ICING CHARACTERISTICS AND MITIGATION STRATEGIES FOR WIND TURBINES IN COLD CLIMATES

By

ANDREA GRAZYNA KRAJ

A thesis presented to the Faculty of Graduate Studies, University of Manitoba in fulfillment of the thesis requirement for the degree of Master of Science in MECHANICAL ENGINEERING

Department of Mechanical and Manufacturing Engineering
University of Manitoba
Winnipeg, Manitoba, Canada

© Andrea Grazyna Kraj, March 2007

THE UNIVERSITY OF MANITOBA

FACULTY OF GRADUATE STUDIES

*****

COPYRIGHT PERMISSION

ICING CHARACTERISTICS AND MITIGATION STRATEGIES FOR WIND TURBINES IN COLD CLIMATES

BY

ANDREA GRAZYNA KRAJ

A Thesis/Practicum submitted to the Faculty of Graduate Studies of The University of Manitoba in partial fulfillment of the requirement of the degree

MASTER OF SCIENCE

ANDREA GRAZYNA KRAJ © 2007

Permission has been granted to the Library of the University of Manitoba to lend or sell copies of this thesis/practicum, to the National Library of Canada to microfilm this thesis and to lend or sell copies of the film, and to University Microfilms Inc. to publish an abstract of this thesis/practicum.

This reproduction or copy of this thesis has been made available by authority of the copyright owner solely for the purpose of private study and research, and may only be reproduced and copied as permitted by copyright laws or with express written authorization from the copyright owner.

ACKNOWLEDGEMENTS

.....

For funding:

- NRCAN
- Manitoba Hydro NSERC Chair in Alternative Energy

For technical support:

- Dr. Eric Bibeau, for providing the opportunity for this project, the support throughout the challenges and trusting in where the wind would blow.
- Department of Mechanical & Manufacturing Engineering, University of Manitoba.
- Dr. Hanesiak, Faculty of Environment, University of Manitoba, for anemometer support.
- Bruce Ellis, UMITF Lab support.
- St. Leon Wind Farm Personnel for onsite experience.
- John Maissan, for wisdom and experience from the cold climate of the Yukon.
- John Yestrau, for unique insight, inspiration, and light along the way.
- Dave Gaden for always having an entertaining thought and the guts to brave the ice and wind at a moments notice.
- Antoine Lacroix for direction and continued support.

For life support:

- Mom & Dad for inspiring the dreams, and breeding the creativity, keeping me grounded, cutting out all the articles and sudoku,
- Greg, for all the smiles and laughter in between,
- Bumbunia, for reminding that you're all proud of me.

- My family and dear friends for being there when the light at the end of the tunnel was just a dream.

- To Japan, for allowing me to be lost.

Twinkling lights below,
Serenity amongst noise,
Soul in search of home.

ABSTRACT

Wind power has gained substantial interest worldwide as a form of alternative and sustainable energy. The optimization of wind energy systems is critical in order to establish wind as a viable and economic resource. An immense potential of untapped wind resources exist in cold climates and is hindered by the uncertainty of the characteristics of the surrounding climatological conditions. One issue facing the optimization of wind power generation in cold climates is ice accumulation on turbine blades. This issue creates concern for efficient energy production, operational safety and when wind represents a significant energy mix ratio for a utility, a concern for grid integration. This research explores mitigation strategies to prevent or delay ice accumulation on wind turbines blades in an effort to enhance the understanding of the icing characteristics and to optimize wind turbine systems in cold climate conditions. Mitigation strategies involve surface, thermal and, the newly developed, *thermface* techniques in both anti-icing and de-icing regimes for both glaze and rime icing conditions. Experiments are conducted on stationary blade configurations in the state-of-the-art University of Manitoba Icing Tunnel Facility. The results of the mitigation techniques depict icing profiles and aerodynamic changes along the blade leading edge over a set period for the simulated icing event and quantify the ice adhesion pressure force, volumetric accumulation amount, metric profile shape extension and the ice accumulation rate. Indication of improved ability to control icing characteristics is presented through the comparison of mitigation strategies to the experimental datum. Results are compiled and summarized in the exclusive Mitigation Forecasting Tool and Profile Shape Catalogue, and are a unique contribution to the scientific community, through the diverse collection of experimental results and novel mitigation solutions.

TABLE OF CONTENTS

LIST OF TABLES

LIST OF FIGURES

1 INTRODUCTION

Wind, as an energy resource, contains the potential to become an important contributor to utility and non-utility power generation in many regions in Canada and in cold climates throughout the world. However, due to climatological factors, many Canadian wind turbine sites are affected by icing problems that impact power generation. Wind power capacity in Canada is expected to increase from 0.4 GW in 2004 to 8.5 GW in 2020, which is equivalent to about 6% of the country's total generating capacity and 3.6% of total electricity production, as indicated in the most recent long-term supply and demand outlook released by Natural Resources Canada [CanWEA 2007]. Almost half of the increase in renewable energy capacity expected over the outlook period will be driven by the expansion of wind generation [NRC 2006]. Worldwide, the conservative IEA projection of the potential for the global market indicates that wind energy could be supplying 5% of the world's electricity by 2030 and 6.6% by 2050, which translates to an annual installed capacity of 24.8 GW and 34.3 MW, respectively [GWEC 2006]. Other models project less conservative figures and are listed in Table 1-1.

Table 1-1: Global wind energy outlook for years 2030 and 2050 [GWEC 2006]

SUMMARY OF GLOBAL WIND ENERGY OUTLOOK SCENARIO FOR 2030							
Global Scenario	Cumulative wind power capacity (GW)	Electricity output (TWh)	Percentage of world electricity (High Energy Efficiency)	Annual installed capacity [GW]	Annual investment (€ bn)	Jobs [million]	Annual CO_2 saving (million tonnes)
Reference	364	892	5 %	24.8	21.2	0.48	535
Moderate	1,129	2,769	15.6 %	58.3	45.0	1.14	1,661
Advanced	2,107	5,176	29.1 %	129.2	84.8	1.44	3,100
SUMMARY OF GLOBAL WIND ENERGY OUTLOOK SCENARIO FOR 2050							
Global Scenario	Cumulative wind power capacity (GW)	Electricity output (TWh)	Percentage of world electricity (High Energy Efficiency)	Annual installed capacity [MW]	Annual investment (€ bn)	Jobs [million]	Annual CO_2 saving (million tonnes)
Reference	577	1,517	6.6 %	34.3	28.8	0.65	910
Moderate	1,557	4,092	17.7 %	71.0	54.2	1.39	2,455
Advanced	3,010	7,911	34.3 %	168.6	112.0	2.80	4,747

Even with the conservative model, the significance of the potential growth of the wind energy market is evident. However, due to the inherent cold climate issues, the potential to harness an abundant source of wind for power generation in such conditions is disadvantaged, as is the optimization of the expected capacity increase.

Icing is an issue of interest to many groups—from private energy companies, to public utilities and landowners. This thesis discusses the experiments performed in the University of Manitoba's Icing Tunnel Facility, (UMITF), for the investigation of icing mitigation strategies for wind turbines in cold climates. Experiments are performed on aerofoils representative of blades currently used in the wind turbine industry, under simulated climatological conditions for severe icing events found in cold climates where wind turbines are commonly employed.

This aspect is important for the Province of Manitoba since it has targeted 1,000 MW of wind penetration by 2016 [Rondeau 2006]. The addition of 200 MW of conventional (hydroelectric) power to this wind target translates to a wind penetration of 15.3% installed capacity [Woods 2007]. This would be the highest wind penetration in North

America with most of the wind farms located in ice prone regions. The importance of understanding icing issues and the resulting loss of wind power is of great concern to Manitoba Hydro and the Province of Manitoba, as an icing event would translate to grid operational issues and affect power delivery to its local and export power markets. Of particular interest, at present, is the 99.9 MW wind farm in St. Leon, Manitoba, which has been developed in a region very well-known for icing events.

1.1 Project Objectives

The objective of this thesis is to further the understanding of icing effects and mitigation strategies on wind turbine blades in cold climates, with emphasis on Canadian regions, and of particular interest, the region of South-Western Manitoba.

The main focus of the research is dedicated to characterizing the ice that forms on wind turbine blades, representative of those used in the wind industry and to investigate icing mitigation strategies.

This research involved characterization of icing properties on a normal blade, implementation of mitigation strategies with development of a new mitigation strategy and further characterization of icing properties for mitigated blades.

1.2 Previous Experience

There is limited experience directly related to wind energy in cold climates in Canada, since this is an emerging area within the wind industry. The two turbines on Haeckle Hill in the Yukon Territory are the first turbines in Canada to have been exposed to cold climate operation that employed mitigation strategies representative of the research in this thesis [Maissan and Kraj 2007b]. Previous experience is this field is driven from research in Europe by members of the International Energy Agency's Annex XIX on Wind Energy in Cold Climates [IEA 2007] and the Finnish Meteorological Institute which has hosted several BOREAS conferences on icing issues for Wind Energy Production in Cold Climates [BOREAS 2000-2005]; as well as from the aerospace industry for icing mitigation on aerofoil sections for aircraft. The knowledge of environmental factors is gathered from the field of climatology and meteorology. These fields of knowledge are fused to gain an understanding of the issues, and potential solutions in order to formulate an information base for wind energy production, specifically icing mitigation for wind turbine blades in cold climates.

2 LITERATURE REVIEW

2.1 Introduction

This section provides a background of information related to wind energy production in cold climates, the related concerns and general status of the industry, as well as the literature pertinent to the development of the experimental design. Included are topics on cold climates, icing, wind turbine performance and safety, the current status of icing mitigation on blades, and mitigation technology.

2.1.1 Summary of Results of Literature Review

The knowledge between the aerospace industry, the power utility industry and the environment are collaborating to enhance the development of the emerging field of wind energy in cold climates. There is a growing awareness for the need to understand the different factors influencing icing conditions, the aerodynamics of blades for the application of energy generation and the methods to mitigate the adverse conditions of icing which these machines encounter in cold climates. Information is sourced from the individual fields of knowledge rather than from the relative field since the area of wind energy in cold climates is concurrently developing. This thesis is a contribution to the fusion of these areas in this emerging field. A summary table of the icing studies presented in the following section is located at the end of this chapter.

2.2 Wind Energy in Cold Climates

There has been extensive development of wind energy in regions that experience cold climates for several reasons. Firstly, the awareness for the need to move towards more sustainable development has been mostly embraced by the countries that can afford this economical transition to an environmentally conscientious approach. Most of these countries are located in regions that are exposed to extremely cold conditions—seasonally or regionally. These cold conditions produce air masses of increased density, ideal for enhanced energy production; however, often associated with dangerous icing conditions. As countries strive to meet the demands of their environmental agendas and take responsibility for the environment as a global community, there is a need to understand the consequences and mitigate the negative risks associated with cold climates on wind energy production in order to effectively harness this substantial resource in cold climate regions.

The International Energy Agency contains Annex XIX, a collaboration called Wind Energy in Cold Climates with the purpose of gathering and providing information about wind turbine icing and low temperature operation [IEA 2007]. This annex references a significant amount of wind turbines located in cold climates around the globe, as depicted by the points in Figure 2-1, note that the Manitoba wind farm is not yet acknowledged on this map. As Canada begins to tap into its significant natural wind resource, it becomes a major contributor to the global wind-energy-in-cold-climates community.

Figure 2-1: Wind turbines located in cold climates [IEA 2007]

Statistics Canada defines Climate as "the average weather that occurs in a specific area over a period of time," where *weather* is defined as daily changes in the atmosphere. Factors that affect local regional climates are latitude, altitude, physiography and the proximity of large bodies of water. Some indicators of climate are: temperature, precipitation, sunshine, wind, atmospheric pressure, humidity, and evaporation. In order to properly characterize a region, measurements must be taken systematically at a site over time in order to accumulate an archive of observations from which climatic summaries can be derived for that location [Statistics Canada 2006].

A common energy production definition of a "cold climate" is a site where turbines are exposed to low temperatures outside the standard operational limit and where turbines face icing, which retards energy production in the winter [IEA 2005]. However, a more accurate and globally minded representation of a cold climate would recognize that a cold climate need not be defined by a single seasonal correlation, as many times in Canadian climates, extreme temperatures, which are characteristic of cold climates, can occur over a range of seasons. A cold climate should neither be defined by the current operational limitations of wind turbine technology, because this definition will become dated as technology development for this unique area advances. Rather, a new definition is proposed. A cold climate specific to wind energy production should be defined by the frequency and consistency that the *region* is exposed to climatological conditions which is primarily a function of typical environmental parameters for an icing event that negatively influence a wind turbine structure and power output. These parameters include air temperature, relative humidity, barometric pressure, and wind speed, as well as air density, altitude, dew-point temperature and solar radiation [Megateli 2006]. Liquid water content (LWC) is also an important parameter relating the amount of moisture in the air mass.

Furthermore, a definition for the *degree* of icing may be useful to characterize the severity of icing and the risks associated with icing in a region, in order to effectively mitigate the risk. Table 2-1 defines the icing degree in relation to the number or icing days, d, per year [Morgan 1998].

Table 2-1: Quantification of icing degrees [Morgan 1998]

Icing degree	Icing days per year
Heavy icing	25 > d >5
Moderate icing	5 > d > 1
Light icing	1 > d
No icing	d = 0

The IEA uses the following guidelines shown in Figure 2-1 to assess a cold climate wind turbine site with safety restrictions, slight icing, heavy icing or low temperature [Laakso 2003].

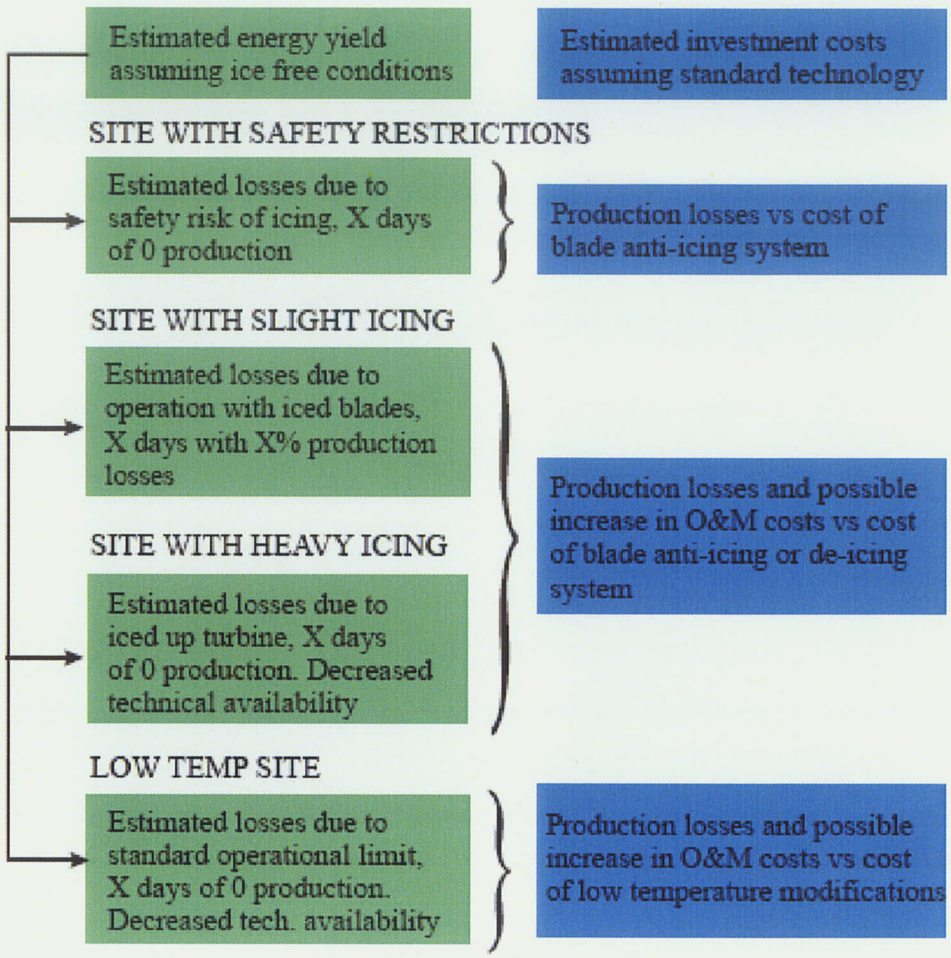

Figure 2-2: Assessment of sites in cold climates [Laakso 2003]

From a Canadian perspective, the majority of the nation is subjected to cold climate conditions for a significant portion of the year. On a national scale of wind energy production, these cold climate conditions affect all of the current wind farm locations, and have the potential to affect proposed projects. With the expansion of the current Canadian wind energy market this is of critical significance to the nation's contribution to efficient wind energy production. Figure 2-3 depicts the current installed capacity in the

Canadian Wind Energy market. Canada's current installed capacity is 1,251 MW - enough to power over 420,000 homes [CanWEA 2006].

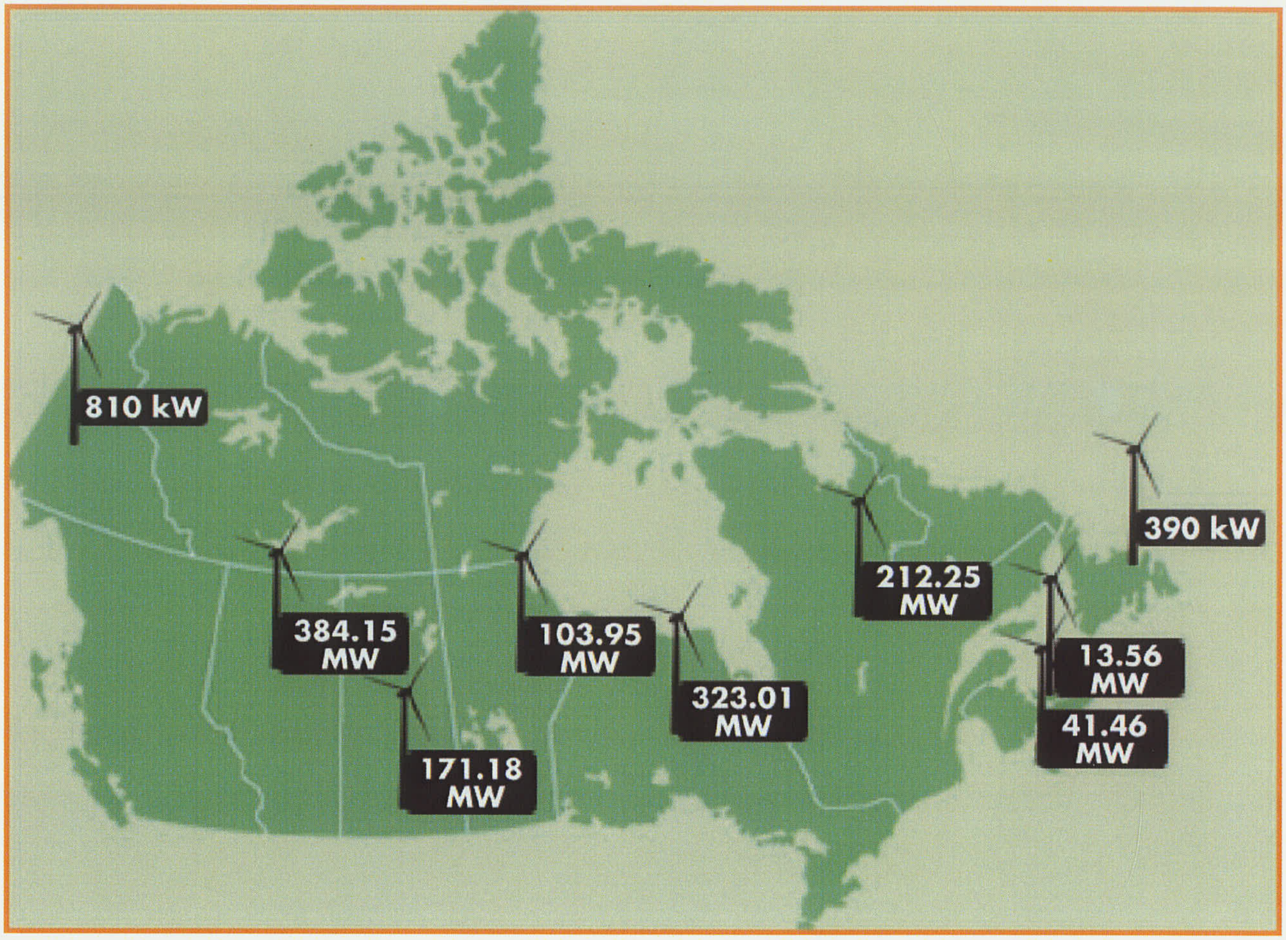

Figure 2-3: Canadian installed capacity, November 2006 [CanWEA 2006]

The Province of Manitoba has announced a committed expansion of 1,000 MW of wind over the next decade [Rondeau 2006]. With this type of drive to enhance wind energy development in the cold climate known to Manitoba, optimized wind energy production is of significant concern to the local energy sector.

Figure 2-4 indicates the areas that are prone to icing in Southern Manitoba [Manitoba Hydro 1984]. This data is a collection of icing data for power cables and ice accumulation on roads and relates to icing effects on wind turbines. Such icing data cannot be used directly to infer power losses expected for wind turbine as the criteria for icing of wind turbines is different. The circle in the figure indicates the region where the wind farm in St. Leon, Manitoba is located, which correlates with the presented severe icing region.

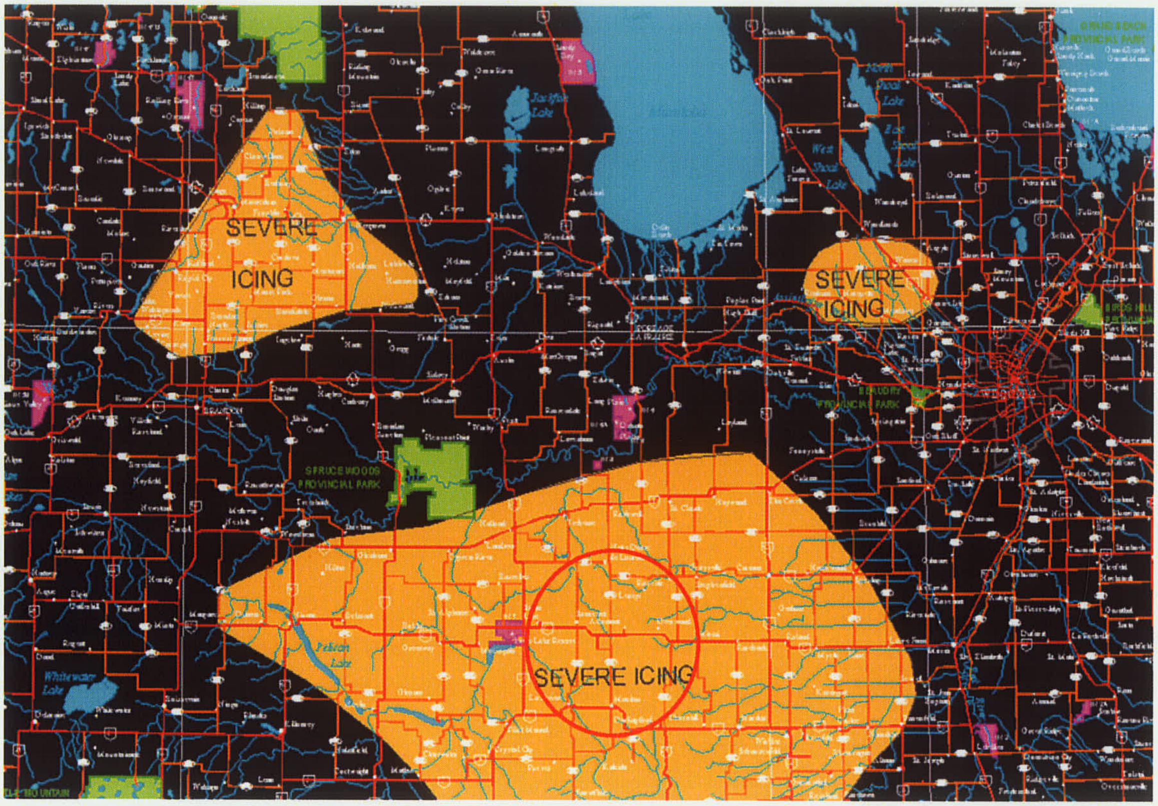

Figure 2-4: Severe icing regions in Southern Manitoba [Manitoba Hydro 1984]

The potential for the wind energy market in Southern Manitoba is shown in Figure 2-5 from the Canadian wind energy atlas, depicting wind speed at the 80 m hub height level as used for the St. Leon wind farm turbines. The icing areas shown in Figure 2-4 coincide with the location of ideal wind resources in Manitoba, as indicated by the circle shown in Figure 2-5.

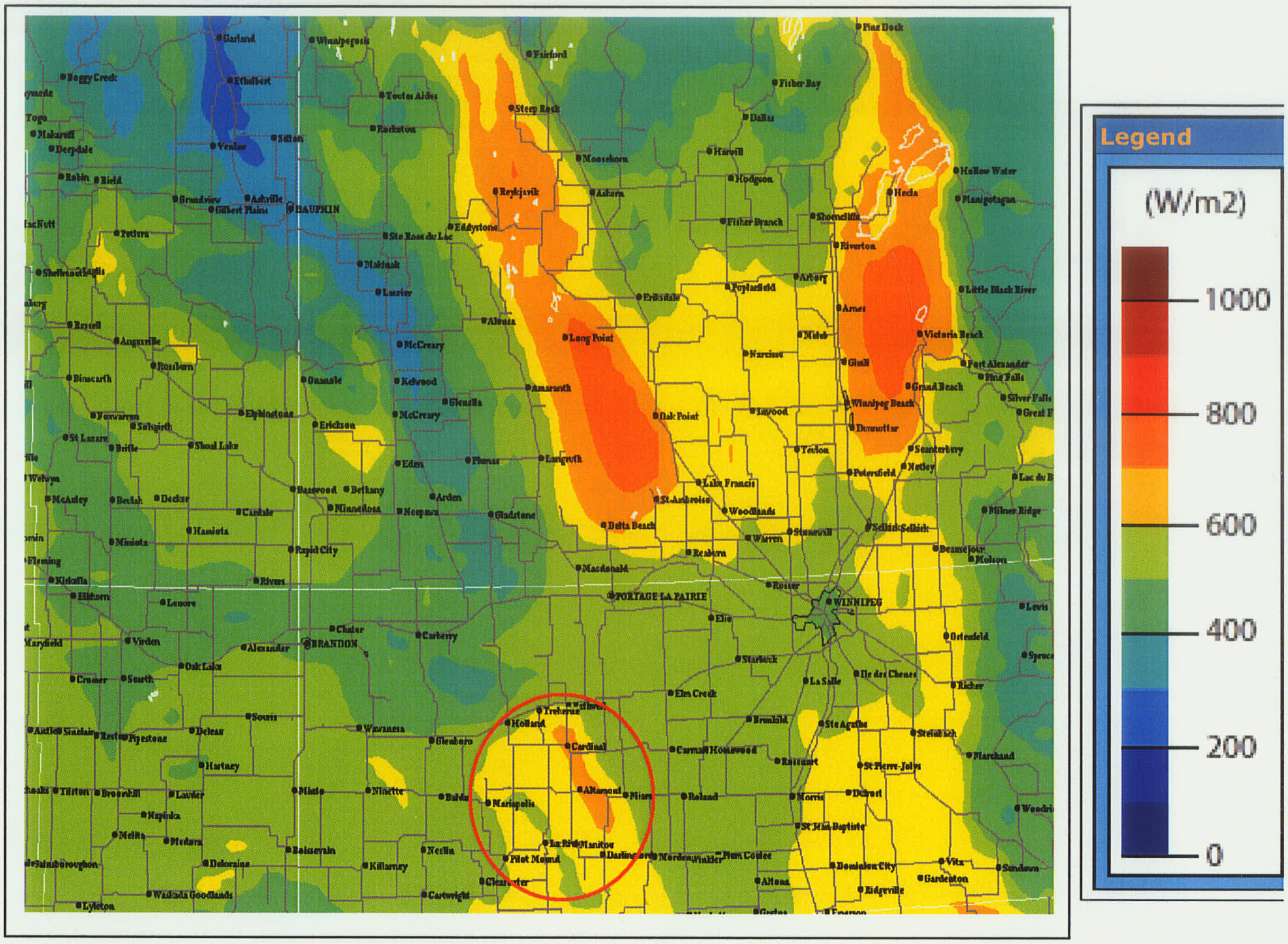

Figure 2-5: Canadian wind energy atlas, wind speed in southern Manitoba at a hub height of 80 m indicating area of wind farm development [Environment Canada, 2006a]

With the above cold climate definition in mind, wind energy in Canadian cold climates can be effectively distinguished by the ability of the climate to negatively impact power generation of the wind turbine specific to the region in which the wind turbine is located. In Southern Manitoba, where this project has been initiated, these characteristics of this cold climate can be experienced in a range of the months from October to May.

Figure 2-6 displays the Canadian climate normals for the station site closest to the St. Leon wind farm in Southern Manitoba, (latitude: 49° 10' N, longitude: 98 ° 4' W, elevation 297.50 m, climate ID: 5021848), [Environment Canada 2006b]. The average daily temperatures between November and March are below zero degrees Celsius. With the ideal combination of wind speed and precipitation, even the months of October and April can produce cold climate conditions.

Temperature:	Jan	Feb	Mar	Apr	May	Jun	Jul	Aug	Sep	Oct	Nov	Dec
Daily Average (°C)	-15.6	-11.7	-4.9	4.7	12.9	17.7	20.1	19.1	13.3	6.2	-4.3	-12.5
Standard Deviation	4.2	4.1	3.1	2.9	2.4	1.8	1.6	1.8	1.5	1.5	3.1	3.9
Daily Max (°C)	-11	-7.2	-0.6	10.4	19.4	23.6	25.9	25.3	19.1	11.2	-0.5	-8.3
Daily Min (°C)	-20.1	-16.2	-9.2	-1	6.2	11.8	14.2	12.9	7.6	1.3	-8	-16.6
Rainfall (mm)	0.4	1.6	6.4	24.5	61.6	84.4	71.2	69.9	52.5	37.8	3.7	2.3
Snowfall (cm)	19.5	17.6	20	11.1	1.7	0	0	0	0.3	7	24	18.5

Figure 2-6: Canadian climate normals 1971-2000 at Morden, Manitoba [Environment Canada 2006b]

The blades of the wind turbines at the St. Leon wind farm are 40 m in length, which is the rotor radius when the blades are attached to the hub. Figure 2-7 provides a scale to emphasize the proportion of ice that can potentially accumulate on blades of this magnitude.

Figure 2-7: 40 m wind turbine blade at St. Leon wind farm prior to assembly

Concerns about cold climate effects on wind energy production influence all components of the wind turbine; from the nacelles, rotors, and blades, to the stability of the tower and the safety of the surrounding region [Laakso 2005a]. The scope of this thesis remains focused on mitigating the negative impact of the cold climates in terms of icing on the blades of the wind turbine.

2.3 Atmospheric Icing

There are a variety of ice accumulations that can occur on a structure. The Finnish Meteorological Institute identifies the following: rime aggregation (in-cloud icing), icing precipitation, wet snow accumulation, and icing from sea water spray [Ahti 2005]. In the Canadian central prairies, marine conditions are irrelevant and only the first three icing conditions are of concern. Freezing rain and freezing drizzle are defined as liquid precipitation which falls when air temperatures are 0°C or less. Other damaging icing situations are caused by wet snow which freezes after contact or by persistent fog or cloud [Chaîné 1974]. The type of ice that forms in the atmosphere is dependent on several factors, such as air temperature, relative humidity, barometric pressure, and wind speed, as well as air density, and altitude; as well as the physical atmospheric processes that create the initial cloud formation. Furthermore, the ice that forms on the substrate of a wind turbine blade is also dependent on the temperature of the substrate surface. There are two distinct types of icing with different characteristics, namely glaze and rime. This experiment solely focuses on the two distinct ice types, as an attempt to best characterize the properties and effects of either of these regimes, since most wind turbines are exposed to icing events that fall into either category. Often, there will be a "mixed" icing regime that is a combination of these two types. The characterization of mixed ice accretion is more involved due to the different proportions of either glaze or rime ice, and could be a complete investigation itself.

2.3.1 Glaze Ice

Glaze ice occurs at temperatures just below freezing, in atmospheric conditions of high liquid water content [Bose 1992]; creating an ice that is clear and dense. Traditionally, glaze ice forms at temperatures between 0°C and -4°C. In the UMITF, glaze ice has been simulated at a temperature of -5°C. In glaze icing, part of the water droplets freeze upon impact and the remainder run along the surface before freezing, forming a smooth lumpy profile shape of high-density clear ice. Glaze ice is expected to be more difficult to remove than rime ice due to its inherent physical properties; however, for the most part this study proves otherwise, which may be a result of the specific experimental configuration. Figure 2-8 depicts the experimental glaze ice formation.

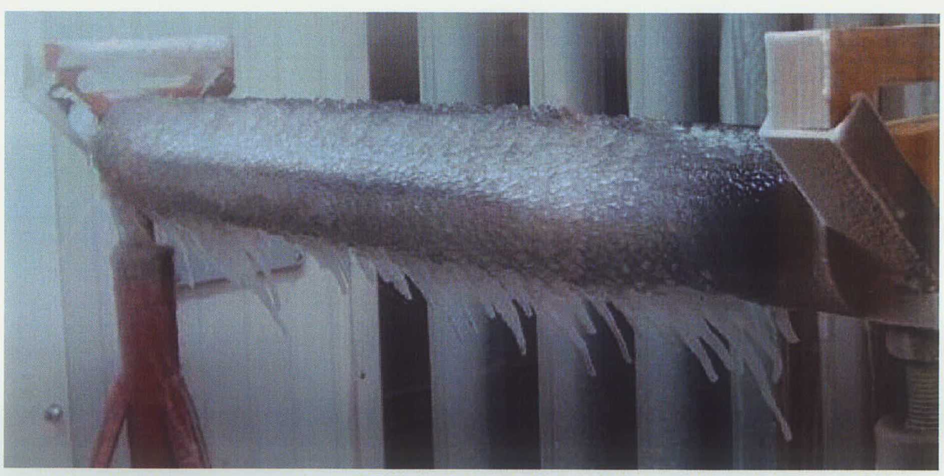

Figure 2-8: Glaze ice with frozen rivulets formed in the icing tunnel

2.3.2 Rime Ice

Rime ice occurs at colder temperatures of low liquid water content freezing before contact with the substrate then accumulating with air pockets in between, forming a white and feathery, less dense type of ice. Traditionally, rime ice forms at surface temperatures between -12°C to -4°C [Bose 1992]. In the UMITF, rime ice has been simulated at a temperature of -15°C. In rime icing, supercooled water droplets freeze immediately upon impact and form a low-density ice, white and feathery in appearance, as shown in Figure 2-9.

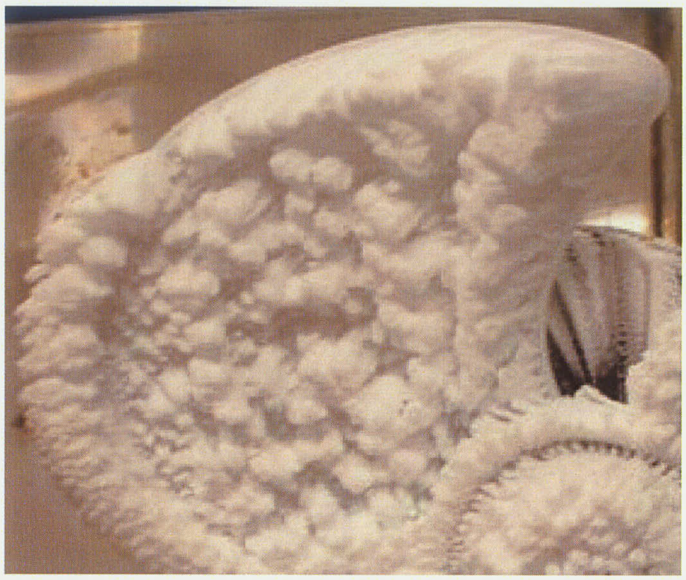

Figure 2-9: Rime ice with feathered texture formed on a rotating blade

2.4 Geographic Distribution of Icing

Literature states that under the current global warming scenario, the regular occurrence of more intense storms is inevitable in the future, with the Canadian western provinces experiencing increased winter temperatures. The impact of this, although not published, could result in more freezing drizzle and freezing rain in autumn, spring and winter due to the warmer temperatures. Referencing the climatic events of the past year, (2006), as a possible indication of future weather patterns, indicates that more cloud and temperatures conducive to freezing precipitation events are to be anticipated [Hanesiak 2006].

2.5 Icing as a Complex 3-Phase System

An icing process is a complex 3-phase system involving solid, liquid and gas phases. The thermal processes leading to icing of structures include multiphase flow with droplets in the freestream, as well as solidification and melting along the moving ice boundary where impinging droplets adhere. This process involves droplet kinetic energy, convective heat transfer, and solid-liquid phase change [Naterer 2003].

As incoming droplets contact the solid surface of the aerofoil, there is a mass conservation balance that must relate the rate of solid (ice) accumulation to the rate of wind transport of droplets onto the surface. The complexity of the extension of this intricate dynamic system of ice accumulation is established through the explanation of the flow field thermodynamic and fluid dynamic principles to determine the ice shapes and rates of ice accumulations with respect to aircraft aerofoil applications [Thomas 1996]. Thomas clarifies that the important phenomena of this process include (1) viscous or kinetic heating, (2) kinetic heating by water droplets, (3) evaporation or sublimation, (4) convection, (5) warming of the droplets from the aerofoil, and (6) heat of fusion. As ice accumulates and changes shape with time, the position and shape of the control volume must also change. The change in aerofoil shape because of accreted ice can alter the boundary layer, thus further increasing the necessity of a flexible control volume. Due to the different freezing characteristics of rime ice and glaze ice, Thomas introduces a freezing factor, f, applicable to all icing phenomena. Furthermore, Thomas provides an in-depth conservation of energy equation for ice accumulating on the surface in a transient process, accounting for the heat rate caused by the liquid water entering the CV (control volume), the sensible heat released by the supercooled liquid water droplets, the kinetic energy of the water droplets, and the viscous flow forces. This energy entering the system is balanced with the energy exiting the system, which includes the heat loss due to evaporation, the heat flowing out of the control volume with the exiting liquid water, the heat rate due to freezing, the convective heat transfer and the conductive heat transfer rate into the skin of the aerofoil.

2.6 The Aerodynamics of the Wind Turbine

The blades of the wind turbine are the most important component of the wind turbine, since it is the blades that capture the energy of the wind and harness the resource. The rotor is composed of the blades that are connected at the hub. It is through the rotor that the energy of the wind is transformed into mechanical energy that turns the main shaft of the wind turbine.

2.6.1 Basic Theory

Aerodynamics is the science and study of the physical laws of the behaviour of objects in an air flow and the forces that are produced by airflows. The front and rear sides of a wind turbine rotor blade have a shape similar to that of a long and narrow triangle with tapered thickness bounded by the curved leading edge at the front and tapering down to the trailing edge at the back; further bounded by the blade tip and the blade root at either edge. The blade root is bolted to the hub. The radius of the blade is the distance from the rotor shaft to the outer edge of the blade tip [Stiesdal 1999]. Figure 2-10 depicts the geometry of a typical wind turbine blade.

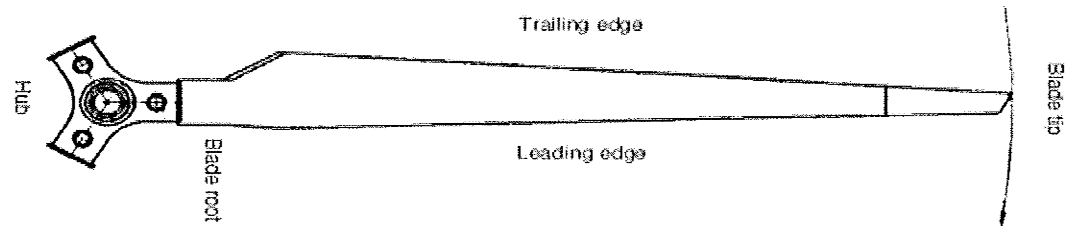

Figure 2-10: Components of a wind turbine blade

2.6.2 Aerodynamic Profile

The shape of the aerodynamic profile is determinative of blade performance. Minor alternations in the shape of the profile can significantly change the power performance of the blade. Blade profiles are traditionally chosen from a widely used catalogue of aerofoil profiles developed in wind tunnel research by NACA (The United States National Advisory Committee for Aeronautics) as early as the 1930's.

Modern wind turbines use the NACA 63 profile series, as shown in Figure 2-11. These profiles have improved power curves compared to the original profile series used for wind turbines, for low and medium wind speed ranges. However, this profile is more sensitive to surface imperfections in certain climates where dirt, grime and insect deposits accumulate and reduce performance, [Stiesdal 1999].

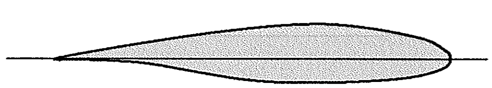

Figure 2-11: NACA 63-series generic profile

This research project uses a NACA 63421 profile blade, consistent with modern turbine blade applications.

2.6.3 Aerodynamic Forces on a Wind Turbine Blade

The flow of a fluid over a surface is governed by Bernoulli's Equation [Prandtl 1934] for a steady, homogenous and incompressible fluid as

$$\frac{w^2}{2}+\frac{p}{\rho}+gh=const. \qquad \text{(Eq 2.1)}$$

Simplification to flow along a definite streamline, such that height, h, is constant and g is the constant for gravity, simplifies the Bernoulli equation, and relates velocity of the fluid velocity, w, to the pressure, p, and the fluid density, ρ, as

$$\frac{w^2}{2}+\frac{p}{\rho}=const. \qquad \text{(Eq 2.2)}$$

In this form of the Bernoulli equation, the balance of the equation implies that as velocity increases the pressure decreases and vice versa.

The flow regime of a fluid over a surface is typically characterized laminar, transitional or turbulent according to its Reynold's number. Reynold's number, Re, is regarded as the parameter that controls the transition from one regime to another [Davidson 2004], as is defined as:

$$\mathrm{Re}_x=\frac{ux}{\nu} \qquad \text{(Eq 2.3)}$$

Where x is the characteristic length, in the case of the wind turbine, it is the chord length of the blade; u is the mean wind speed, and ν the kinematic viscosity of the fluid, in this case the fluid is air. The Reynold's number represents the ratio of inertial to viscous forces in a fluid. The laminar regime is typically associated with low Re, while the turbulent regime is associated with high Re and the transitional regime occurs in a given region between these regimes. The approximation of an aerofoil as a flat plate indicates that the transitional regime would occur at approximately Re = 500, 000 [Fox 2004].

2.6.3.1 Lift

Lift is a force created by a pressure distribution acting over the area of a surface subjected to a flow. Lift acts on the body in the direction perpendicular to the flow. The aerofoil is characteristically designed with a rounded upper surface and a curvature or "cambered" under-surface so that the airflow beneath the blade is slowed, while above the blade the airflow speed is increased. This increase in velocity over the upper surface creates a related pressure drop, such that the pressure on the cambered surface is greater than above, thereby generating lift as shown in Figure 2-12.

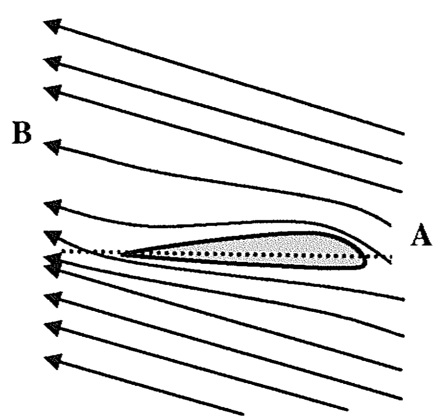

Figure 2-12: Streamlines around an aerodynamic profile

2.6.3.2 Drag

Drag at high Reynolds numbers is a force created by both a pressure distribution acting over the area of a surface subjected to a flow and a friction factor. Drag acts on the body in the same direction as the flow. The aerofoil is characteristically designed to minimize drag which opposes lift. The optimized blade position seeks an ideal lift-to-drag ratio, such that lift is maximized and drag is minimized and stall is prevented. The ideal surface finish of the blades is one method to minimize drag.

2.6.3.3 Critical design of the aerodynamic profile

The aerodynamic profile of a wind turbine blade is twisted along the blade axis to accommodate for changes in the resulting wind angle. As wind speed increases the angle of attack increases, and the aerodynamic properties of the profile will change. There is a critical region of optimized performance correlated to angle-of-attack. Beyond this region lift decreases, drag increases and the profile "stalls". A stall is a situation during which airflow is no longer laminar or flowing smoothly, over the profile. Rather, the air detaches from the rear side of the blade and strong turbulence occurs. This separation of air masses normally commences progressively from the trailing edge, so the profile gradually becomes semi-stalled and eventually fully-stalled as shown in Figure 2-13.

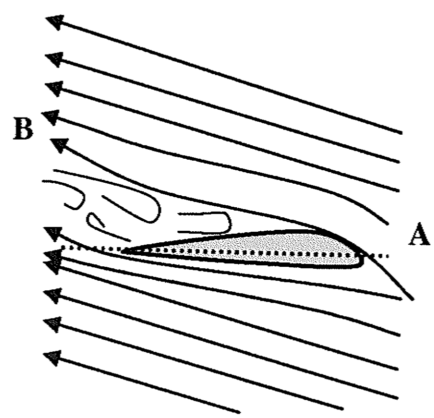

Figure 2-13: Flow separation with induced stall

Any change to the surface of the aerodynamic profile may behave as a trip to the flow and induce separation of the boundary layer creating turbulence and potential stall; thus, any physical changes can be considered potential threats leading to aerodynamic losses.

2.7 Wind Turbine Blade Design

A successful blade design must satisfy several objectives: maximize annual energy yield for the specified wind speed distribution; limit maximum power output; resist extreme fatigue loads; restrict tip deflections to avoid blade-tower collisions; avoid resonances; and minimize weight and cost [Burton 2001, p.377]. Blade design consists of aerodynamic design and structural design. Aerodynamic design focuses on the selection of optimum geometry of the blade external surface, referred to as the *blade geometry* and is defined by the aerofoil family and the chord, twist and thickness distributions. The structural design consists of blade material selection and spar design. The typical construction of a blade consists of a load bearing member, the spar, the stiffening structures composing the frame called shear webs, and that which encloses the structure and makes it whole—the skin, as shown in Figure 2-14.

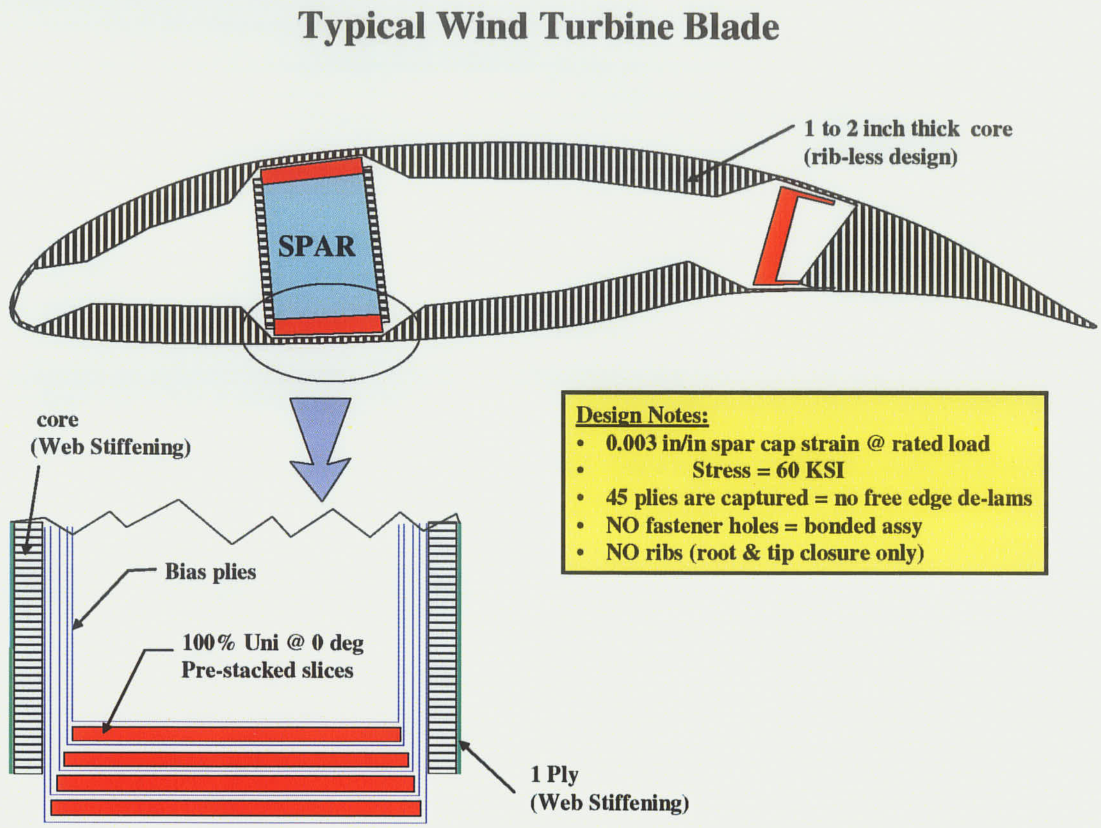

Figure 2-14: Typical blade construction [Roeseler 2006]

The ideal material for blade construction will combine the necessary structural properties—high strength to weight ratio, fatigue life and stiffness, with low cost and the ability to be formed into the desired aerofoil shape [Burton 2001, p.380]. Various designs and materials are used for construction. Traditional blades used wood, aluminum, or fiberglass; however, modern design concerns for efficient strength-to-weight ratios in turbine blades are leading towards aerospace materials such as carbon fibre composites. Figure 2-15 identifies some of the innovative modern materials being used for the various structural elements.

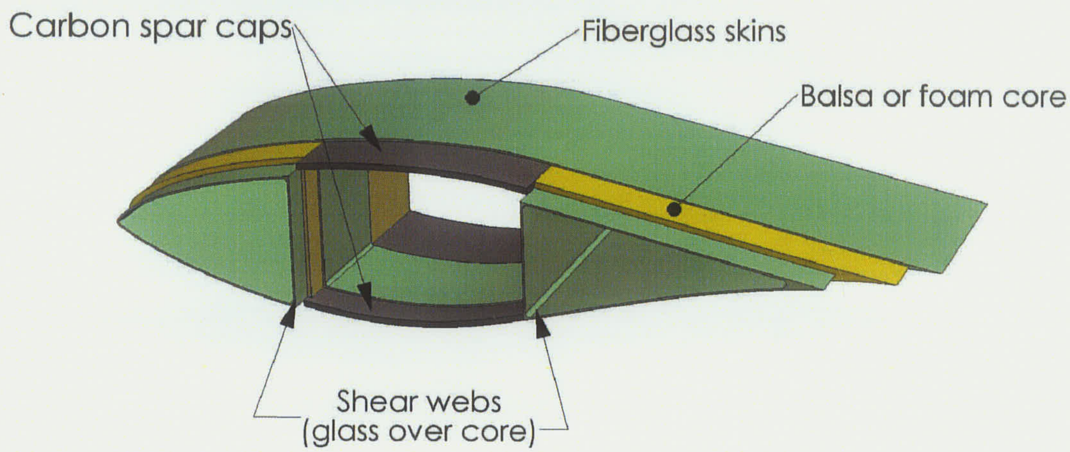

Figure 2-15: Innovative materials in wind turbine blade design [Roeseler 2006]

These modern materials can be varied and integrated along the entire wind turbine blade to optimize the performance needs and load bearing properties of the blade, as is shown in Figure 2-16.

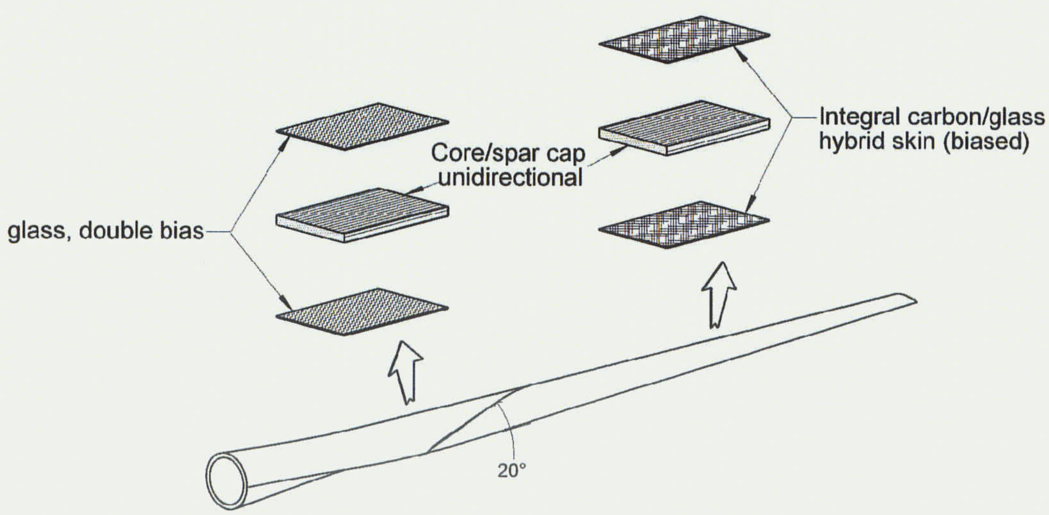

Figure 2-16: Concept for biased carbon-fiberglass blade skins [Roeseler 2006]

2.8 Wind Turbine Performance

The performance of a wind turbine is characterized by the variability of power, torque and thrust with wind speed. The power is determined by the amount of energy captured by the rotor. The rotor is composed of the turbine blades.

2.8.1 Effect of Icing on Wind Turbine Performance

Optimized aerodynamic performance is dependent on the blade lift to drag ratio [Kraj 2003]. It is an undisputed fact that ice accretion on rotor blades changes the surface and geometric dimensions of the blades and affects the aerodynamic design properties [Rissanen 2005, Durstewitz 2003, Antikainen 2003, Kimura 2000]. Changes to the aerofoil profile shape due to ice accumulation lead to the transient change in chord length of the aerofoil and result in a significant extension to chord length, also known as leading edge "thickness", after only a period of 10 minutes, for which the aerodynamic blades are not designed. The changes in the blade aerodynamic profile shape directly affect the lift, as well as create trigger points for non-laminar flow over the blade surface [Rissanen 2005] resulting in less-efficient energy capture. With a less-effective lift-to-drag ratio the turbine is not capable of efficient wind energy production [Kimura 2000], and in turn may compromise financial interests.

Furthermore, ice accumulation adds weight to the aerofoil and changes the mass distribution along the blade [Rissanen 2005, Antikainen 2003] which can lead to additional (symmetrical or asymmetrical) loading and vibrations, which in turn compromise the fatigue life of the blade material. The compromise of the structural integrity of the machine not only hinders performance, but operational safety as well.

These effects identify further uncertainties and issues related to additional loading from ice accretion and low temperature operation, such as the structural safety and lifetime of the blades, or a sudden loss of ice that causes large asymmetric loading and vibration dynamics [Antikainen 2003]. A summary of these results is listed in Table 2-2, with degree ranking correlated to the consequential effects of the result.

Table 2-2: Potential results of ice accretion on wind turbine performance

1st Degree	2nd Degree	3rd Degree	4th Degree
Increased loads (static/dynamic)	Yaw angle declination	Ice throw / drop	Ice impact safety concerns
Reduced aerodynamic efficiency	Turbulence	Noise	Reduced power production
Vibrations	Blade material stress	Structure degradation	Structure Safety Concerns
Untrue sensor signals	Plant stoppage	Restart problematic	Financial losses

2.8.1.1 Reduction in Output Power

The power output, *P*, from a wind turbine is given by the well-known expression:

$$P = \frac{1}{2} C_P \rho A U^3 \qquad \text{(Eq 2.3)}$$

where, ρ, is the density of air at 1.225 kg/m^3 at standard conditions, C_P, is the power coefficient, A, is the rotor swept area, and, U, is the wind speed [Burton 2001, p.6]. The power coefficient describes the fraction of the power in the wind that may be converted by the turbine into mechanical work. It has a theoretical maximum value of 0.593, known as the Betz Limit; however, lower peak values are achieved in practice. The tip-speed ratio is defined as the ratio of the rotor tip speed to the free wind speed. The power coefficient of a rotor varies with the tip speed ratio, and is a maximum for a unique tip-speed ratio.

The significance of the wind speed to influence output power is evident in the cubed wind speed factor. A doubling of wind speed leads to an eight-fold increase in power. Thus, this represents the incentive to develop wind farms in areas of high wind speed. Furthermore, turbine towers are heightened to harness the wind speeds that increase with height to make further use of this natural occurrence. This poses another concern due to the increased frequency of in-cloud icing that more commonly occurs at higher altitudes, in which the turbine blade encounters a collision with super-cooled water droplets [Durstewitz 2003, Kimura 2000] that freeze upon impact with the structure immediately forming an unfavorable thin ice layer.

When the aerodynamic design of the blade profile is compromised through icing, energy capture is inhibited and reduced output power results [Battisti 2005, Peltola 2003]. Ice induced leading edge roughness has been shown to negatively influence blade aerodynamics, as already mentioned, and significant power degradation can be expected from a thin ice layer on a wind turbine blade [Laakso 2005b], as is shown in Figure 2-17.

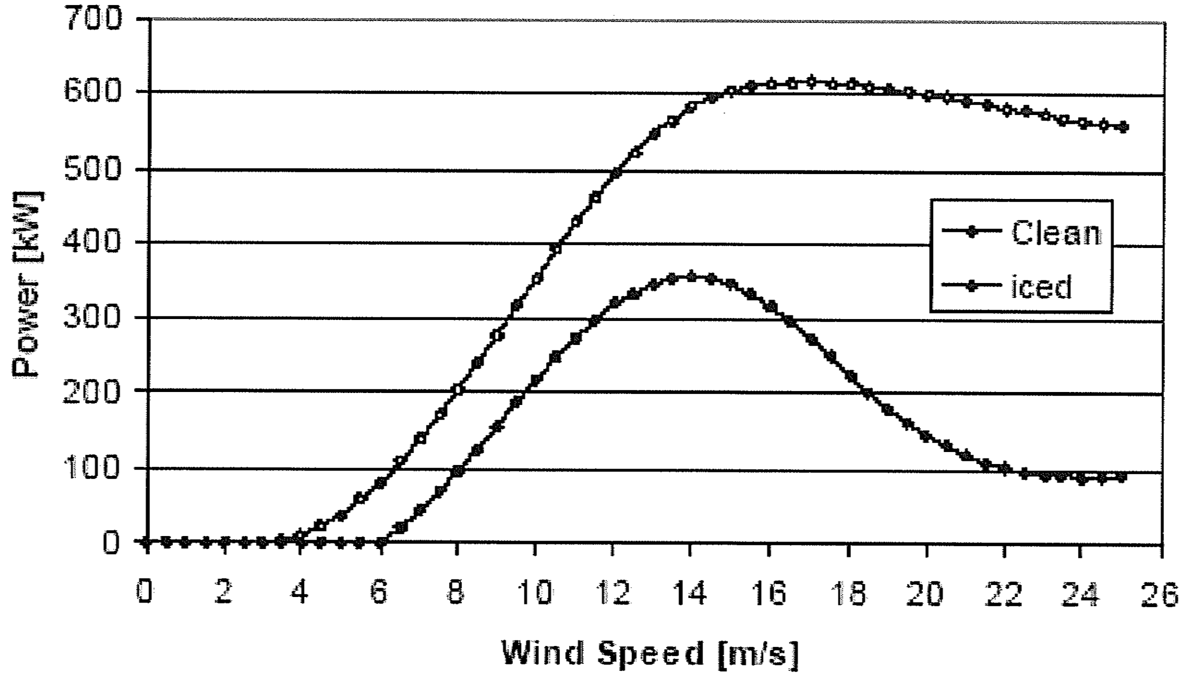

Figure 2-17: Power degradation due to icing of wind turbine blade [Laakso 2005b]

Additionally, icing of the turbine blades is regarded as an equivalent concern for power reduction [Rissanen 2005, Antikainen 2003]. A reduction in power output means less electricity production and thus, reduced financial efficiency. Furthermore, if icing conditions last for a longer period of time, the economic viability of the project may not be secured [Durstewitz 2003].

2.8.1.2 Increase in Rotor Loads

Blades are naturally subjected to loading through such events as wind gusts and material properties. In the case of extreme loading, wind gusts induce blade bending moments. Over an extended period of time, fatigue loading becomes a concern. Fatigue loading is a function of material properties. As a result, fatigue damage can be dominated by the small number of high range stress cycles associated with unusual wind conditions, rather than routine medium range cycles. Fatigue damage also results from stress cycles with high mean levels, characteristic of composite materials [Burton 2001, p.399]. High wind or yaw cycles are a major source of fatigue damage, although the contribution of cycles at wind speeds below stall may also be significant due to the rapid variation of moment with, and at, that wind speed as well as the increased amount of cycles. The relative contributions of different wind speeds to life-time fatigue are dependent on the shape of the bending moment and wind speed characteristics. Fatigue also results from gravity loading and fluctuations in the in-plane aerodynamic loadings that dominate for large wind turbines. In extreme operating conditions, tip deflections of up to 10 percent of blade radius may occur and create a risk of blade-to-tower collisions.

When ice accumulates on the blade, its weight creates a load in itself which amplifies the already existing load conditions. Since the blades are not designed for the non-uniform ice loads, the increased loads pose a threat to the integrity of the blade structure, as well as to the resulting performance of the turbine. Damages to the blades that may potentially end in complete failure of the blade also pose a costly risk to the machine and owners. The risk from excessive loading that the failure of a blade poses on the surrounding safety of the wind farm area is also a concern.

2.8.1.3 Vibration

One of the most important objectives of blade design is the prevention of resonant oscillations, which intensify fatigue damage and can lead to rapid failure [Burton 2001, p.407]. Blade resonance is carefully mitigated in its design by maximizing the damping and ensuring that the blade flap wise and edgewise natural frequencies are well separated from the rotational frequency and its harmonics, such as the blade passing frequency, as well as those of any other vibration modes. Since the accumulation of ice on the blade surface is a transient process it is continuously changing and does not guarantee level accumulation on all the blades of the wind turbine at the same point in time. This inconsistency can lead to non-proportional loading among the blades which can negatively impact the harmonics of the rotating system, leading to structural damage of the blades, and in severe cases to tower failure. This is another costly risk to the wind turbine system.

2.8.1.4 Non-optimized Blade Aerodynamics

A wind turbine blade operates on basic aerodynamic principles for a body submersed in a flow. The power generated by the wind turbine relies in the ability of the energy in the wind to lift the blade. The essence of the aerodynamic profile, as designed, has already been mentioned, and any changes to the as-designed for conditions will create non-optimized performance characteristics for the blade. Any ice that accumulates on the blades changes the profile shape of the blade, creates trigger points for non-laminar flow, and adds weight to the blade, which makes lift more difficult. With non-optimized blade aerodynamics, wind turbine performance is directly compromised.

2.8.1.5 Solidity

Solidity represents one aspect of turbine performance and is defined as the total blade area divided by the swept area [Burton 2001, p.174-175]. As ice accumulates on the blades, and extends the chord length, the blade area increases. Thus, it is inferred that the severity of icing can potentially dictate the severity of an increase in solidity of the machine. An increase in solidity would narrow the performance curve and make the turbine very sensitive to tip speed ratio changes. If the solidity increases excessively, the turbine has a relatively low maximum C_P and thus, a reduced power performance.

2.8.1.6 Blade Icing and Safety

With the extensive development of wind resources in cold climates worldwide, there is a growing awareness for safety issues regarding icing on wind turbine blades and its removal. Not only is icing seen to be counter productive for energy generation, but that the removal of the ice to improve production lends itself to another concern—ice throw and the damage to the surrounding environment, which can include humans, objects as a result of human interaction and the turbine structure itself. In recognition of this fact, formulas have been developed to attempt a prediction of ice throw and the threat that the impending ice may pose on the surroundings. A basic formula for calculating the zone of likely ice throw for rotating and stopped turbines as follows [Laakso 2005a, p.27]:

Rotating: $$d = (D + H)1.5 \qquad \text{(Eq 2.4)}$$

Stand still: $$d = \frac{v(D/2 + H)}{15} \qquad \text{(Eq 2.5)}$$

In the case of the wind turbines located in Southern Manitoba, in a moderate wind speed of 7 m/s, (25.2 km/h, 15.6 mph), where the wind turbine blades have a 40 m radius located at a hub height of 80 m, this results in a maximum falling ice distance, d, for a rotating turbine of 240 m and for a turbine at stand still of 56 m.

As a means of managing such risk, proper risk assessment is suggested [Siefert 2003a, Laakso 2005a, p.27] and advised to include the results of the risk assessment as part of specifications for turbine and equipment manufacture, installation and operation.

2.8.2 Performance Improvements in Icing Conditions

Despite the many risks associated with operating wind turbines in cold climates, there is a potential ability to effectively and efficiently harness the abundant energy in cold wind. The power of a turbine is governed by various design parameters. In cold climates and adverse icing conditions, the wind turbine must be able to maintain ideal performance characteristics by reducing the adhesion of ice to the surface of the blades, thereby preventing ice accumulation or enabling the accumulated mass to shed from the blade surface. Through mitigation efforts to prevent or at least delay ice accumulation on the blade, the wind turbine is able to perform comparatively to turbines in more favourable conditions.

2.8.2.1 Droplet shedding

The ability of a droplet to not adhere, but rather shed from a surface is critical to mitigating ice accumulation and improving the resulting performance of the wind turbine. The contact angle at which the liquid/vapor interface meets the solid surface indicates the wettability of a surface, which is controlled by three main factors—surface energy, surface roughness, and homogeneity. Surfaces with a high degree of roughness and low surface energy show super-hydrophobicity [Mohammadi 2004]. For such surfaces, water droplets rest on the surface without actually wetting to any significant extent. A *hydrophobe* refers to the physical property of a molecule that is repelled from a mass of water [Wikipedia 2006]. Water on a hydrophobic surface will exhibit a high contact angle. In accordance with physical laws, matter seeks to be in a low-energy state and bonding reduces chemical energy. Since water is electrically polarized, it is able to form hydrogen bonds internally, providing its many unique properties. However, since hydrophobes are not electrically polarized and unable to form hydrogen bonds, water repels hydrophobes, in favour of bonding to itself. Thus, hydrophobic surfaces are extremely difficult to wet and prompt high contact angles with water to form. Highly hydrophobic surfaces have large contact angles in the range of 70 to 90 degrees, whereas super-hydrophobic surfaces have contact angles greater than 90 degrees, as high as 150 or even 180 degrees [Mohammadi 2004, Wikipedia 2007]. Figure 2-18 depicts the contact angle between a liquid droplet and a surface.

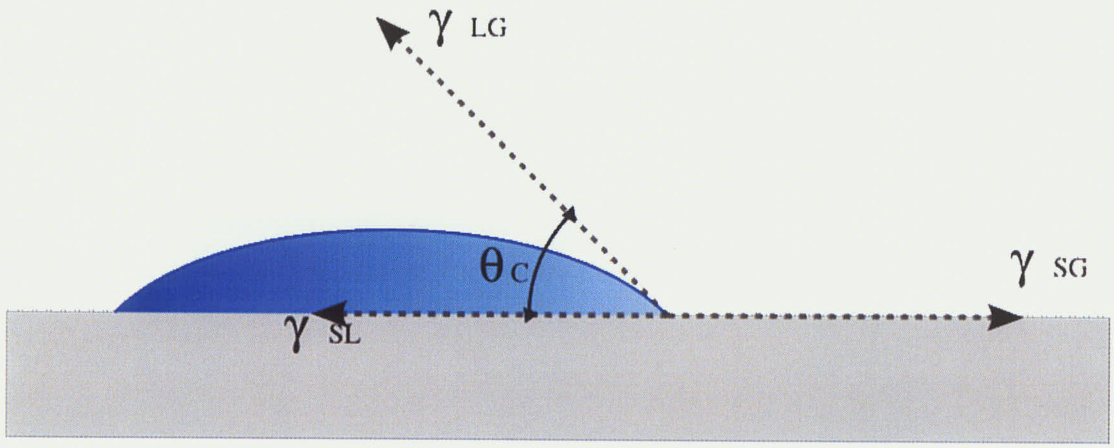

Figure 2-18: Liquid droplet showing contact angle less than 90°

The premise of the ice-phobic surface is the same. By creating the very high contact angles with water, the droplet is shed before it can freeze and adhere to the surface. Once a droplet can not readily adhered to the surface, normal aerodynamic forces may be sufficient enough to remove the droplet from the surface and prevent ice accumulation.

Furthermore, droplets or ice may be shed when the force of bonding at the interface is reduced and normal aerodynamic forces act upon and remove the accreted mass. A means to reduce the bond at the interface is through thermal mitigation methods in which the generated heat is conducted to the ice-substrate interface, where a thin film of water is formed. This breaks the adhesive bond between the ice and the outer surface so that the ice can be swept away by the aerodynamic forces [Thomas 1996].

2.8.2.2 Reduction in Adhesion Force

Reducing the force of ice adhesion from a surface is a key factor to improving the ability to shed ice with ease. As investigated by the B.F. Goodrich Company [Loughborough 1952], the force of adhesion of ice on a flat plate is approximated to be linear with temperature, increasing 8.5 psi or 5,976 Pa for each degree centigrade decrease in temperature, such that assuming a blade surface temperature of approximately -10°C, corresponds to an ice adhesion force of 85 psi or 59,760 Pa. The significance of this value indicates that a reduction in the adhesion force of the ice would greatly improve ice shedding and the resulting performance of the turbine. Due to limited information regarding testing of ice adhesion force on a curved surface, an important objective of this experiment was to develop a method to measure the adhesion force of ice on the curved aerofoil surface at the experimental temperature. In order to do this, a test apparatus and method was developed that enabled the measurement of ice adhesion force on a curved surface to be conducted in the UMITF immediately after a simulated icing event. Although this was not the primary objective of this experimental research, it is a significant contribution to the field of experimental icing measurement.

2.9 Overview of Current Blade Icing Mitigation Measures

Current techniques for ice shedding from aerofoil blades are commonly found in literature related to aerospace and aircraft applications. These methods include anti-icing and de-icing techniques ranging from freezing point depressants and surface deformation, to thermal melting [Fitt 2001]. Typical thermal systems either use hot compressor gas, hot exhaust gas, hot oil or electrical energy. Since hot oil is not a clean, light-weight option, and the use of excessive electrical energy would defeat the purpose of generating electricity, these methods are not viable options for wind turbines.

Furthermore, electro-thermal heaters are commonly used as well. The heat generated by these methods is conducted to the ice-substrate interface, where a thin film of water is formed. This breaks the adhesive bond between the ice and the outer surface so that the ice can be swept away by the aerodynamic forces. Additionally, cycling of the heater power helps to control and reduce energy requirements [Thomas 1996]. Inflatable devices have also been experimented with in the past; however, their complexity and added weight are not ideal for wind turbine systems.

An investigation of the issues associated with overall operation of wind turbine component in cold climates was conducted, and involved experimental testing of one type of thermal blade anti-icer and an analytical assessment of the thermal anti-icing method [Lacroix, 2001]. This study confirmed that without protection, ice accumulates at the leading edge and pressure side of the aerofoil, reducing power production, and concluded that a complete wind turbine ice protection system should include mitigation techniques and sensors for ice and temperature monitoring.

2.10 Icing Mitigation Technology

This thesis explores three icing mitigation strategies: surface, thermal and the combination thereof, termed *thermface* mitigation. The designation, *thermface,* is an original term created as part of this thesis to represent the novel mitigation strategy developed in this thesis.

2.10.1 Passive Mitigation

Passive methods use the inherent physical properties of the blade surface to eliminate or prevent the presence of ice. Passive techniques do not involve any visible or active participation in the mitigation.

2.10.1.1 Surface Mitigation Methods

The appeal of a surface mitigation strategy is that it requires the least amount of direct energy, yet can effectively control icing since it takes advantage of the physical properties of the blade surface. A surface mitigation method has the ability to reduce the adhesion force of ice on the surface and initiate the prevention, or delay the onset, of ice accretion. Numerous papers [Nushi 2003, Laforte 2002, USACE 2003, and Garti 1995] have been reviewed for non-stick coatings that exhibit the characteristics of wear resistance, durability and low ice adhesion, as well as availability and safe application—factors that are important to wind turbine applications. The correlation between the influence of a high contact angle for droplets on a surface and their enhanced ability to shed from the surface has been studied and revealed to highly influence the ability of a coating to be hydrophobic or ice-phobic [Mohammadi 2004]. This characteristic has remained important in the selection of ideal coating candidates for testing. Over 15 coatings, commonly available or highly recommended in related applications, have been reviewed in detail. Figure 2-19 lists several of these coatings in comparison to their ice adhesion reduction factor. Some of the coatings, despite their high reduction factors, have been rejected from this experiment due to their irrelevance to the applications of wind turbine blades—greases and lubricants are not viable options. The remaining potential candidates have been evaluated on relevance to application, physical properties in terms of adhesion reduction, and availability.

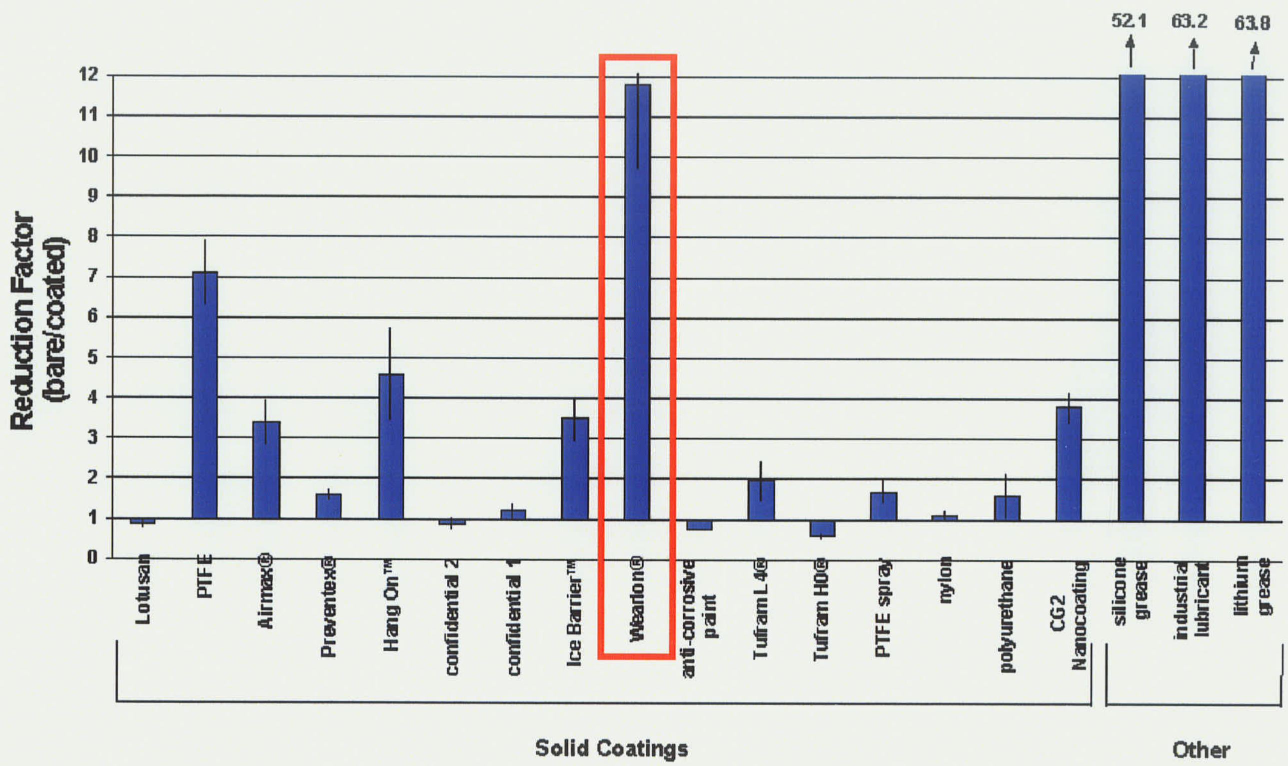

Figure 2-19: Centrifuge Ice Adhesion Reduction AMIL's Results [AMIL 2006]

As is shown in Figure 2-19, Wearlon has the highest reduction factor, thus the following have been short listed as potential candidates for testing, due to their compatibility with mitigation objectives:

- Wearlon super-icephobic
- Wearlon super-hydrophobic

- Tufram L4
- Tufram H0

Since the icing environment is highly erosive, Teflon has been ruled out due to its lack of wear resistance capability. Tufram coatings are primarily used for aluminum components as a means to enhance the surface hardness, wear and corrosion resistance and permanent lubricity. Despite their benefits of adherence and impact resistance, non-stick properties, hydrophobicity and extreme weather resistance, these coatings were not selected for this experiment since the information presented these coatings as more compatible with metallic substrates than those used in the wind turbine blade industry [Tufram 2002].

Wearlon is a water-home block-copolymer chemistry that grafts silicone to an epoxy backbone. The properties of the coating can be adjusted by controlling the ratio of silicone to epoxy. The silicone is the non-stick, hydrophobic, lubricious and soft component while the epoxy contributes to the hardness and the adhesion [Wearlon 2005a, 2005b]. Wearlon describes its hydrophobic coating as having high contact angles with water of greater than 90 degrees, low surface energies of less than 40 dynes/cm, and excellent spreading with organic solvents. The icephobic coating is a two-component water based silicone epoxy with increased silicone that enhances the non-stick ice-phobic properties. It is designed for applications that require more non-stick ability without heavy abrasion, and thus is slightly softer than its hydrophobic companion; however, it contains additives that reduce the inherent slip of the polymer. Both the icephobic and hydrophobic coatings are water-based systems. The correlation between a high contact angle for droplets on a surface and their enhanced ability to shed from the surface is highly influenced by the ability of a coating to be hydrophobic or ice-phobic [Mohammadi 2004].

Therefore, only the following have been selected for experimentation, for their favourable characteristics in icing conditions: Wearlon *Super-Icephobic* and *Super-Hydrophobic.* The icephobic coating is designed to perform best in icing conditions, whereas the hydrophobic coating is designed for repelling water droplets.

2.10.2 Active Mitigation

The active methods require physical action during the mitigation process to eliminate or prevent the presence of ice. Active ice protection techniques can involve anti-icing and de-icing methods. Anti-icing prevents or delays the formation of ice while de-icing attempts to remove the ice once an amount has accumulated.

2.10.2.1 Thermal Mitigation Methods

The thermal mitigation method involves the application of a heated membrane to the surface of the blade. The heating of the membrane is actively controlled such that either anti-icing or de-icing regimes are created. Due to the limitation of traditional thermal mitigation methods for aerofoils and the desire for innovative solutions, new technology for thermal mitigation was investigated. The technology of Thermion® heaters was originally developed for the aerospace industry. Thermion flexible heating material is a thin, conductive textile consisting of nickel coated carbon fibers formed into a non-woven fabric. A magnified view of Thermion material is shown in Figure 2-20, depicting millions of conductive fibres. It is manufactured using a specialized paper making technology that produces a fabric of controlled material weight, thickness and electrical resistivity.

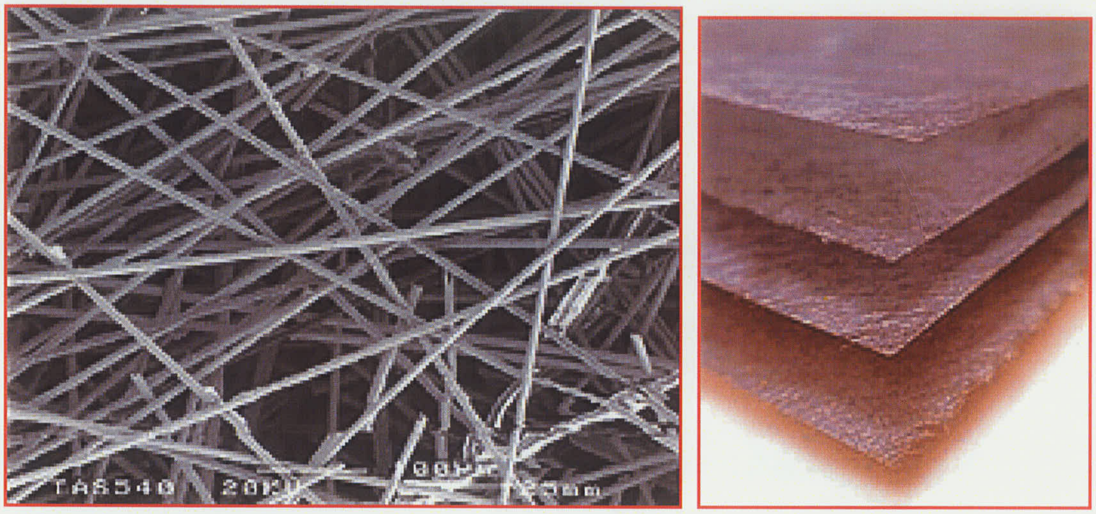

Figure 2-20: Magnified view of Thermion material [Thermion 2005a]

A Thermion heating element can replace most conventional foil or wire elements with a continuous, precise source of uniform heat across a small or large area for a fraction of the cost. Thermion flexible heating elements provide improved thermal uniformity, and low thermal mass such that the heaters are extremely responsive in heat-up and cool-down cycles. Figure 2-21 depicts Thermion heating in contrast to traditional methods.

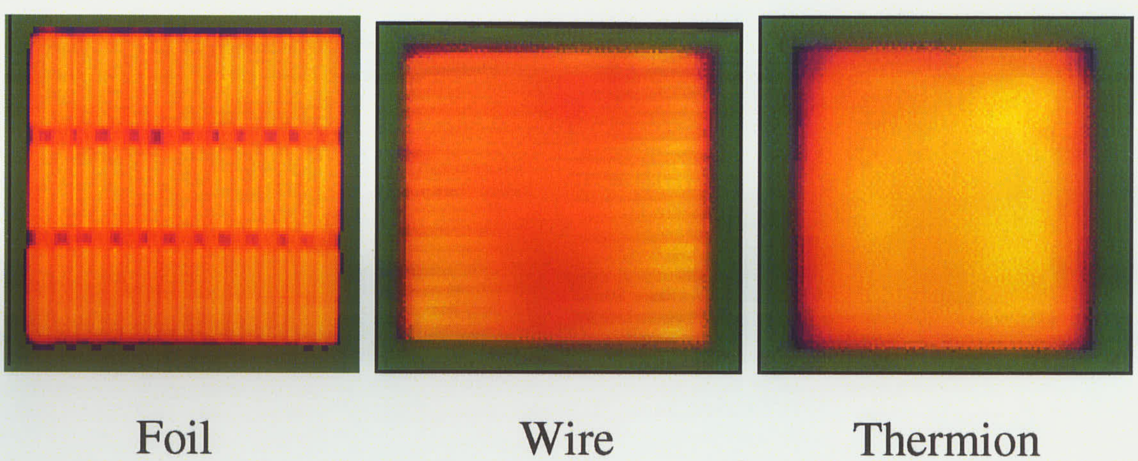

Figure 2-21: Thermal images of temperature uniformity [Thermion 2005b]

Furthermore, Thermion® heaters are highly resistive to mechanical damage and thermal fatigue because they do not rely on a single conductor and thus can withstand harsh environments [Thermion 2005c]. Thermion® heaters successfully underwent rigorous testing in the NASA-Glenn Icing Research Tunnel as part of the Rotorcraft Industry Technology Association (RITA) multi-partner rotor blade ice protection program. This successful demonstration of the Thermion technology has led to a number of programs with military and commercial rotorcraft manufacturers. Many of the benefits of the Thermion heaters are drawn upon in rotor blade leading edge de-icing applications due to the particularly harsh operating environment.

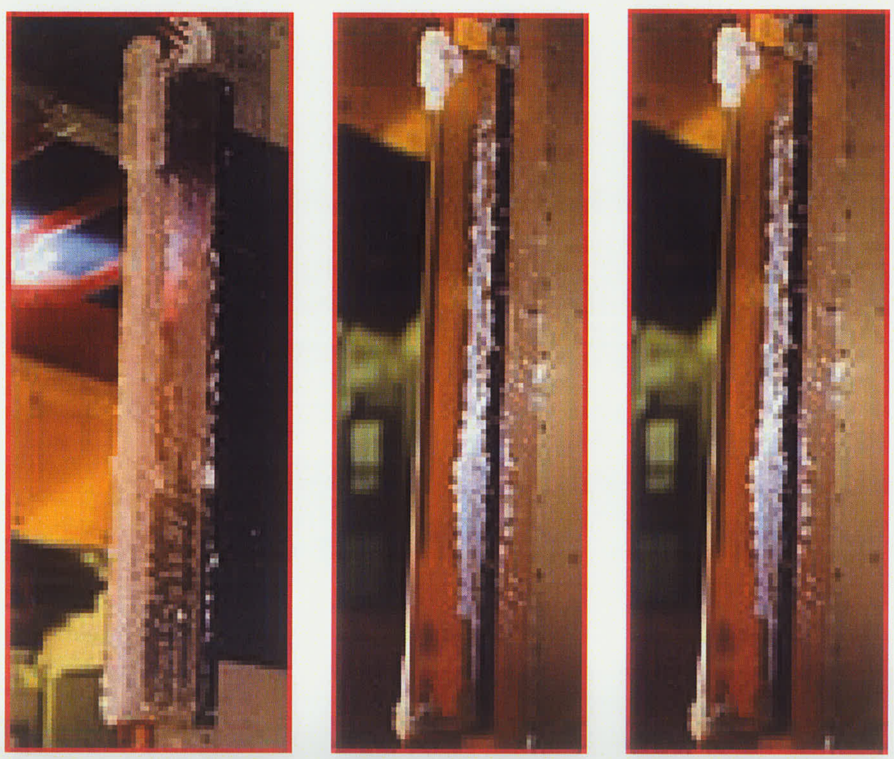

Figure 2-22: Heaters in NASA-Glenn icing research tunnel [Thermion 2005d]

2.10.3 Combined Mitigation Methods

Currently, there is little information about the combination of mitigation strategies and the definition thereof. By definition in this research, combined mitigation methods involve mitigation strategies that directly act upon the ice, such as the combination of blade coatings and blade heating, and are referred to as "direct" mitigation, as opposed to indirect methods which do not directly act upon the ice itself, for example, methods that work to detect the need for icing mitigation, such as sensors. The only reference to a similar means of mitigation as involved in this study includes the turbines in the Yukon Territory on Haeckle Hill in which black ice-phobic coating and heated blades are used for mitigation [Maissan and Kraj 2007a]; however, the particular design is dated and does not incorporate the combination of hydrophobic coatings with the new heater design, as in this study.

Furthermore, there is a general regard that [Maissan and Kraj 2007a] an indirect method combined with a direct mitigation method suffices to be labeled as a combined mitigation strategy; however, as an important clarification for the future development of combined mitigation strategies, this would not be a truly descriptive definition, since the use of an indirect method, such as a sensor for ice detection does not act to mitigate the ice itself. Thus, caution is raised for such a definition and in the interpretation of combined mitigation methods as described in research that implements any indirect method, such as ice detectors through sensors [Peltola 2003, Vattenfall 2001, Norling 2000] or cameras [Cattin 2005] with a direct method, such as blade heating (electro-thermal or hot-air), coatings or pneumatic control, since only a single direct method is used, and is not a true direct combined mitigation method, as is presented in this research.

Additionally, it has been observed that a single mitigation strategy alone, such as coatings, is not sufficient enough to combat the effects of icing on a turbine blade [Kimura 2003] and from experimental experience that the electro-thermal blade heating strategy provides serious advantages as a direct mitigation approach [Botura 2003, Maissan 2006], which emphasize the potential in combined mitigation methods and the need to develop this strategy further.

2.11 Summary of Icing Research Studies

The icing research studies presented in the previous section are summarized in Table 2-3, in the following pages.

Table 2-3: Summary of icing research studies 1990 to 2007

Study	Measurements	Conditions	Findings/comments
Ahti, 2005	-Ice load forecasts in Finland, -defines 4 ways of ice accumulation on a structure	-for rime: temperatures below 0 Celsius; object in fog or cloud -for wet snow: +0.2-0.8 Celsius; heavy precipitation	1.rime aggregation (in cloud icing) 2. icing precipitation 3. wet snow 4. water spray icing in sea areas
AMIL 2006	-Various icephobic coatings evaluated for ice adhesion reduction -Centrifuge for testing	-controlled centrifuge cold chamber -adhesion force measured by centrifuge effects	-reduction factor provided for various coatings
Antikainen 2003	-Modeling, verification and classification of ice loads in wind turbines -meteorological -turbine -loads -tools	-data taken from measurements on wind turbine at Pyhatunturi, Finland and another at Suorva, Sweden. -uses TURBICE and ADAMS/WT for modeling	-dynamic modeling for various ice shapes, masses and configurations -results verified by measurements
Battisti, 2005	Evaluation of anti-icing energy and power requirement for wind turbine rotors in cold climates	-model for estimation of anti-icing heat requirement and power required to operate thermal IPS	-yearly energy required to heat blades -anti-icing power demand -by probability distributions of site meteorology parameters
Bose 1992	-Horizontal-axis wind turbine in Newfoundland -3-D ice formation on blade -Glaze ice	- 1 m blades - 0 to 4 m/s winds - 0°C temperatures -natural freezing precipitation	- Characterization of blade rotation effect on ice accumulation - obtain data during actual icing event
Botura 2003	-Development of ice protection system for wind turbine applications -Goodrich Corporation De-icing and specialty systems	-pneumatic de-icing system -lab test rig for 100-ft blades-Goodrich icing wind tunnel -electro thermal ice protection system, preliminary work	-capability of Goodrich DSS to transition aircraft ice protection to wind turbines -pneumatic system is effective for ice control -electro thermal for further investigation
Cattin 2006	-Alpine test site Gutsch: monitoring of a wind turbine under icing conditions in Switzerland	-blade heating by hot air -ice detection involved as improvement to mitigation -safety risk of icing	-ice throw is a safety issue -not all ice can be removed from blades by the heating process -Ice detection by combined methods
Chaîné 1974	-Wind and ice loading in Canada	-series of topographical maps of icing regions	-icing regions of Canada
Dursetwitz 2003	-On-site cold climate problems, -Central Europe	-hands on experience from operators and research results	-insight to amount of time which effects turbine operation -examples of on-site problems of operators and equipment

Study	Measurements	Conditions	Findings/comments
Fitt 2001	-De-icing by slot injection -injection of hot fluid through slot in plate to remove ice from a plate in a cold cross flow	-aviation industry, ice on aircraft wings -aerofoil theory used -flow and energy eqns	-nonlinear singular integro-differential eqn, coupled to convection/diffusion eqn and Stefan condition -numerical soln for several cases
Ganander 2003	-Design load aspects due to ice loading on wind turbine blades -structural dynamics and turbine safety due to ice loads	-2-parameter ice model -measurements taken at Suorva wind turbine	-identification of type of ice conditions -fatigue loading, prelim results
IEA 2005	-Wind energy in cold climates -collate information on available adapted wind turbine technology and to formulate recommended practices	-site assessment -follow up measurements -estimation of production losses -measured performance of anti- and de-icing methods	-current international status on cold climate characterization for wind turbines
Kimura 2003	-The effect of anti-icing paint on the adhesion force of ice accretion on a wind turbine blade -commercially available water repellents and coatings	-wind tunnel tests; load tests conducted -2D aerofoil -supercooled liquid water droplets -sub-zero temperatures	-prevention of icing on wind turbine blades could not be effected by a single coating alone -icing occurs even on coated surfaces -adhesion force reduced when repellent agent used
Kimura 2000	-Estimation of reduction of power production due to icing from the existing meteorological data -method to estimate power production in icing areas	-wind tunnel test on aerofoil model -ice imitations Measure effects of ice deposits	-calculation of duration of wind speed, classification of ice by a code of meteorological data -power production
Kraj 2006a – 2006e	- stationary horizontal aerofoil in icing tunnel - simulated icing events - glaze and rime ice - heaters and coatings	- 0.5 m aerofoil NACA 63421 - 0 to 30 m/s - -20°C to 0°C	- measured adhesion force on curve surface - developed thermface mitigation technique -characterized icing phenomena
Laakso 2005a	-Expert group study on wind energy projects in cold climates -IEA member countries contribute	-site considerations -measurement programs -project design -installation -operation and maintenance -decommissioning -public safety	-provide solns for the cold climate specific challenges and reduce cost of wind energy by lowering social, technological, economic risks
Laakso 2003	-State-of-the-art of wind energy in cold climates, -IEA member countries contribute	-international collaboration on gathering and providing information on wind turbine icing and low temperature operation -monitor technology and establish guidelines	-SOTA arctic wind energy presented -knowledge on climatic conditions and resources, technical solns, operational experience
Laakso 2005b	-Review on blade heating technology and future prospects	-hot air heating -electrical surface heating element -analyze range of both heating methods	-market prospects summarized -theoretical capability of the heating methods reviewed based on theoretical calculations

Study	Measurements	Conditions	Findings/comments
Laforte 2002	-How a solid coating can reduce the adhesion of ice on a structure	-7 solid icephobic coatings -ice density -hydrophobic character -roughness surface characteristics -coating degradation after 7-8 de-icing operations -UV radiation -metallic surfaces	-reduction of 37% adhesion force by most efficient icephobic coatings -weak deterioration of surface coating slightly reduces ice adhesion, related to roughness of coating and not hydrophobicity
Loughborough 1952	-Physics of mechanical removal of ice from aircraft -approximation to stresses produced on a de-icer surface	-calculate value for adhesion of ice to rubber -defines the adhesion problem -adhesion to rubber surface	-lower adhesion produced by silicones results from breaking of the silicone film -states that adhesion force is linear with temperature
Maissan 2007	-Memoire CCVK 58 IEA Annex XIX – Short Version	-outline of the proposed project to organize collected data on WTs in CCs	-Lists sites with icing and gives site characteristics
Megateli 2006	-Meteorological and metrological characterization of icing events	-icing event characteristics listed -icing factors include, barometric pressure, wind speed, air temperature, relative humidity	-summarizes icing events typical environmental parameters -instrumentation efficacy & icing events
Morgan 1998	-Assessment of safety risks arising from wind turbine icing	-authorative set of guidelines -risk assessment methodology developed	-risk of being struck by ice thrown from WT is small at distances greater than 250m in moderate icing climate
Norling 2000	-Suorva—artic wind turbine in northern Sweden -100km north of the Arctic Circle -Bonus Mk IV, 600KW output, 44 m diameter -rotor speed of 27 or 18 rpm -3 blades have JE-system heating of carbon fibre surface on outer part of blades -heating regulated by control system from ice detector and thermistors	-tackles uncertainties of WT operation in northern climates -public acceptance -environmental impact -acoustics -power performance -icing -availability -OM costs -icing conditions of relative humidity 95%, temperature below 0C, occur 2-4% of the time	-High-power-effect problems solved by turning blades 1.5 deg., and using stall strips -lowest temperature to date -37C -energy demand for de-icing less than 3%
Peltola 2003	-Prevention of icing effects -current status of adapted technology reviewed -blade heating system developed in Finland -heating systems in different climatic conditions	-heating energy consumption -reliability -effects of blade heating system -long-tem power performance -theoretical calculations and analyses	-icing deteriorates energy output -custom designed carbon fibre blade heating elements -JE-System consumed 1-4% of annual energy production

Study	Measurements	Conditions	Findings/comments
Rissanen 2005	-Modeling and measurements of dynamic loads of an arctic wind turbine -3 commercial programs used together for continuous and simultaneous simulation -measurements provided from Olos wind farm	-2 simulation examples given -ADAMS used for modeling turbine dynamics -PSCAD/EMTDC used to model electrical components -Matlab/Simulink used to combine simulations	-icing effects on WT performance addressed -simulation environment now suitable for grid fault sims and icing studies -control and condition monitoring systems can be simulated with these tools -1Hz power measurements can be used for ice detection
Seifert 2003a	-Risk analysis of ice throw from wind turbines -icing during operation, estimates of accreted masses and sizes	-trajectory calculations for various wind speeds -eqns provided for ice throw from rotating and stand-still turbines -risk assessment guidelines provided	-area of risk of an operating turbine in larger than of a stand-still turbine -web cameras useful for visual observations -ice throw needs to be accounted for in the planning phase
Seifert 2003b	-Technical requirements for rotor blades operating in cold climate -various shapes of leading edge icing	-trailing edge icing -blade surface icing -special strategies of operation for different control systems such as pitch, stall, active stall controlled turbines	-recommendation To optimize operation of supervisory systems of blade heating -effects of icing on rotor blades in terms of natural frequencies, blade fatigue, ultimate loads
Thomas 1996	-Aircraft anti-icing and de-icing techniques and modeling	-recommendations for alternate icing mitigation strategies for aircraft; including combined methods -eqns given	-glaze and runback are difficult problems to solve; interactive boundary-layer method recommended
Vattenfall 2001	-Vindmannen—efficient wind power in the mountains -Suorva, Sweden	-discusses extra equipment for operation in CC -blade heating system -heated sensors -ice detector -heated gearbox Low-temperature oils	-cold air increased density provides high generation levels -heating system used to counteract ice formation is successful
Woods 2007	-Ice and wind factors in wind turbine output in southern Manitoba	-geographic considerations -climatic factors -sensing, control, mitigation in CCs -icing maps	-icing is an issue in southern Manitoba -200MW hydro + 1000MW wind power results in wind penetration of 15.3% installed capacity
Yukon Energy, 2004	-Viewing Whitehorse from above: a guide to Haeckel Hill -2 turbines -combined surface and heated mitigation strategies -subject to rime and glaze icing	-Bonus 150KW Mark III -Vestas V47-660KW -normal operating range to -30C	-rime ice is single biggest obstacle to wind power generation -over 100 days of icing -without icing mitigation would result in 25% more loss in energy production

3 INVESTIGATION OF ICING MITIGATION STRATEGIES

3.1 Objective

The objective is to improve the understanding of icing effects and mitigation strategies on wind turbine blades in Canadian cold climates which required:

- Preparation and development of new test apparatus to adapt the current experimental apparatus for wind turbine blade applications
- Calibration of the experimental wind tunnel
- Characterization of icing properties on a normal blade
- Implementation of mitigation strategies
- Development of a new mitigation strategy
- Characterization of icing properties for mitigated blades
- Comparison of the resulting icing properties amongst the mitigation strategies

3.2 Mitigation Strategy

The basis of the mitigation strategy stems from the notion that the bond of the ice to the substrate of the blade is a critical factor in the ability of a chosen technique to effectively mitigate icing. Therefore, the techniques were selected with the intention to improve the resistance to ice adhesion and accretion on the aerofoil surface.

The initial phase of the mitigation study implements a passive technique as an effective solution that employs the natural characteristics of the surface. Subsequently, an active mitigation strategy is investigated in the form of a thermal technique. Finally, the combination of the surface and thermal mitigation techniques results in the creation of a new mitigation strategy, termed *Thermface.* This strategy involves both passive and active elements as a means to optimize the capabilities of the individual surface and thermal strategies.

3.2.1 Stage 1: Surface Mitigation

The initial approach of the mitigation strategy was to investigate a strategy that required the least amount of effort to employ, yet effectively mitigated icing. Thus, the surface mitigation technique was investigated. The correlation between a high contact angle for droplets on a surface and their enhanced ability to shed from the surface is highly influenced by the ability of a coating to be hydrophobic or ice-phobic [Mohammadi 2004].

The following have been selected for experimentation, for their favourable characteristics in icing conditions: Wearlon *Super-Icephobic* and *Super-Hydrophobic.* The icephobic coating is designed to perform best in icing conditions, whereas the hydrophobic coating is catered towards repelling water droplets. The surface mitigation was implemented for the plain, hydrophobic and icephobic samples under both glaze and rime icing conditions.

3.2.2 Stage 2: Thermal Mitigation

Subsequently, an active mitigation strategy was investigated, which employed a non-traditional type of thermal heater. The thermal mechanism is a controllable, lightweight system, compatible with modern composite materials that have been adapted as an electro-thermal ice protection system where heat is generated at the point of use. Thermion® heaters are made from finely dispersed metal coated carbon fibre elements that may be integrated into composite or polymer material structures and are ideally suited for leading edge blade ice protection applications due to their lightweight and uniform heat distribution capability, contrary to traditional wire heaters [Thermion 2006c]. The heat generated by this method is conducted into the ice-substrate interface, where a thin film of water is formed. This weakens the adhesive bond between the ice and the outer surface so that the ice can be swept away by aerodynamic forces. Furthermore, cycling of the heater power helps to control and reduce energy requirements [Thomas 1996], suggesting the use of various thermal regimes to further enhance the effectiveness of the mitigation strategy. By controlling the duration and timing of heat application both anti-icing and various de-icing regimes are explored in both glaze and rime icing regimes. The heated area Watt density of the heater is 775 W/m^2 (0.5 W/in^2).

3.2.2.1 Anti-icing Regime

The anti-icing regime is a means of preventing or delaying ice accretion from occurring on the surface of the specimen, such that the experiment was designed to implement heat at the beginning of the icing test and continue for the entire duration of the icing test, a period of 20 minutes.

3.2.2.2 De-icing Regime

The de-icing regime is a means of mitigating the ice once the specimen has already been exposed to the ice, such that the experiment was designed to implement heat at the midpoint of the icing test, and continue for the remaining duration of the experiment. The heat was initiated at the 10 minute point in the 20 minute experiment and continued for the remaining 10 minutes of the experiment.

In summary:

Anti-icing regime	Heat during entire experiment
De-icing regime	Heat during the second half of the experiment

Note that increased heat flux intensity has the potential to melt the ice causing liquid water droplets to run back along the aerofoil surface, which can lead to ice formations or remitting droplets at the trailing edge and further dynamic complexity of the system.

3.2.2.3 Cost of Thermal Mitigation

The selected and tested Thermion heaters parameters are shown in

Table 3-1. Figure 3-1 provides a visual reference of the sample heater. The requirements and dimensions of the sample heaters and aerofoils have been extended for a full-scaled wind turbine blade representative of the blades at the St. Leon wind farm, such that one turbine blade approximately requires 10.4 kW of power for the heated mitigation, and a single 3-bladed turbine requires 31.2 kW. For a wind farm the size of St. Leon, consisting of 63 turbines, the total required power is approximately 2 MW. Thus, for this 100 MW wind farm, this is only 2% of the wind farm capacity. Since icing mitigation would only be required for a maximum of 6 months of the year, this is more realistically reduced to only 1% of the wind farm capacity.

Table 3-1: Thermion heater parameters

Units	Size	Operating Voltage	Output Power	Heated Area	Heated Area Watt Density
Imperial	2" x 5"	12 V	5 W	10 in^2	0.5 W/ in^2
Metric	0.0508 m x 0.127 m	12 V	5 W	0.00645 m^2	775 W/ m^2

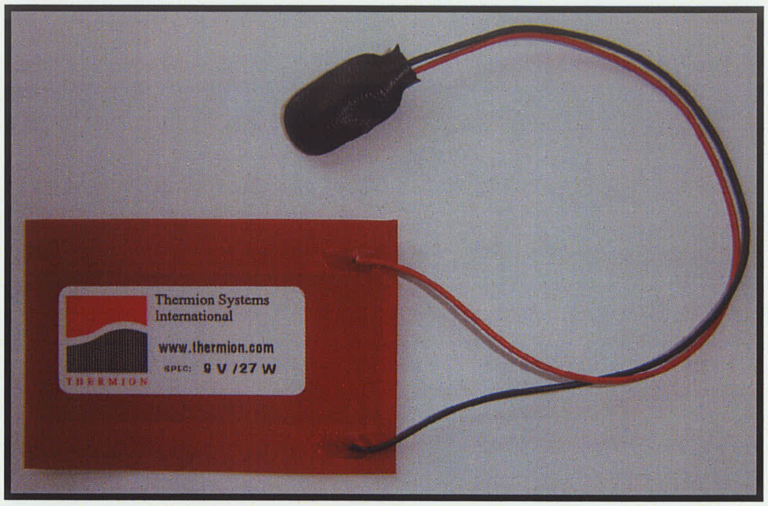

Figure 3-1: Sample thermion heater

Energy production is increased in winter months, due to a colder and denser air mass. This production increase has the potential to offset the cost of the ice-protections heating systems. Since the system would have a protection system, energy production could be optimized by more readily operating the system at critical times rather than stopping production. This could further off-set the cost of the system, such that the system practically pays for the 1% power requirement itself, while enhancing energy production opportunities. Details of the approximated calculation for the cost of thermal mitigation are located in Appendix D.

3.2.3 Stage 3: Thermface Mitigation

The combination of mitigation strategies is explored as means of a more controlled-passive deicing technique, providing insight to the combined effectiveness of these mitigation strategies. The cycling of power for the electro-thermal heaters allows integration with other techniques to optimize mitigation efforts.

3.3 Mitigation Measurement and Analysis

The following section provides an indication of the icing characteristics that were investigated through this project for the various mitigation strategies. Comparison of the various mitigation techniques indicates their effectiveness amongst another in the given conditions.

3.3.1 Profile Shape Changes

Aerofoil profile shape is critical to the aerodynamic optimization of a system in the environment it is to operate. In the case of wind turbines in cold climates, aerodynamic optimization of the system must account for the environmental factors for which it will be exposed. The profile shape dictates the lift and drag that the blade encounters in the flow of the system. The balance of the lift and drag that is imposed on the blade in a flow dictates the resulting aerodynamic performance of the system. A blade aerofoil profile is carefully selected for optimized performance in the system that it will be used. In the case of this study, the NACA 63421, a typical blade profile used in the wind energy industry, is the profile of choice. The surface finish is critical to maintaining laminar flow over the aerofoil as long as possible before the onset of flow separation, as any trip on the surface can instigate turbulence and a resulting loss in aerodynamic performance, which can potentially lead to complete failure. Thus, changes in profile shape due to icing accumulation on the blade surface of a wind turbine are of critical significance to monitor, prevent and control, in order to ensure optimized performance of the system. The collected leading edge (LE) profiles provide an indication of ice shape, symmetry and consistency.

3.3.2 Adhesion Force

Adhesion force is of critical significance in developing an effective mitigation strategy. To properly understand how to mitigate the effects of this significant force, it is necessary to understand how the adhesion of ice behaves on the curved surface of an aerofoil. Due to the limitations of previous knowledge on the topic of adhesion force on curved surfaces, a new test apparatus was developed specific to the specimens of this research project. From the information gathered, a knowledge base was developed that characterizes the force with which the ice adheres to the curved LE and provides an indication of the mitigation intensity that is required to alleviate the adverse effects of ice adhesion.

3.3.3 Accumulation Amount

The ice specimens were melted for a liquid volume measurement to gauge the amount of water that had accumulated along the leading edge. The results provide an indication of the mass of the ice accumulated on the leading edge surface, and indicate the potential load concerns for the turbine blades which can lead to power losses.

3.3.4 Accumulation Rate

Collected image data was processed using graphics software to determine changes in ice accumulation rate. The results provide an indication of the rate at which ice accumulates on the surface in a given test condition, dependent on climatic condition and mitigation strategy. This accumulation can also be interpreted as ice thickness at the leading edge. The results also provide an indication of the intensity of the mitigation strategy that is required to effectively control the adverse effects of ice accumulation.

Figure 3-2: Accumulation on leading edge of aerofoil in test chamber

3.3.5 Profile Shape Extension

Ice growth at the leading edge of the blade aerofoil results in length changes which influence the aerodynamic properties of the blade. As the profile shape extends, it lengthens the chord of the aerofoil which leads to greater planform area for lift to act upon; however, due to the inconsistent extension along the length of the blade, uneven lift patterns result and lead to harmonic imbalances and aerodynamic losses. Despite the expanded blade area, undesirable effects on turbine solidity can also result. Image data was processed to obtain the amount of LE extension due to ice accumulation, thereby characterizing the severity of the negative impact that the shape extension parameter may impose.

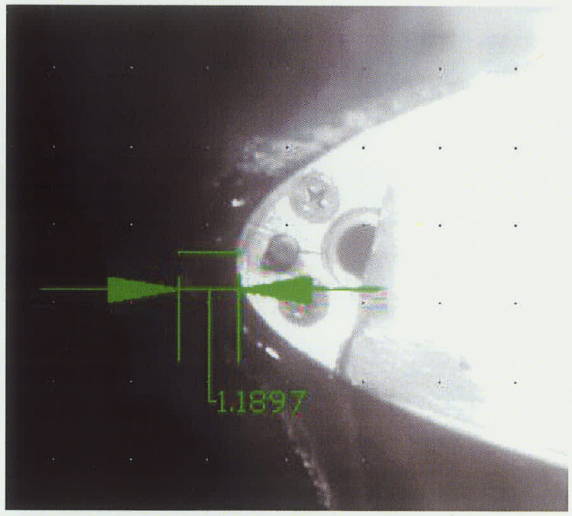

Figure 3-3: Leading edge profile extension measurement in AutoCAD

3.3.6 Profile Shape Catalogue

Collected image data is compiled into a catalogue referencing ice LE profile growth for each icing event and related mitigation strategy. It is summarized into images at the beginning, mid and end point of the test duration (0, 10, 20 minutes). The catalogue provides an indication of the resulting ice accumulation among the various mitigation strategies and allows for visual interpretation of the icing event.

3.3.7 Mitigation Forecasting Tool

The MFT is a compilation of resulting test data that can be compared amongst itself prior, during or after an icing event. It provides an indication of what is occurring among the various icing characteristics during an icing event, which can be used to gauge the mitigation intensity that is required to control a specific icing characteristic in comparison to other characteristics for the various strategies.

4 EXPERIMENT

The University of Manitoba accommodates a unique experimental facility for aerodynamic icing research. The capability and size of this facility make it exclusive in Canada, the only exception being the NRC research facility in Ottawa. Previously, the facility was intended to be used for power-line icing and helicopter intake icing research, and through this research project, has been expanded to wind turbine blade icing research. Since the basis of this research work is experimental, all collected data and results are produced within the limitations of the following experimental design.

4.1 Facility

Icing experimentation is performed in the Icing Tunnel Facility located in the Engineering Complex at the University of Manitoba. The UMITF consists of a spray system to emit droplets into the flow and a refrigeration system for cooling of the air as shown in Figure 4-1 [Naterer 2002].

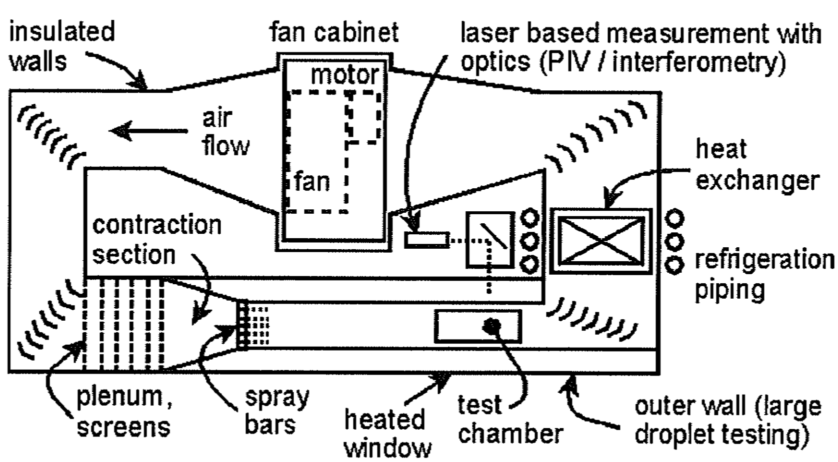

Figure 4-1: Top view of spray flow and icing tunnel

Experiments are conducted using stationary aerofoils placed within the inner duct (1 m^2) of the wind tunnel. Scaled test specimens are subjected to cooled airflows containing water droplets that are released into the flow stream from a customized spray bar located upstream of the aerofoil test piece.

Air atomizing nozzles can produce a reliable spray pattern with water mean droplet diameters ranging from 10^{-3} to 10^{-5} meters, per manufacturers specifications for the nozzles employed in the UMITF facility. The droplets travel in a trajectory towards the test specimen, are cooled along the way and freeze upon impact with the test specimen forming various ice shapes and characteristics, according to the climatological conditions of the conducted experiment.

4.2 Wind Tunnel Calibration

The calibration of the wind tunnel was not previously performed for the system. Thus, a series of tests were conducted to obtain data on the wind speeds at varying temperatures within the inner duct of the tunnel where the icing experiments were to take place. A pitot tube-manometer was placed upstream, while a 3-cup anemometer with digital output was placed further downstream. The resulting readings were statistically accurate, verifying the calibration of the system and identifying particular wind speeds at specific temperatures. The wind tunnel parameters set for this calibration involved a range of motor frequencies between 8 to 40 Hz, and a range of temperatures between +25 °C to -30 °C resulting in a range of calculated actual wind speeds between 3 and 24 m/s, depending on the motor setting and correlating tunnel temperature. The resulting values are located in Appendix A. The pitot tube-manometer instrumentation is a more accurate method of measuring flow rates than the 3-cup anemometer; however, the results accurately collapse to follow similar curves between both methods, which validate the wind speed measurement. The only inconsistency to directly affect the reading of the 3-cup anemometer may have been the pitot-tube located upstream; despite its placement at a distance such that it had minimal impact on the following anemometer. Furthermore, the spray bar upstream of the Pitot tube disturbs the flow; however, since the spray bar is part of the icing tunnel functionality, its position remains constant throughout experimental testing, thus, the impact it has remains constant on the flow through the tunnel and is a negligible factor for this particular experiment.

4.3 Experiment Design

The following section describes the experimental components and apparatus in the design of the mitigation strategies.

4.3.1 Scope

This experimental research project is the initial work of any contribution to the topic of icing mitigation strategies at the University of Manitoba, thus foundational elements to understanding the problem of icing on wind turbine blades needed to be developed; however, there was also a drive to understand icing mechanics, and if possible, to make a contribution towards the development of a new mitigation strategy. Furthermore, the experimental apparatus was never previously used for this application and the modification of the experimental apparatus for this icing application, including calibration of the system, was required.

To understand the fundamental dynamics of the complex three-phase system, the initial phase of the experiment was designed to minimize unnecessary variables. Thus, rotation dynamics were not investigated and the blade specimens were held in a fixed stationary position. From the literature review at the time of experimental design, information about the effect of the angle of attack of the blades on icing mechanics was limited. Thus, in order to develop a fundamental understanding of the problem within the scope and time frame of the project, a single angle of attack was selected for testing. To keep the problem simplified, a zero angle of attack was used with the stationary blade specimens. It is understood that zero angle-of-attack is not completely realistic, but was necessary to eliminate unnecessary variables and develop a baseline for further work.

Two distinct icing types were selected, glaze and rime, which occur under distinctly different conditions, most notably by temperature. The combination of icing types was not directly explored, as this would extend beyond the time frame of the project.

The surface mitigation strategies were limited to three different surfaces; one remained a datum, while the two others were different type coatings.

The thermal mitigation was limited to a single technique; however with two different heating regimes: anti-icing and de-icing.

The combinations of these techniques lead to the development of a third mitigation strategy, termed *Thermface*, resulting in 18 degrees of freedom to analyze. Thus, one can understand that adding just another variable, such as a different angle of attack would increase this system to 36 degrees of freedom, and the complexity is imminent in scale.

Due to the nature of the ice, all test measurements needed to be taken immediately after the icing event, some at experimental temperature, while the measurements that could be taken during an event were as such, completed per test.

4.3.2 Climatological Conditions

The two distinct types of icing regimes are glaze and rime, and have been selected for this experiment. Glaze ice occurs at temperatures near the liquid freezing point, in atmospheric conditions of high liquid water content, creating an ice that is clear and dense. Rime ice occurs at colder temperatures of lower liquid water content freezing before contact with the substrate, then accumulating with air pockets in between, forming a white and feathery, but less dense type of ice. From the wind tunnel calibration, the climatological conditions for testing were selected based on the parameters that created the most representative climatological conditions for glaze and rime icing.

In the UMITF, to obtain glaze and rime icing with a wind condition representative of climatological conditions in the region of interest, the experimental testing required the motor to be fixed at 15.5 Hz which corresponds to 7.37 m/s at -5°C and 7.97 m/s at -15°C, for glaze and rime conditions, respectively. Other parameters that needed to be balanced to ensure these icing conditions could be properly simulated included water liquid-line temperature and air-line pressure for the air atomizing nozzles to create the ideal Liquid Water Content (LWC) for the system. An imbalance in LWC can create too "wet" or "dry" an ice, and must be balanced with the flow speed and distance to the object that is subjected to icing in order to ensure the liquid properly cools and does not prematurely evaporate or solidify before contact with the specimen substrate, as all these factors contribute to the resulting ice form and characteristics.

4.3.3 Experimental Parameters

An icing event is characterized by several naturally occurring parameters such as barometric pressure, wind speed, relative humidity and air temperature. For a simulated icing event in controlled conditions, these parameters along with other conditions must be set and closely monitored to ensure the icing event occurs as required. In icing related applications, the actual droplet size distribution in clouds is represented by a single variable called the droplet's median volume diameter (MVD). The MVD is the midpoint in the liquid water content (LWC) distribution over the range of cloud droplet sizes that are present in a given moment of time. Thus, the MVD varies with the number of droplets in each size category. The overall average LWC and MVD have been conservatively approximated for this experiment in accordance with published data [Battisti 2005] and the properties of the air atomizing nozzles in the spray bar apparatus of the UMITF to represent icing droplet concentrations and sizes that are slightly greater than those of a freezing fog or stratiform cloud and lesser than those of a convective (cumuliform) cloud. For this particular experimental design, the set parameters for simulated climatological conditions, along with the limitations of the aerofoil test specimen geometry are listed below in Table 4-1 where LWC and droplet diameter are approximated based on manufacturer's specifications for nozzle performance.

Table 4-1: Experimental Parameters

Parameter	Value
Experimental equipment conditions	
Spray bar water flow (m^3/s)	9.46
Spray bar water temperature (°C)	1.89
Spray bar air pressure (Pa)	344,737
Wind tunnel set velocity, v_t (Hz)	15.5
Test specimen parameters	
Chord length (m)	0.5000
Aerofoil specimen width (m)	0.06350
Angle of attack (degrees)	0.00
Weather conditions for glaze icing	
Liquid water content, LWC (kg/m^3)	0.0028
Diameter of droplet, d (m)	0.00001
Freestream temperature, T_i (K)	268.0
Freestream pressure, P_o (MPa)	0.1013
Measured local wind velocity, V_w (m/s)	7.37
Weather conditions for rime icing	
Liquid water content, LWC (kg/m^3)	0.0028
Diameter of droplet, d (m)	0.000017
Free stream temperature, T_i (K)	258.0
Free stream pressure, P_o (MPa)	0.1013
Measured local wind velocity, V_w (m/s)	7.97

4.4 Apparatus

The experimental apparatus consists of the UMITF, specimen test rig and the specimen mounted within the UMITF.

4.4.1 Test Specimen

The test specimen is based on the shape of a NACA 63421 aerofoil profile with aluminum frame and fiberglass sheeting. The selected NACA profile is commonly used in the wind turbine blade manufacturing industry. For this experimental series, six test pieces with various mitigation strategies were required to investigate the surface, thermal and thermface mitigation strategies. The specimen without a heater or coating was used as a datum. The selected coatings were applied to the aerofoil test specimens using specialized paint application equipment and procedures. The icephobic coated specimen is black, whereas the hydrophobic coated specimen is white, and the plain, uncoated specimen is the original fiberglass composite colour, yellow. The specimens are shown in Figure 4-2 as mounted for testing.

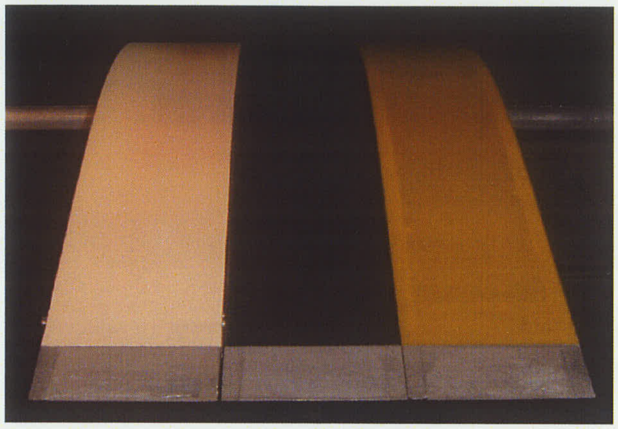

Figure 4-2: Aerofoil test sections: (L-R) hydrophobic; icephobic; plain

All thermally mitigated specimens had two 0.508 x 0.127 m, 12 V / 5 W heaters, mounted on each of the upper and lower leading edge surfaces. All thermface specimens contained both coatings and heaters. Figure 4-3 depicts the red thermal heaters as mounted in the leading edge of the aerofoils.

Figure 4-3: Aerofoil test sections with thermal heater mounted at leading edge

The aerofoil test specimens were mounted at zero angle of attack downstream of the spray bar. The thermal components required wiring to a power source which provided constant heat at full capacity throughout the duration of the test.

4.4.2 Procedure

4.4.2.1 Preparation

In preparation for experimental testing the cooling of the water system must be initialized a minimum of one hour in advance of testing to ensure the water temperature is appropriate for icing. While this occurs, the specimen is prepared in the inner tunnel. The selected specimens are mounted on a rod and fixed in the tunnel accordingly, if heat is to be used, the wires are connected to the appropriate samples. A thermometer is mounted on the inner tunnel duct behind the specimen as a second reference measurement for the temperature in the tunnel. The computer and system for image collection is started and the Flow-Manager data-acquisition software initiated. A light is mounted in the exterior tunnel to provide added light source for photographing the experiment. The windows are cleaned of debris. The camera is adjusted in the frame to ensure proper positioning. The camera lens is focused manually while visually referencing collected continuous images through the software program until the best focused image is achieved. A ruler is attached to the specimen and a photograph taken for calibration of the images. The view reference for specimen scaling is adjusted in the software program accordingly. The ruler is then removed and the surfaces of the aerofoil specimens are cleaned with ethyl alcohol to remove residual oils and grease from handling. The doors are closed and an initial image of the specimen is taken at 0 minutes.

The test procedure is then initialized. An experimental iced specimen is depicted in Figure 4-4.

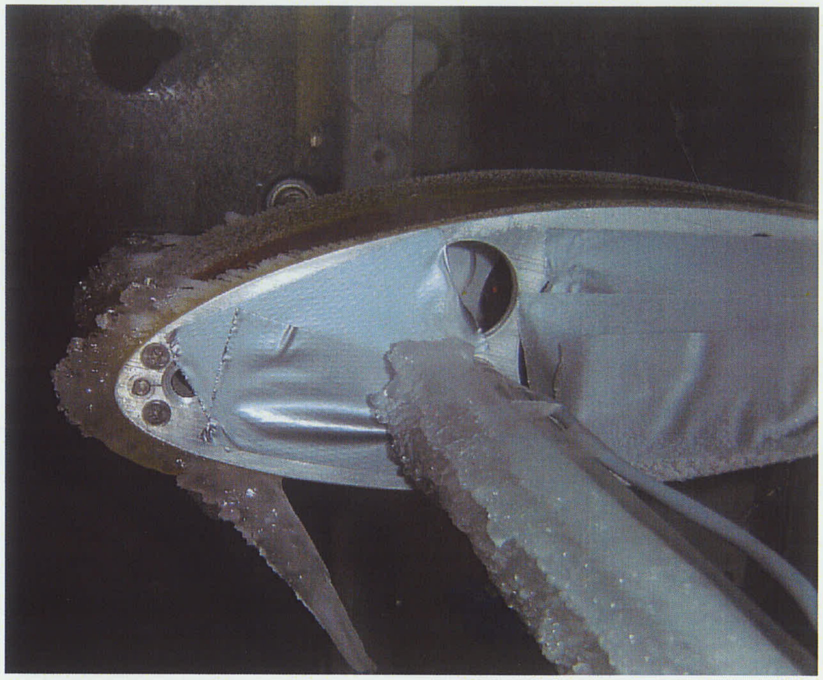

Figure 4-4: Iced specimen in tunnel

4.4.2.2 Test Procedure

All previous safety measures in accordance with the wind tunnel safety manual are performed prior to activating the system. Firstly, the desired temperature for cooling is set on the thermostat followed by initializing the motor of the blower to create a slight wind. The system takes approximately 30-45 minutes to cool, depending on the temperature and wind speed that has been set. In the meantime, the temperature of the water system is monitored to ensure the water has reached the desired temperature and the airline for the spray bar is activated before the tunnel temperature drops below the freezing point to prevent the nozzles from becoming blocked by ice particles. As soon as the desired tunnel temperature is reached, the water system is activated and set to the desired flow rate, at which the nozzles begin spraying. An immediate visual verification is required to ensure that the four nozzles are spraying evenly. Image collection is initiated after 1 minute of spraying and continues each minute, as timed by the clock on the computer, for the entire 20 minute duration of the icing test. If heating is used, then the power source is activated at either the initial point of testing for anti-icing, or at the mid-point of the test duration for de-icing.

Multiple test runs were completed with a minimum of three trials per test strategy. Results were averaged in the analysis of icing characteristics to account for experimental error and natural variations.

4.4.2.3 Post Testing

After the test period, the image collection, water system, heater and tunnel wind speed are stopped. The air remains circulating in the nozzles to clear any remaining particles. The heating wires are detached and the specimens are removed from the inner tunnel, and then carefully separated before removing each specimen individually with diligence to ensure ice specimen along the leading edge is not damaged. Each specimen is then mounted in the adhesion force test apparatus and loaded at the experimental temperature until failure. The ice specimens are then measured for geometric configuration and later melted for volumetric accumulation amount. The related data is processed to obtain information on LE profile shape changes; accumulation rate, accumulation weight amount and profile shape extension, as well as adhesion pressure. The data is then compared amongst mitigation techniques to determine changes in icing characteristics and provide a recommended mitigation strategy.

4.4.3 Image Data Collection and Analysis

A high resolution black-white digital camera and data acquisition system was used to collect images of the side-view aerofoil profile and the ice accretion at one minute intervals for the duration of the 20 minute icing test. Collected image data was processed using graphics software to investigate changes in leading edge profile shapes, calculate the leading edge shape extension, and determine the accumulation rate for the various mitigation strategies.

4.4.4 Adhesion Force Test

Due to the limited and dated information on adhesion test methods for ice on substrates, and lack of relevant information for testing the force of adhesion on a curved surface, an adhesion test for this experiment needed to be developed. Due to the complexity of the cold climate environment that the tests needed to be conducted in, sensitive equipment could not be used. Furthermore, placing any piezoelectric devices on the surface would alter the ice profile that was part of the experiment. Due to these restrictions a simplified test was developed that used weights and the inverse mold of the aerofoil profiles, in resistance, to shear off the ice and obtain a force measurement in the environment and temperature that the ice was formed. A wedge was placed inside the mold at the trailing edge to support the aerofoil and keep the test piece level. Weights were then loaded in increasing intervals at a gradual and steady pace until the ice failed to adhere to the substrate. The measured failure weight was converted through calculations to obtain the adhesion force at the leading edge of the aerofoil. Figure 4-5 and Figure 4-6 contain images of the apparatus and the procedure of mounting the specimen in the test apparatus.

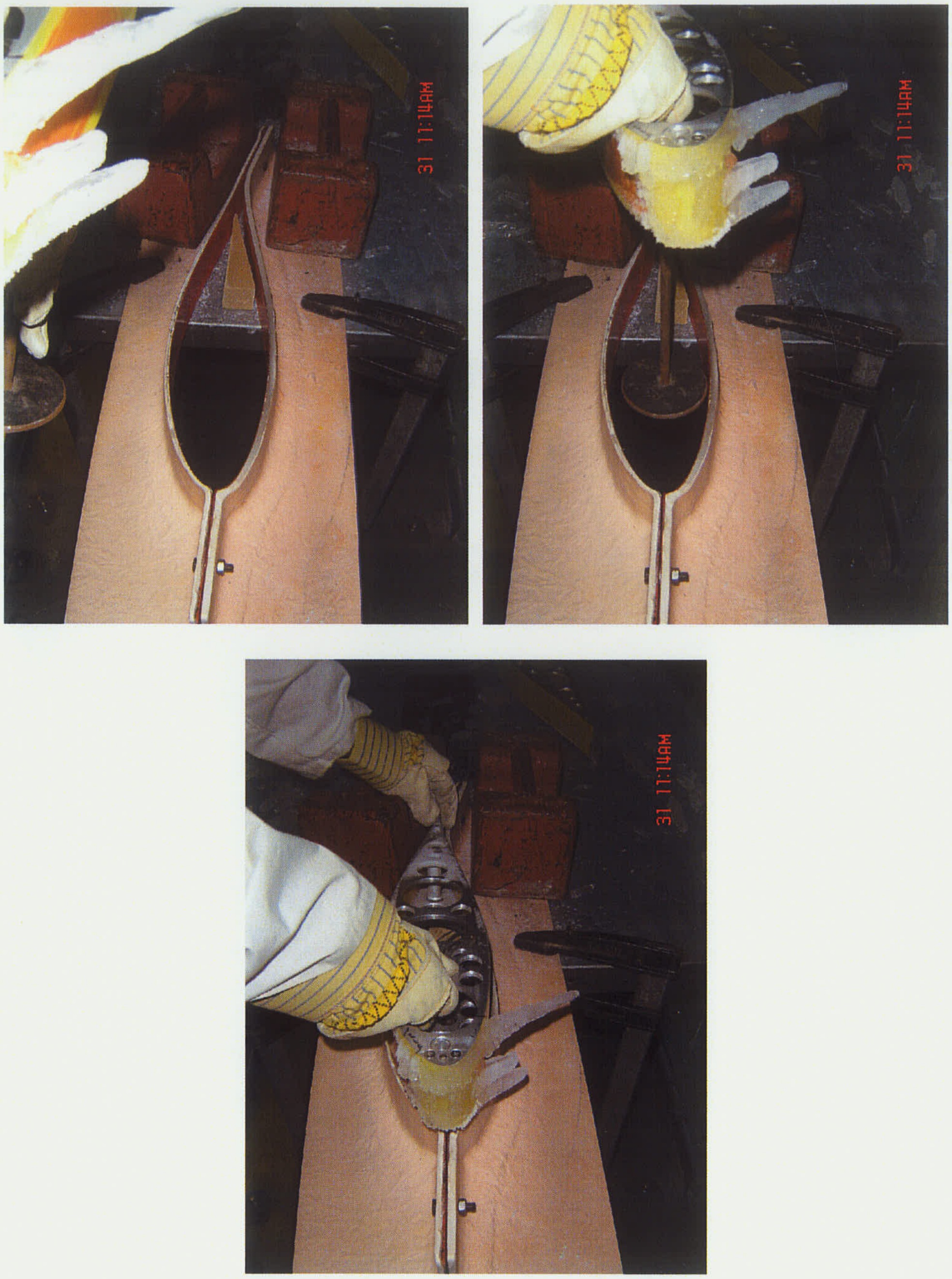

Figure 4-5: Adhesion force test apparatus and mounting procedure.

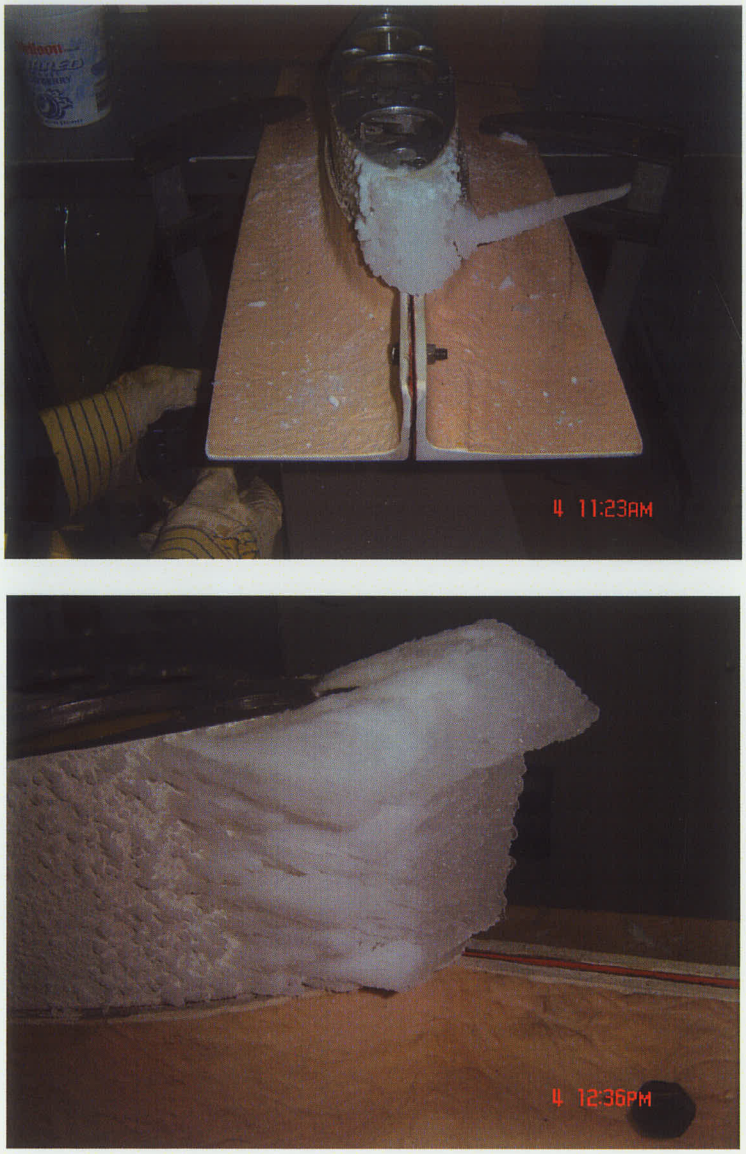

Figure 4-6: Loading of weights and LE ice profile in contact with the test mold.

4.4.5 Iced Area Measurement

Following the adhesion force test, the remaining leading edge ice specimen was traced onto paper and geometry measured to obtain an area calculation. This information was gathered for further use in the calculation of shear pressure of the ice on the blade leading edge regardless of specific ice shape geometry.

Figure 4-7: Sample of leading edge ice specimen geometry

4.4.6 Accumulation Amount Measurement

Due to the varying geometrical volumes of the ice profiles, the resulting test specimens were melted to obtain a liquid volumetric measurement of the amount of ice accumulation. The liquid volume was measured in a graduated cylinder, and results recorded to the icing experiment spreadsheet.

4.5 Uncertainties and Possible Sources of Error

Some of the image data collected during the icing tests became clouded from ice build up on the tunnel window and did not produce as clear an image as possible. Although, this was not desired, it did not affect the majority of the resulting images. Due to the nature of the destructive testing for adhesion force, a minor percentage of the ice fragments could not be collected leading to slight uncertainty in the actual amount of ice that adhered to the LE. However, in all cases the majority of the LE specimen sheared from the surface as one solid piece and remained intact, such that this issue posed only a minor uncertainty to the data collected. Due to the nature of the experiment design this uncertainty was carried through to the next measurements. However, a fragment from the external edge of the ice profile would not affect the geometrical measurement for the area calculation and would only be relevant to the volumetric accumulation measurement.

There is some evidence to suggest that the heat generated as part of the mitigation strategy may have altered the type of ice to form at the substrate. In the case of rime conditions, this created glaze ice at the substrate, and resulted in higher than expected adhesion force values for typical rime ice, signifying that the ice behaves more like glaze adhesion, thus suggesting that the heater may negatively influence adhesion reduction in such situations. This is difficult to visually observe at the substrate-ice interface, however can be deduced from the behaviour of the ice. Furthermore, due to unforeseen mechanisms of the experimental process, at times a mixed form of ice accretion resulted on the blades, despite steady conditions of the experimental facility. This may have been influenced by the mitigation strategies itself.

The water used in the lines of the UMITF spraying apparatus is filtered to ensure it is cleansed of impurities so that fine atomizing nozzles do not become plugged, as they are critical to maintaining proper spray and difficult to perform maintenance on once mounted in the in tunnel. Moreover, the "clean" ice in an experimental setup may not have the impurities of real climatic conditions for icing; however, it is suggestive that those impurities would only act as stress points and induce stress fractures in the ice, leading to a further reduced adhesion force than resulted in these tests. The probability of occurrence and influence of those impurities remains an area for further research.

5 RESULTS & DISCUSSION

Through the transient process of ice accumulation on the surface of the aerofoil section, the blade encounters several physical changes. The physical changes investigated in this project include LE profile shape changes, ice adhesion force, volumetric accumulation amount, accumulation rate and the leading edge profile shape extension. The profile shape changes culminate in a catalogue for visual representation of the icing events. The percentage reduction of icing characteristics is presented in charts. The results are summarized in the Mitigation Forecasting Tool. Further details of results are located in the appendices. Appendix E contains original collected data and percentage reduction tables for the various icing characteristics that were measured. Appendix F contains calculations for loads to determine adhesion force in the test rig. Appendix G contains the summary charts of the following presented results in a larger scale, including charts from published papers. Appendices H through L contain the published papers from conferences, which can be referred to for further specific details regarding each of the mitigated icing characteristics.

The experimental work of this thesis is novel and previous works do not exist for direct comparison, especially in the entirety of collected data for icing characteristics and analysis carried out in this work; as well as for the effects of mitigation strategies on icing characteristics and the comparison between mitigated and non-mitigated blades. Icing issues on blades have been modelled before; however, mostly only for ice accretion shape [Lacroix 2001]. Experiments have been conducted; however, not in as controlled conditions, as in this experiment, due to the limitations of wind-icing facilities available.

5.1 Leading Edge Aerofoil Profile Shape Changes

A visual profile of ice formation on the LE surface illustrates the varying amounts of ice accumulation and changes in profile shapes between different surfaces. If unmitigated, ice will accumulate unevenly on the leading edge of the blade surface; however, when mitigation techniques are implemented, results indicate that the ice accumulation is reduced and more controlled. The images presented below, in Figure 5-1 to Figure 5-6, are shown at either the mid-point (10 min.) or end stage (20 min.) of the test duration.

Surface Mitigation in Glaze:

The hydrophobic coating provides the most controlled, symmetric and reduced amount of accumulation on the blade LE. Furthermore, both coatings appear to better control the resulting ice profile shape as compared to the plain, un-mitigated sample.

Glaze (t = 20 min.)

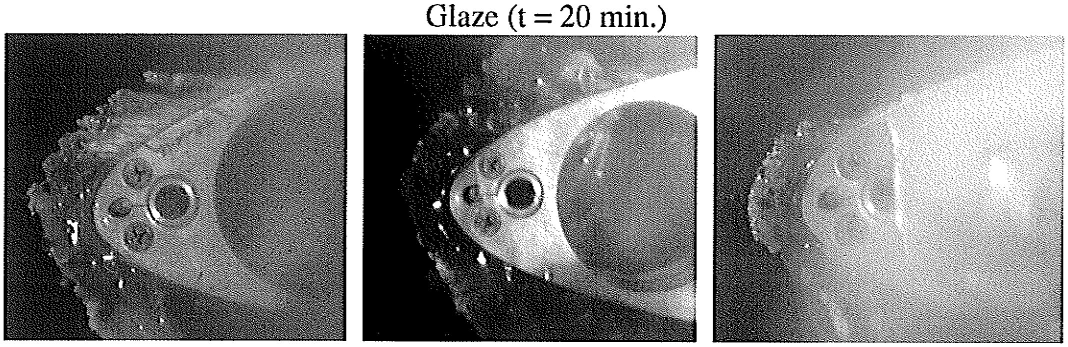

(a) Plain (b) Icephobic (c) Hydrophobic

Figure 5-1: Experimental icing of aerofoil leading edge, coatings, glaze

Surface Mitigation in Rime:

Both the icephobic and hydrophobic coatings provide more controlled accumulation. The hydrophobic profile appears to reduce accumulation slightly more than the icephobic c

Rime (t = 10 min.)

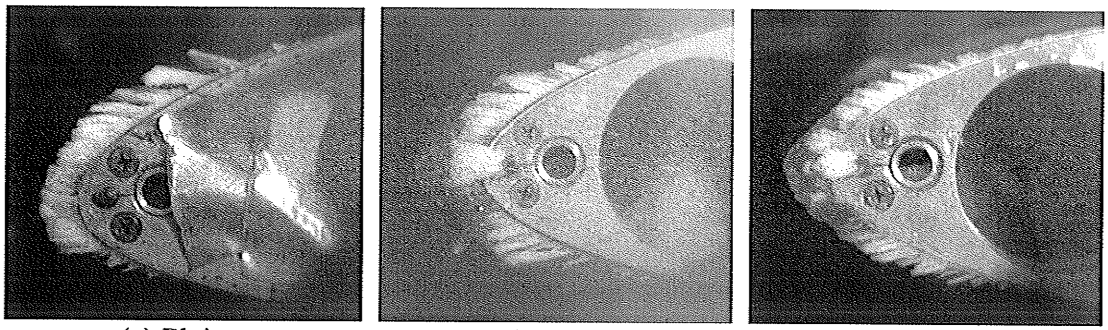

(a) Plain (b) Icephobic (c) Hydrophobic

Figure 5-2: Experimental icing of aerofoil leading edge, coatings, rime

Thermal Mitigation in Glaze:

Anti-icing on a plain surface is more effective than the de-icing regime at reducing accumulation and controlling profile shape changes in glaze icing conditions.

Glaze (t = 10 min.)

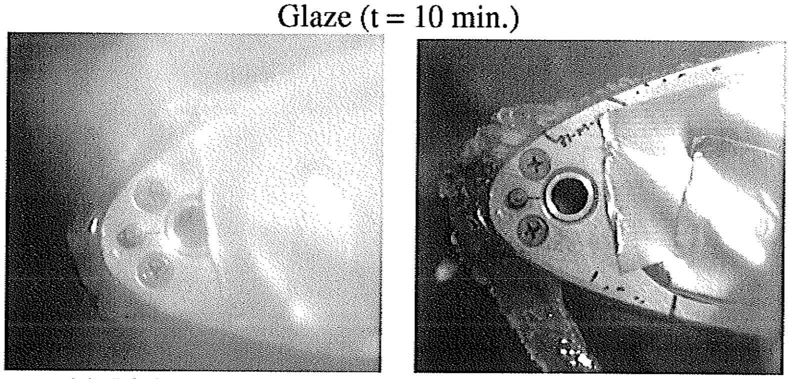

(a) Plain + Anti-icing (b) Plain + De-icing

Figure 5-3: Experimental icing of aerofoil leading edge, thermal regimes, glaze

Thermal Mitigation in Rime:

Anti-icing on a plain surface is more effective at reducing accumulation and profile shape changes in rime icing conditions. However, as can be seen, a glaze layer forms at the interface of the ice and substrate surface, leading to glaze-like ice characteristics and behaviour at the interface, due to the heating of the blade surface as part of the mitigation strategy. Attention must be addressed to this consequence of mitigation. This results despite the same heat flux levels in either heating regime.

Rime (t = 20 min.)

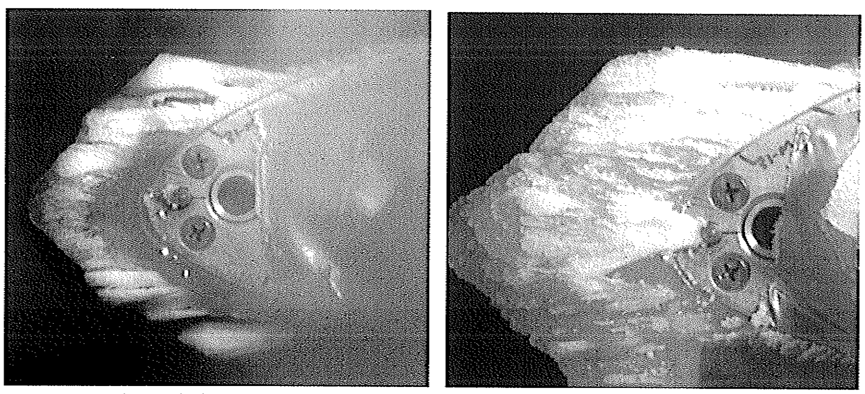

(a) Plain + Anti-icing (b) Plain + De-icing

Figure 5-4: Experimental icing of aerofoil leading edge, thermal regimes, rime

Thermface Mitigation in Glaze:

The hydrophobic coating appears more effective at controlling ice accumulation and profile shape change than the icephobic coating in glaze conditions. Anti-icing depicts a lesser amount of accumulation and shape change than the de-icing regime.

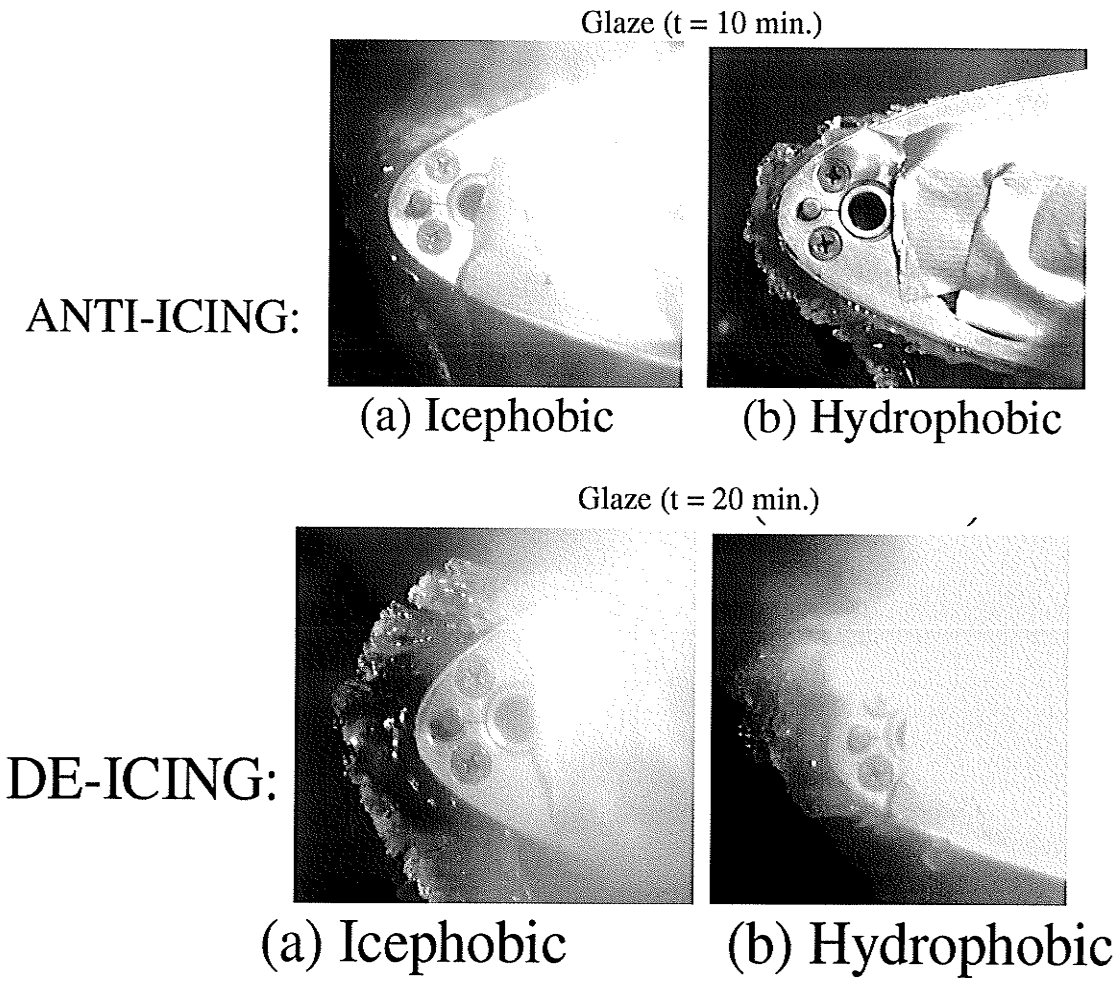

Figure 5-5: Experimental icing of aerofoil leading edge, thermface regimes, glaze

Thermface Mitigation in Rime:

The icephobic coating appears more effective at controlling ice accumulation and profile shape change than the hydrophobic coating in rime conditions, as is evident by the reduced amount of ice accumulation along the aerofoil. Anti-icing depicts a lesser amount of accumulation and shape change than the de-icing regime.

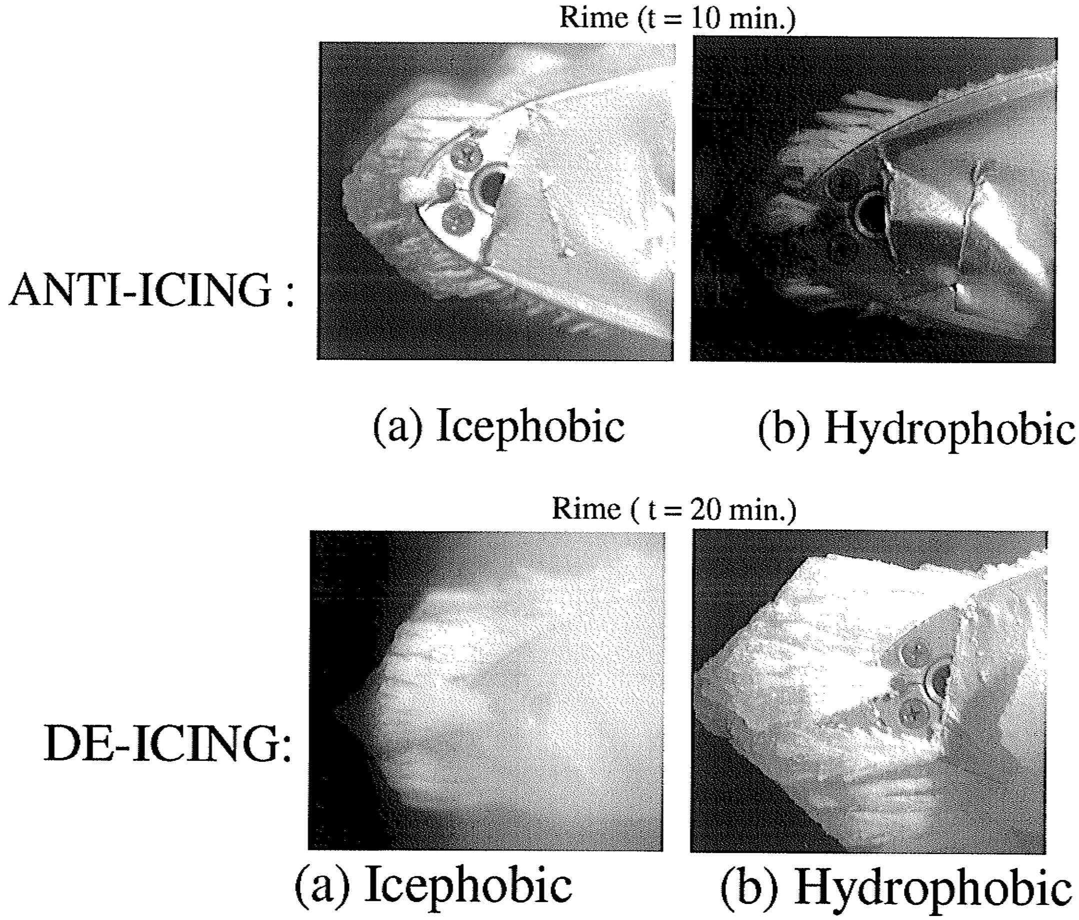

Figure 5-6: Experimental icing of aerofoil leading edge, thermface regimes, rime

5.2 Adhesion Force

Comparing glaze and rime icing results indicate that on an uncoated plain surface, the adhesion force of glaze ice is 60% less adhesive than rime ice. Figure 5-7 shows the overall comparative results for adhesion force. The most effective surface mitigation in glaze conditions is the hydrophobic coating which reduces adhesion force by 70%. In the rime condition, the icephobic coating is more effective, reducing adhesion by 26%. Evidently, in surface mitigation, the hydrophobic coating is most effective in glaze conditions while the icephobic coating is most effective in rime conditions. This can be attributed to the physical properties of the coatings: the hydrophobic coating is designed to be effective at repelling water droplets that occur in glaze ice formation, while the icephobic coating is designed to repel solid-ice, as in rime conditions. The results identify the differences in the surface strategies and indicate that this distinction is related to the applied climatological conditions. This validates the significance and effectiveness of applying the proper coating in the conditions for which it is designed.

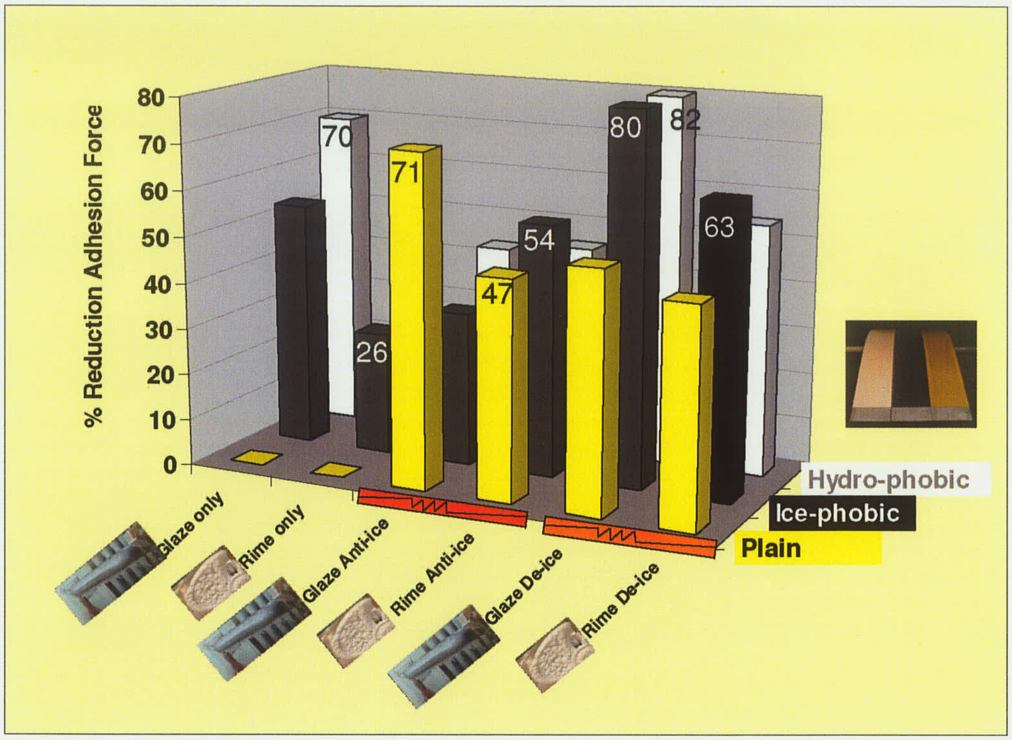

Figure 5-7: Percentage reduction in adhesion force

For thermal mitigation, anti-icing is more effective than the deicing regime, in both glaze and rime icing conditions, reducing adhesion 71% and 47% respectively. Furthermore, the results indicate that the glaze responds more effectively than rime to this thermal mitigation strategy.

For the thermface mitigation, in both icing conditions, the de-icing regime is more effective than the anti-icing regime. In glaze conditions it performs equally well among the icephobic and hydrophobic coatings, reducing adhesion by 80%; whereas in rime conditions, it is best paired with the icephobic coating, reducing adhesion by 63%. Furthermore, the deicing regime also consumes less energy, which is ideal for energy production systems. Isolating the thermal variable indicates that for glaze icing, the thermal regimes are not solitarily effective at reducing adhesion force, and thus are most effective when paired with a secondary mitigation strategy. Moreover, isolating the surface variable indicates that for glaze icing, there is no apparent adhesion reduction for either coating with the anti-icing regime, suggesting a supplementary result that the coatings may impede ice removal by preventing conductive heat transfer to the surface, as a result of their inherent thickness.

The de-icing regime is the most effective in either icing condition; whereas in glaze, either surface mitigation is just as effective as the other, but in rime, the icephobic is more effective. Therefore, an effective mitigation strategy for either icing condition employs the icephobic coating and the de-icing regime.

There is a discrepancy between the experimental findings in this report and the common assumption that the adhesion force of the higher density glaze ice exceeds that of the lower density rime ice. However, there is an opposite finding in this project. One observation suggests that the thermal mitigation creates a glaze-like layer at the substrate-ice interface with resulting glaze-like behaviour at the critical interface of the adhesion force test and thus, higher adhesion force values result for rime ice. However, it was also found in the non-thermally mitigated cases—such as the surface mitigation, or even the plain surface without any mitigation, that rime ice is always more adhesive than the glaze ice. Thus, the above theory is relevant, however, requires further investigation before a definite conclusion can be stated. The results presented herein were measured on a curved surface and within the environmental chamber at experimental temperature.

5.3 Accumulation Amount

In comparison of the amount of ice, in liquid state that accumulates along the LE of an aerofoil for both icing conditions, there is 14% less accumulation in glaze than in rime. The comparison is percentage reduction of accumulation amount is shown in Figure 5-8. The most effective surface mitigation in glaze icing is the icephobic coating, reducing accumulation by 29%, and in rime is the hydrophobic coating reducing accumulation 39%.

The most effective thermal mitigation strategy on a plain uncoated surface, in glaze conditions, is the anti-icing regime, reducing accumulation by 34%. In rime conditions, accumulation is not significantly reduced; in fact, only the anti-icing regime reduces accumulation by 8%, whereas for deicing, the amount of accumulation appears to supersede the effectiveness of the mitigation technique, suggesting that it does not have the capacity to be effective in the given conditions.

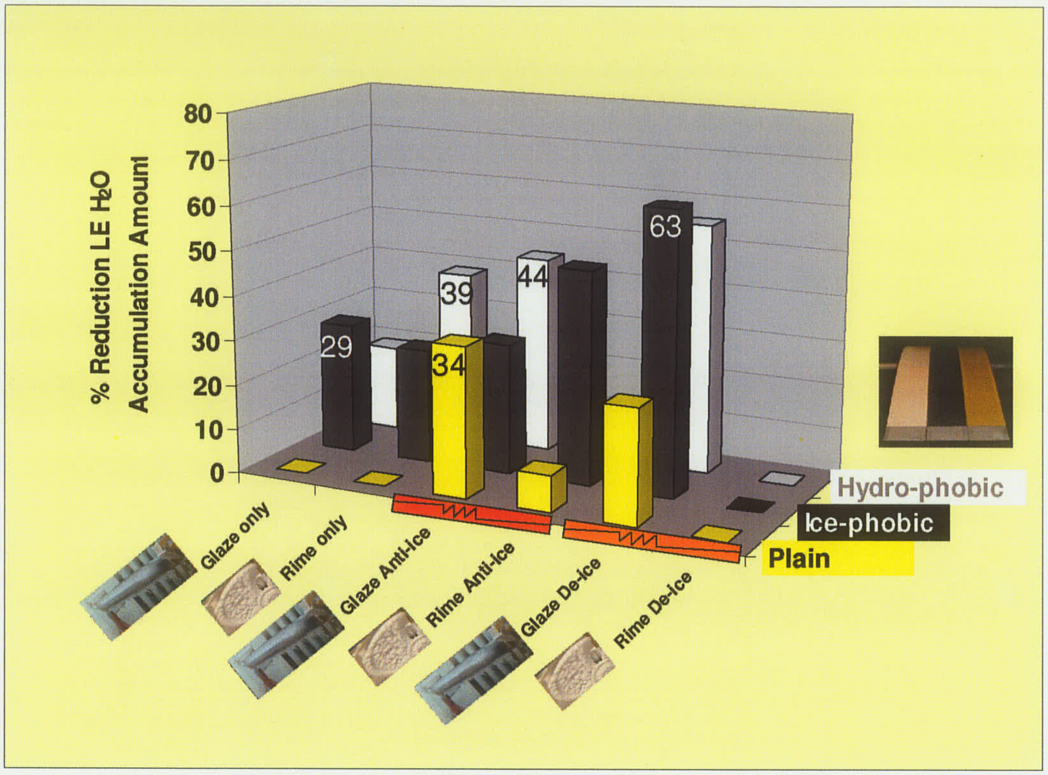

Figure 5-8: Percentage reduction in accumulation

The most effective thermface regime for glaze conditions involves combining the de-icing regime with the icephobic coating, which reduces accumulation 63%. In rime conditions, the only effective solution is the icephobic coating with the anti-icing regime, reducing accumulation 48%. The inability of the mitigation strategy to be effective with the de-icing regime in rime conditions indicates that the thermal technique has nearly reached its maximum capacity of effectiveness, yet the combination with the surface mitigation remains more effective than the thermal technique alone. In light of energy consumption, the deicing regime utilizes less energy, however it is limited in effectiveness of reducing accumulation in rime conditions, despite being the preferred regime. Thus, to effectively mitigate icing accumulation amount in rime conditions, greater energy consumption is required through the anti-icing regime.

Evidently, both the thermal and surface mitigation strategies, independently, are significantly effective at reducing accumulation along the leading edge of an aerofoil. However, the combined mitigation of the thermface strategy provides the most substantial reduction in accumulation. Thus, the recommended mitigation strategy for reducing accumulation in either glaze or rime conditions would be to implement the icephobic coating in combination with a deicing regime, but with attention to enhanced thermal duration as needed in rime conditions due to the limitation of de-icing to effectively reduce accumulation. Furthermore, this strategy is effective at reducing adhesion force as well.

5.4 Accumulation Rate

The comparison of percentage reduction of ice accumulation rate for various mitigation techniques are contained in Figure 5-9.

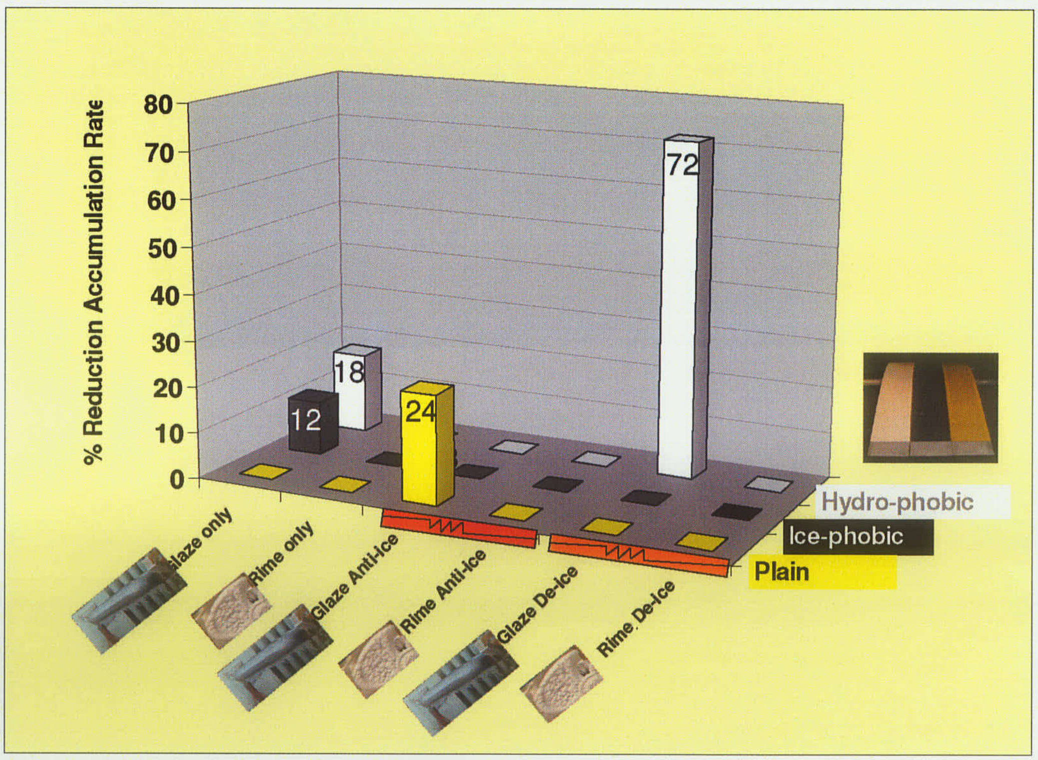

Figure 5-9: Percentage reduction in accumulation rate

In comparing the rate of accumulation between glaze and rime icing conditions, results indicate that on an uncoated plain surface, glaze ice accumulation rate is 5% less than rime. When surface mitigation is used, the rate of ice accumulations on a wind turbine blade is more effectively reduced. By employing the icephobic coating, icing accumulation rate (IAR) is 52% less in glaze than in rime, while using the hydrophobic coating IAR is 80% less in glaze than in rime.

Comparing the surface mitigation techniques, in glaze conditions, the IAR is reduced by 12% with the icephobic coating and 18% by the hydrophobic coating as is shown in Figure 5-9. In rime conditions, surface mitigation does not effectively reduce IAR, suggesting that the mitigation strategy has reached its maximum capacity to be effective for the given climatological conditions.

In comparison of the thermal mitigation techniques, for glaze conditions, the anti-icing regime effectively reduces IAR by 24%, whereas the deicing regime is ineffective for reducing IAR. In rime conditions, neither thermal mitigation regime effectively reduces IAR suggesting that the technique has reached its maximum capacity to be effective in the given conditions.

The thermface strategy employing the hydrophobic coating with the deicing regime reduces IAR by 72% in glaze conditions and is the only thermface strategy to perform effectively. In rime conditions, there is not a single overall mitigation strategy that indicates a reduction in IAR. Isolating individual variables for further insight to these results indicates that the icephobic coating with anti-icing provides a reduction in IAR when compared to both surface and thermal mitigations individually. This thermface technique effectively reduces IAR by 20% over surface mitigation alone and 14% over anti-icing thermal mitigation alone; thereby suggesting that it would be the most effective mitigation strategy in rime conditions for controlling IAR.

Evidently, IAR is more easily mitigated in glaze than in rime conditions. The most effective mitigation strategy is the thermface technique where in glaze conditions, the hydrophobic coating with the de-icing regime is employed, and in rime, the icephobic coating with the anti-icing regime is employed. These results are indicative of the correlation between the sensitivity of the behaviour of the ice to the employed mitigation strategy, (i.e. rime icing, as the more severe case requires a more intense mitigation technique to effectively control the icing accumulation rate).

5.5 LE Profile Shape Extension

In comparison of the amount of ice, in solid state that accumulates at the LE of an aerofoil causing an extension in shape profile, less extension occurs in glaze than in rime ice by 8%. From Figure 5-10, the results of the percentage reduction in profile shape extension indicate that surface mitigation efforts are only effective in glaze conditions, in which the hydrophobic coating reduces shape extension by 25% and the icephobic coating by 16%. Evidently, the hydrophobic coating is slightly more effective. Surface mitigation in rime conditions is not effective, suggesting that the rime icing conditions subdue the surface mitigation efforts for reducing shape extension.

The most effective thermal mitigation strategy on a plain uncoated surface, in glaze conditions, is the anti-icing regime, reducing shape extension by 29%, whereas the deicing regime does not effectively reduce shape extension. In rime conditions, shape extension is not significantly reduced by either de-icing or anti-icing regimes, suggesting that the mitigation effort does not have the capacity to be effective in the given conditions.

The thermface strategy employing the hydrophobic coating with the deicing regime reduces shape extension by 75% in glaze conditions, and the icephobic coating with the deicing regime, although not as effective, still contributes to mitigating shape extension. In rime conditions, there is not a single overall mitigation strategy that indicates a reduction in shape extension. However, isolating individual variables for further insight to these results indicates that the icephobic coating with anti-icing provides a reduction in shape extension when compared to both surface and thermal mitigations individually. This thermface technique effectively reduces shape extension by 21% over surface mitigation alone and 15% over anti-icing thermal mitigation alone; thereby suggesting that it would be the most effective mitigation strategy in rime conditions for controlling shape extension.

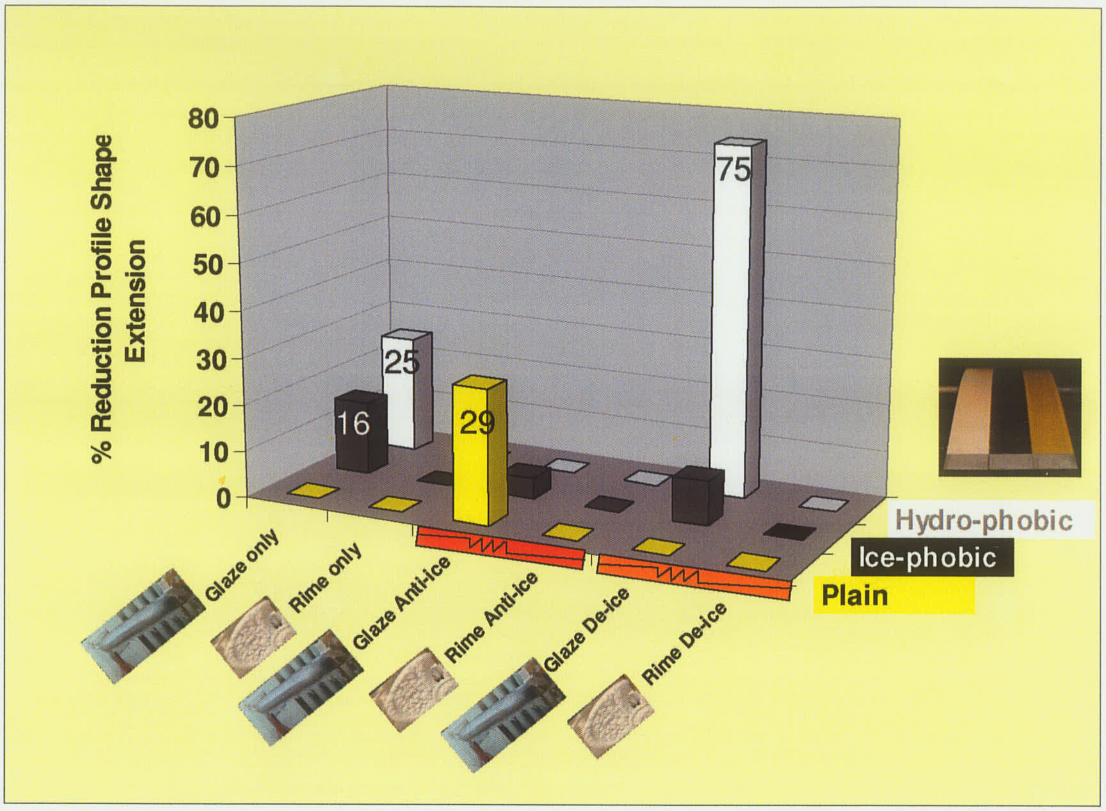

Figure 5-10: Percentage reduction in profile shape extension at leading edge

Evidently, it is more difficult to control profile shape extension in rime than in glaze conditions, however it is not impossible. Both surface and thermal techniques are independently effective, and when combined are substantially more effective, as is evident in glaze conditions, and even slightly in rime conditions.

5.6 Profile Shape Catalogue

The profile shape catalogue is a culmination of all the collected visual data for the simulated icing events over a period of 20 minutes. It provides a visual representation of the changes in shape of the aerofoil profile, while providing and indication of the amount of ice that accumulates, the amount the profile extends, and a visual suggestion of the rate of ice accumulation over the experimental duration. A sample of the resulting icing event profile shapes are depicted in

Table 5-1, at the beginning (0 min.), mid (10 min.) and end (20 min.) stages of the icing event for the three mitigation strategies in both glaze and rime icing conditions, indicating the ice growth at the LE for the various mitigation strategies. The complete profile shape catalogue is located in Appendix B.

Table 5-1: Sample Aerofoil Profile Catalogue

Experiment List					LE Shape Profile Intervals (1 min / 10 mins. / 20 mins.)
Test Description		specimen	thermal regime		1 min / 10 mins. / 20 mins.
Surface	glaze	plain	-	-	
Surface	rime	icephobic	-	-	
Thermal	glaze	plain	-	de-icing	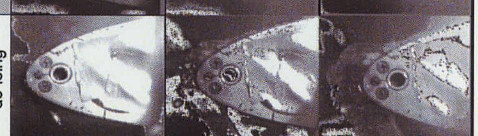
Thermal	rime	plain	anti-icing	-	
Thermface	glaze	hydrophobic	anti-icing	-	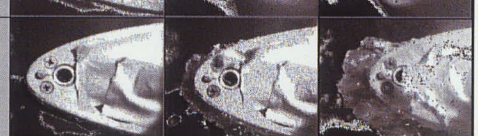
Thermface	rime	hydrophobic	-	de-icing	

5.7 Mitigation Forecasting Tool (MFT)

The experimental results have been consolidated into a Mitigation Forecasting Tool (MFT). The MFT is composed of relevant icing characteristic data during and after an icing event for the proposed mitigation strategies in the given simulated climatological conditions. It has been designed to provide an idea of what to expect during and after an icing event in terms of accumulation rate, profile shape extension, weight amount of ice accumulation and adhesion pressure. Adhesion pressure provides an idea of "how sticky" the ice is to the surface, or in other words, how difficult the ice is to remove from the substrate per square inch. Profile shape extension is used to determine the changes in blade aerodynamics in terms of extended chord length which is a direct influential parameter for blade optimization, while ice weight accumulation provides the information to assess how much "heavier" and unstable the blade can become, which has a direct influence on turbine vibration and blade aerodynamics. Icing accumulation rate indicates the amount of ice to accumulate (length scale) at the leading edge, in a given time and provides an indication to the required intensity of a mitigation strategy to effectively mitigate an icing event. Figure 5-11 relates the collected data in a timeline format during and after an icing event. The figure is used to forecast icing characteristics and performance measures of mitigation strategies, as well as provide a comparison of values amongst strategies for a given icing characteristic.

For example, during an icing event, the accumulation rate in rime conditions is the greatest for the sample with only the hydrophobic surface mitigation and least with the plain, unmitigated specimen; whereas in glaze conditions, accumulation rate was the greatest in on the uncoated specimen with the de-icing regime and least with the thermface mitigation of the hydrophobic coating with the de-icing regime. Immediately, it is evident that the mitigation strategies presented in this study are inadequate for the imposed rime icing conditions; however, they are effective for mitigating glaze ice.

If after an icing event, a critical icing characteristic is selected, such as adhesion pressure, the MFT indicates that in rime the thermface strategy employing the icephobic coating with the de-icing regime has the least pressure and can be selected for effective control of this parameter in an icing event. If, however, this mitigation strategy needs to be balanced with other icing characteristics the MFT shows that it is not the best in terms of shape extension amount or accumulation amount. A further decision can be made to determine the ideal mitigation strategy for a particular need or in simply gaining a perspective for how the mitigation strategy performs amongst other strategies for the various icing characteristics. Further details of the mitigation forecasting tool are located in Appendix C.

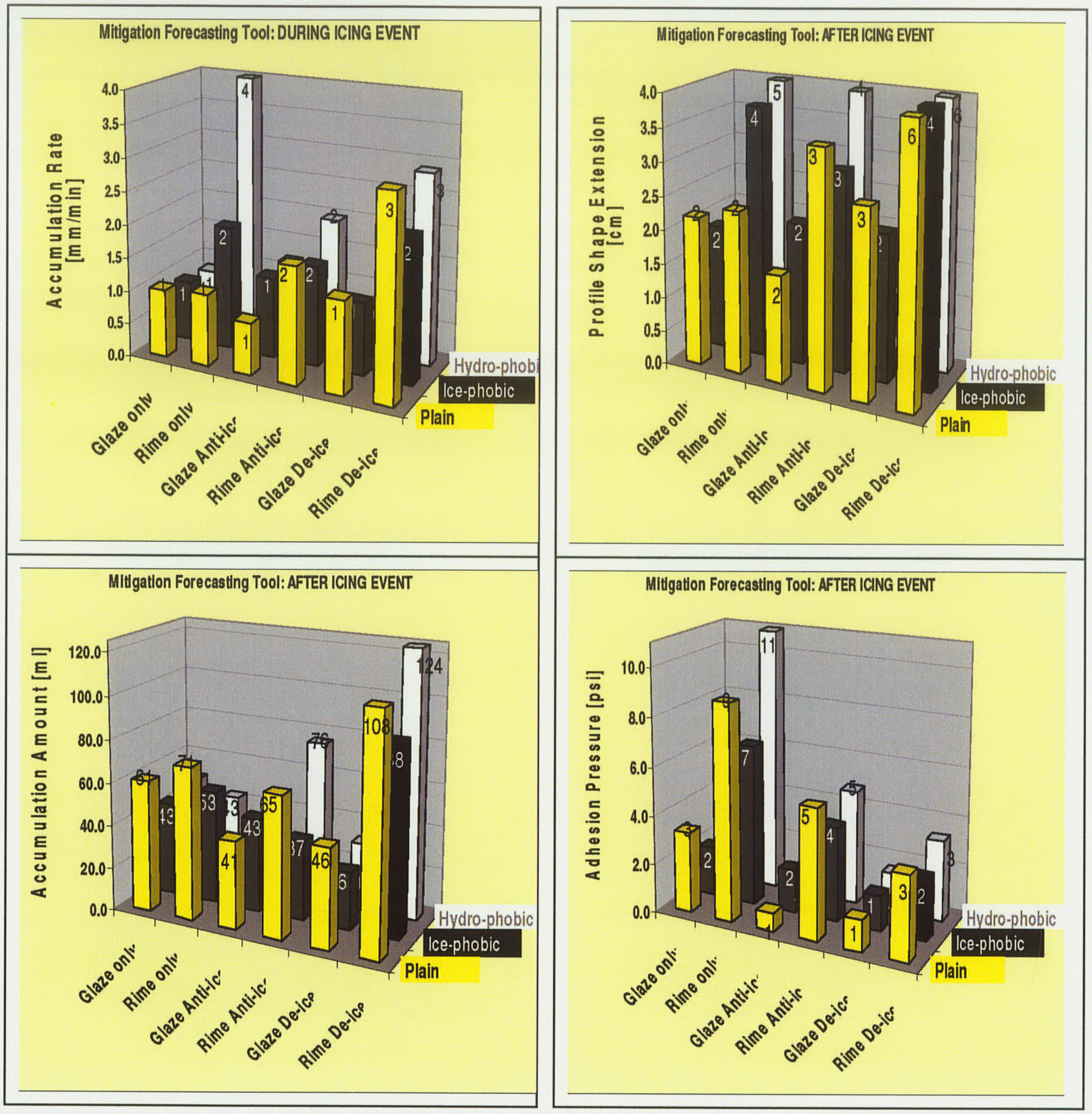

Figure 5-11: Mitigation Forecasting Tool

5.8 Dynamic Similarity

The experimental focus of this thesis was placed on identifying icing characteristics and the effects of mitigation strategies imposed on scaled-down blades subjected to icing, without the initial intension of scaling the immediate results for actual wind turbines. However, it is possible to identify how the results of this thesis pertain to a full-scale blade.

Dynamic similarity for aerofoils exists when the Mach numbers and Reynold's numbers are equal between the experimental and actual conditions. Since the flow remains incompressible for wind turbine analysis, Mach number does not need to be considered, and only Re is important. Furthermore, since the experiment was designed to simulate actual climatological conditions, the parameters for the air conditions would be equivalent, and only the characteristic length would vary between the experiment and actual conditions. From a simple evaluation of the approximated average chord length of the actual turbine blade, 1.68 m, and the experimental specimen chord length, 0.5 m; it is evident that the actual turbine is scaled 3.36 times larger than the specimen.

Thus, for dynamic similarity to exist for this experiment, (i.e. equivalent Reynold's numbers), the velocities tested in the wind tunnel represent wind speeds that the turbine would experience reduced by a factor of 3.36. In other words, the icing characteristics that occurred in glaze or rime conditions in the tunnel at 7.37 m/s and 7.97 m/s respectively, would actually represent icing that occurs at 2.19 m/s and 2.37 m/s for glaze and rime conditions, respectively, on an actual wind turbine.

6 CONCLUSION & RECOMMENDATIONS

6.1 Icing Characteristics

Wind Energy production in adverse cold climates can be enhanced by implementing the presented mitigation strategies, which significantly control the ice profile shapes, reduce the accumulation rate, adhesion force, accumulation amount and profile shape extension of ice on a blade surface and influence the formation of a more symmetric LE ice profile.

The explicit contributions of this thesis are the experimental collected data, which has not previously been collected for such a diverse range of icing characteristics, and icing conditions; in addition, collected for mitigation strategies. Furthermore, the analysis of the data and comparison amongst results is a unique contribution to the scientific community, especially in terms of experimental results which are often difficult to find, let alone collect, due to the complexity of the required apparatus for such an experiment. Creation of the MFT is exclusive, as such results have never before been published in this diverse form; as well, the profile shape catalogue is distinctively detailed with experimental results rarely available in one location, as in the compilation provided in this thesis. Moreover, the direct contribution of this thesis to the advancement of technology for mitigating icing effects is the development of a novel mitigation strategy, and it's designation as *Thermface*, which has successfully provided enhanced icing mitigation in comparison to other approaches.

6.2 Mitigation Strategies

For reducing adhesion force and accumulation amount, it is shown that in glaze or rime conditions, the thermface strategy employing the de-icing thermal regime with the icephobic surface coating is the most effective mitigation, with the necessity to extend the duration of the thermal regime to best mitigate accumulation amount in more severe icing conditions, such as rime.

For controlling icing accumulation rate and profile shape extension, glaze icing will be effectively mitigated with the minimalist strategy while rime icing requires the most intense strategy, indicating the sensitivity of the behaviour of the ice to the employed mitigation strategy. The specific solution for each icing condition is the hydrophobic coating with the de-icing regime in glaze, and the icephobic coating with the anti-icing regime in rime.

The Mitigation Forecasting Tool indicates the performance measures for various mitigation strategies as a means to predict results and resolve an optimal solution, when a critical icing characteristic is selected.

The Profile Shape Catalogue is a useful tool for visual reference of the results of the icing event.

6.3 Recommendations

Furthermore, the combination of mitigation strategies must be carefully designed so that they are employed in the climatological conditions best suited for their use and within their scope of capability so that they do not adversely affect the capabilities of one another.

Other areas for further investigation include varying the heat flux; varying the delivery rate of the droplets to the specimen, which would involve changing the experimental parameters or diversification of experimental parameters; focusing on the creation of a sub-film to break the adhesive bond; and modeling the phase change of the accumulation through computational fluid dynamics. Investigation of "dirty" ice may better replicate actual icing conditions. Furthermore, an investigation of adhesion force for "mixed" ice conditions due to the indirect effects of mitigation strategies on the formation of the ice type would be valuable to clarify the uncharacteristically high rime adhesion force values. Also, variation of the Reynold's number and consideration of scaling effects between the test specimen and the actual blades needs to be investigated, as well as variation of the angle of attack of the blade position in the flow, in stationary position. Extension of the experiment to rotation of blades should be considered.

7 REFERENCES

Ahti, K. "Ice load forecasts in Finland," BOREAS VII, Saariselka, Finland. 7-8 March, 2005.

AMIL, "Icephobic coatings evaluation". May 2006. <www.amil.chichoutimi.qc.ca/amil/amil/icephobiccoatings/index.htm>. accessed 11-May-06.

Antikainen, P., et al, "Modeling, verification and classification of ice loads in wind turbines," Boreas VI, Pyhätunturi, Finland, 9-11 April 2003.

Battisti, L., et al., "Evaluation of anti-icing energy and power requirement for wind turbine rotors in cold climates," BOREAS VII Proceedings, Saariselka, 7-8 March 2005.

BOREAS V Proceedings, Levi, Finland, 29 Nov-1 Dec, 2000. <www.fmi.fi/research_meteorology/meteorology_13.html>. accessed Jan-07.

BOREAS VI Proceedings, Pyhätunturi, Finland, 9-11 April 2003. <www.fmi.fi/research_meteorology/meteorology_13.html>. accessed Jan-07.

BOREAS VII Proceedings, Saariselkä, Finland, 7-8 March, 2005. <www.fmi.fi/research_meteorology/meteorology_13.html>. accessed Jan-07.

Bose, N. "Icing on a small horizontal axis wind turbine-part 1: glaze ice profiles." Journal of wind engineering and industrial aerodynamics, 45.1, 1992: 75-85.

Botura, G., Fisher, K., "Development of ice protection system for wind turbine applications," Boreas VI, Pyhätunturi, Finland, 9-11 April 2003.

Burton, T., Sharpe, D., Jenkins, N., Bossanyi, E. Wind Energy Handbook. Wiley& Sons, Ltd., Chichester, 2001, 6, 377-380.

CanWEA, "Canadian installed capacity". November 2006. <www.canwea.ca/Map_of_Installations.cfm>. accessed 21-Nov-06.

CanWEA, "Wind generation to experience strong growth," Windlink, January 9, 2007, Issue #6.

Cattin, R., et al., "Alpine test site Gutsch: monitoring of a wind turbine under icing conditions," Switzerland, 2006.

Chaîné, P.M., et al. Wind and ice loading in Canada, 1974. Toronto: Atmospheric Environment Canada, 1974.

Davidson, P.A., Turbulence: An introduction for scientists and engineers. University of Cambridge, Oxford University Press Inc., New York, 2004.

Dursetwitz, M., "On-site cold climate problems," Boreas VI, Pyhätunturi, Finland, 9-11 April 2003.

Environment Canada, 2006a, "Canadian wind atlas," <www.windatlas.ca>, accessed 2-Dec-06.

Environment Canada 2006b, "Canadian climate normals 1971-2000 for data site Morden, Manitoba," <www.climate.weatheroffice.ec.gc.ca/climate_normals/results_e.html>, accessed Nov-06.

Fitt, A.D. and Pope, M.P., "De-icing by slot injection," Acta Mechanica. 147.1-4 (2001) 73-86.

Fox, R.W., et al., Introduction to Fluid Mechanics. 6^{th} Ed. John Wiley & Sons Inc., 2004.

Ganander, H., Ronsten, G., "Design load aspects due to ice loading on wind turbine blades," Boreas VI, Pyhätunturi, Finland, 9-11 April 2003.

Garti, N. et al, "New non-stick epoxy-silicone water-based coatings part 1: physical and surface properties," Proceeding of the 5th international zebra mussel and other aquatic nuisance organisms conference, Toronto, Canada, (Feb, 1995), 151-169.

Global Wind Energy Council (GWEC). Global wind energy outlook 2006, p38 September 2006.

Hanesiak, J, and Kraj, A. Re: request: icing maps., 5-Dec-2006.

IEA-Annex XIX, Wind Energy in Cold Climates, <http://virtual.vtt.fi/virtual/arcticwind>. accessed 2007.

IEA, "Wind energy in cold climates," IEA task XIX wind energy annual report, 2005, p. 41.

Kimura, S., Sato, T., Kosugi, K., "The effect of anti-icing paint on the adhesion force of ice accretion on a wind turbine blade," Boreas VI, Pyhätunturi, Finland, 9-11 April 2003.

Kimura, S., Tammelin, B., Säntti, K., "Estimation of reduction of power production due to icing from the existing meteorological data," Boreas V, Levi, Finland, 29 November – 1 December, 2000.

Kraj, A. G., Aerodynamic optimization of a biplane configuration through differential evolution, Department of Mechanical and Industrial Engineering, University of Manitoba, 2003.

Kraj, A. G. and Bibeau, E. L., Icing characteristics and mitigation strategies for wind turbines in cold climates-part 1, WREC, Florence, Italy, 2006a.

Kraj, A. G. and Bibeau, E. L., Icing characteristics and mitigation strategies for wind turbines in cold climates-part 2, Global Wind Power, Adelaide, Australia, 2006b.

Kraj, A. G. and Bibeau, E. L., Icing characteristics and mitigation strategies for wind turbines in cold climates-part 3, Renewable Energy, Makuhari, Japan, 2006c.

Kraj, A. G. and Bibeau, E. L., Application of coatings for icing mitigation of wind turbines in cold climates (poster), Renewable Energy, Makuhari, Japan, 2006d.

Kraj, A. G. and Bibeau, E. L., Impact of mitigation strategies on icing accumulation rate for wind turbines in cold climates, CanWEA, Winnipeg, Canada 2006e.

Laakso, T., et al. Expert group study on wind energy projects in cold climates. 1stEdition 2005. Finland: IEA Annex XIX, 2005a.

Laakso, T., et al. State-of-the-art of wind energy in cold climates. Exhibit MH-NCN-1031 Section E, Finland: IEA Wind Energy in Cold Climates Annex XIX, April 2003.

Laakso, T., Peltola, E., "Review on blade heating technology and future prospects," BOREAS VII Proceedings, Saariselka, 7-8 March 2005b.

Lacroix, A., "Wind turbine operations in cold weather: an overview of the issues with a focus on icing and its mitigation," Department of Mechanical and Manufacturing Engineering, University of Massachusetts Amherst, August, 2001.

Laforte, C., Laforte, J.L. & Carriere, J.C., (2002), "How a solid coating can reduce the adhesion of ice on a structure," The tenth International Workshop on Atmospheric Icing of Structures, IWAIS, June 2002.

Loughborough, D.L., "Physics of mechanical removal of ice from aircraft," Aeronautical Engineering Review, 11.2 (Feb 1952) 29-34.

Maissan, J., "Comments on impact of mitigation strategies on icing accumulation rate for wind turbines in cold climates, Andrea G. Kraj, CanWEA 2006," 20-November-2006.

Maissan, J., "Memoire CCVK 58 IEA Annex XIX – Short Version," 10-January-2007.

Maissan, J., and Kraj, A. Icing mitigation. 9-January-2007a.

Maissan, J., and Kraj, A. RE: First Canadian wind turbines in cold climates?, 9-January-2007b.

Manitoba Hydro. "Improving reliability in ice prone areas", Ice Storm Task Force, 1984.

Megateli, R. "Meteorological and metrological characterization of icing events," CanWEA Proceedings, Winnipeg, Canada, October 22-25, 2006.

Mohammadi, R., Wassink, J., Amirfazli, A., "Effect of surfactants on wetting of super-hydrophobic surfaces," American Chemical Society, (Aug 6, 2004), 1-6.

Morgan, C., Bossanyi, E., Seifert, H., "Assessment of safety risks arising from wind turbine icing." BOREAS IV. Hetta, Finland, 31 March-2 April, 1998.

Naterer, G. F. et al," Experimental facility for new hybrid ice/spray flow tunnel with laser based droplet measurement," American Institute of Aeronautics and Astronautics, Inc., 2002-2867, 1-10.

Naterer, G.F. Heat Transfer in Single and Multiphase Systems. New York: CRC Press, 2003.

Norling, J., "Suorva—artic wind turbine in northern Sweden," CADDET Renewable Energy Newsletter, Vattenfall AB, Sweden, March 2000.

NRC, "Canada's energy outlook: the reference case 2006," Natural Resources Canada, Analysis and Modeling Division, 2006.

Nushi K. & Kasai S., "Computation of aerodynamic performance deterioration of wind turbine blade due to ice accretion," Proceedings of ASME FEDSM'03, 4th ASME_JSME Joint Fluids Engineering Conference, (July 6-10, 2003) 2567-2573.

Peltola, E., Laakso, T., Antikainen, P., Peuranen, S., "Prevention of icing effects," Boreas VI, Pyhätunturi, Finland, 9-11 April 2003.

Prandtl, L. and Tietjens, O. Applied Hydro- and Aeromechanics. Dover Publications, Inc., New York, NY, 1934, 3.

Rissanen, S., Uski, S., "Modeling and measurements of dynamic loads of an arctic wind turbine," BOREAS VII Proceedings, Saariselka, 7-8 March 2005.

Roeseler B., "Composite wings and wind power," WIGO open session, 27 October, 2006.

Rondeau, J. "Rondeau opens national wind energy conference," Winnipeg, Canada. 23-October 2006. <http://news.gov.mb.ca/news/index,print.html?archive=&item=178>. accessed 2-Dec-06.

Seifert, H., "Risk analysis of ice throw from wind turbines," BOREAS VI, Pyhätunturi, Finland, 9-11 April 2003a.

Seifert, H., "Technical requirements for rotor blades operating in cold climate," Boreas VI, Pyhätunturi, Finland, 9-11 April 2003b.

Statistics Canada, "Natural background: extreme weather conditions, Canadian climate trends and events, teacher answer sheet," Canada.

<http://www.statcan.ca.proxy1.lib.umanitoba.ca/english/kits/hae2000/xtrem3.htm>. accessed 6-Dec-2006.

Stiesdal, H., The wind turbine: components and operation, bonus-info 1998, newsletter, Autumn 1999, 5-10.

Thermion 2005a. " Flexible heating elements-technology," <http://www.thermion.com/heaters/technology.html>, accessed 5-May-2005.

Thermion 2005b. "Flexible heating elements-advantages," <http://www.thermion.com/heaters/advantages.html>, accessed 5-May-2005.

Thermion 2005c, "Thermion technology," Thermion Systems International Information Package, 5 May, 2005.

Thermion 2005d, "Rotorcraft," <http://thermion.com/aerospace/rotorcraft.html>, accessed 5-May-2005.

Thomas, S.K., et al., "Aircraft anti-icing and de-icing techniques and modeling," Journal of Aircraft, 33.5 (September-October 1996): 841-854.

Tufram, "'Synergistic' surface enhancement coatings protect aluminum and aluminum allows against wear, corrosion, sticking and galling." General Magnaplate Corp. 30 December, 2002. <www.magnaplate.com> accessed 18- May-05.

US Army Corp of Engineers (USACE), Cold Regions Research & Engineering Laboratory, "Progress in evaluating surface coatings for icing control at corps hydraulic structures," Ice Engineering, ERDC/CRREL Technical Note 03-4, October 2003, 1-8.

Vattenfall, "Vindmannen—efficient wind power in the mountains," Vattenfall Support AB, Inhouse. Stockholm 09-2001.

Woods, J. "Ice and wind factors in wind turbine output in southern Manitoba," Report prepared for Emerging Energy Systems, Manitoba Hydro. February 2007.
Yukon Energy, "Viewing Whitehorse from above: a guide to Haeckel Hill,".

Wearlon 2005a, "Wearlon coatings technical data," <http://www.wearlon.com/ETechData.html> accessed 5-May-05.

Wearlon 2005b, "Wearlon: Wearlon anti-graffiti, Wearlon non-stick, Wearlon foul-release, Wearlon M…," <http://www.wearlon.com/EHome.html> accessed 5-May-05.

Wikipedia, "Contact_angle." *Wikipedia, the free encyclopedia.* 5 Jan. 2007. <Reference.com http://www.reference.com/browse/wiki/Contact_angle>.

Wikipedia, "Hydrophobe." *Wikipedia, the free encyclopedia.* 16 Dec. 2006. <Reference.com http://www.reference.com/browse/wiki/Hydrophobe>.

8 APPENDICES

A. UMITF CALIBRATION DATA

B. SHAPE CATALOGUE

C. MITIGATION FORECASTING TOOL

D. COST OF THERMAL MITIGATION CALCULATION

E. COLLECTED DATA & RESULTS CALCULATIONS

F. ADHESION FORCE CALCULATIONS

G. CHARTS FOR PERCENTAGE REDUCTION OF ICING CHARACTERISTICS

H. ICING CHARACTERISTICS AND MITIGATION STRATEGIES FOR WIND TURBINES IN COLD CLIMATES: PART 1

I. ICING CHARACTERISTICS AND MITIGATION STRATEGIES FOR WIND TURBINES IN COLD CLIMATES, PART 2: PROFILE SHAPE EXTENSION

J. ICING CHARACTERISTICS AND MITIGATION STRATEGIES FOR WIND TURBINES IN COLD CLIMATES, PART 3: ACCUMULATION RATE

K. IMPACT OF MITIGATION STRATEGIES ON ICING ACCUMULATION RATE FOR WIND TURBINES IN COLD CLIMATES

L. APPLICATION OF COATINGS FOR ICING MITIGATION OF WIND TURBINES IN COLD CLIMATES

APPENDIX A

UMITF CALIBRATION DATA

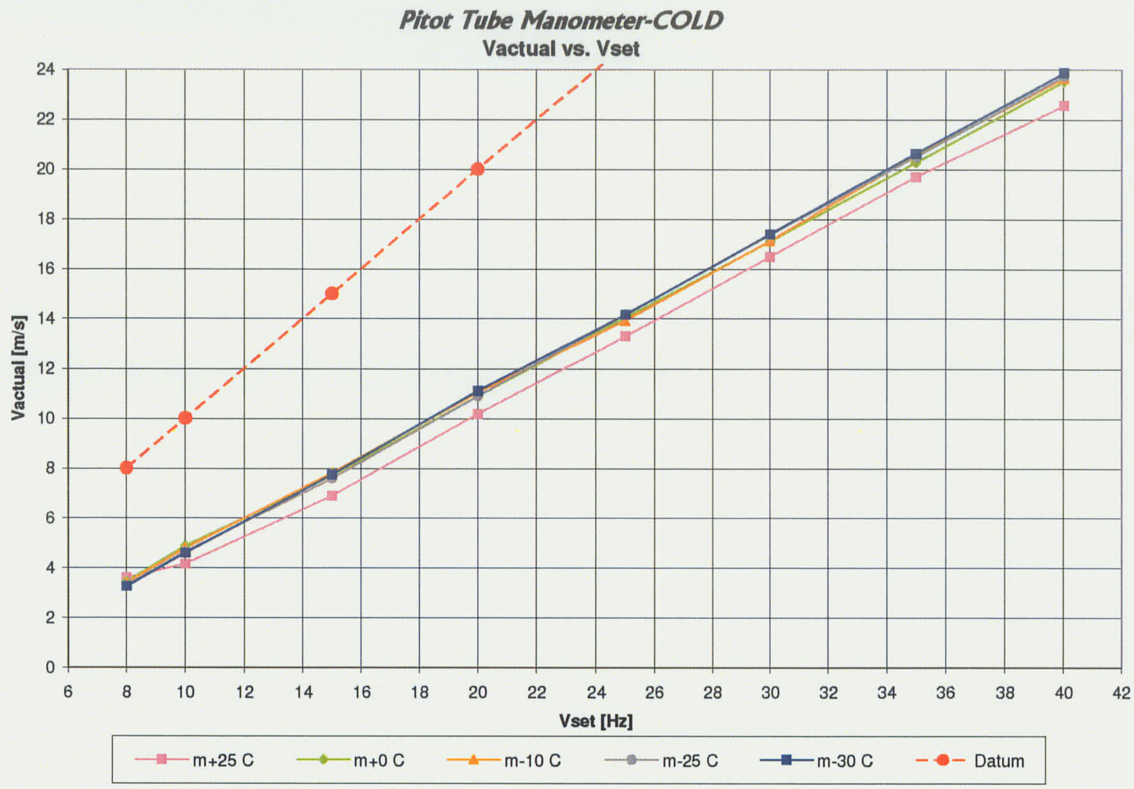
Pitot Tube Manometer-COLD
Vactual vs. Vset
Vactual [m/s]
Vset [Hz]
m+25 C
m+0 C
m-10 C
m-25 C
m-30 C
Datum

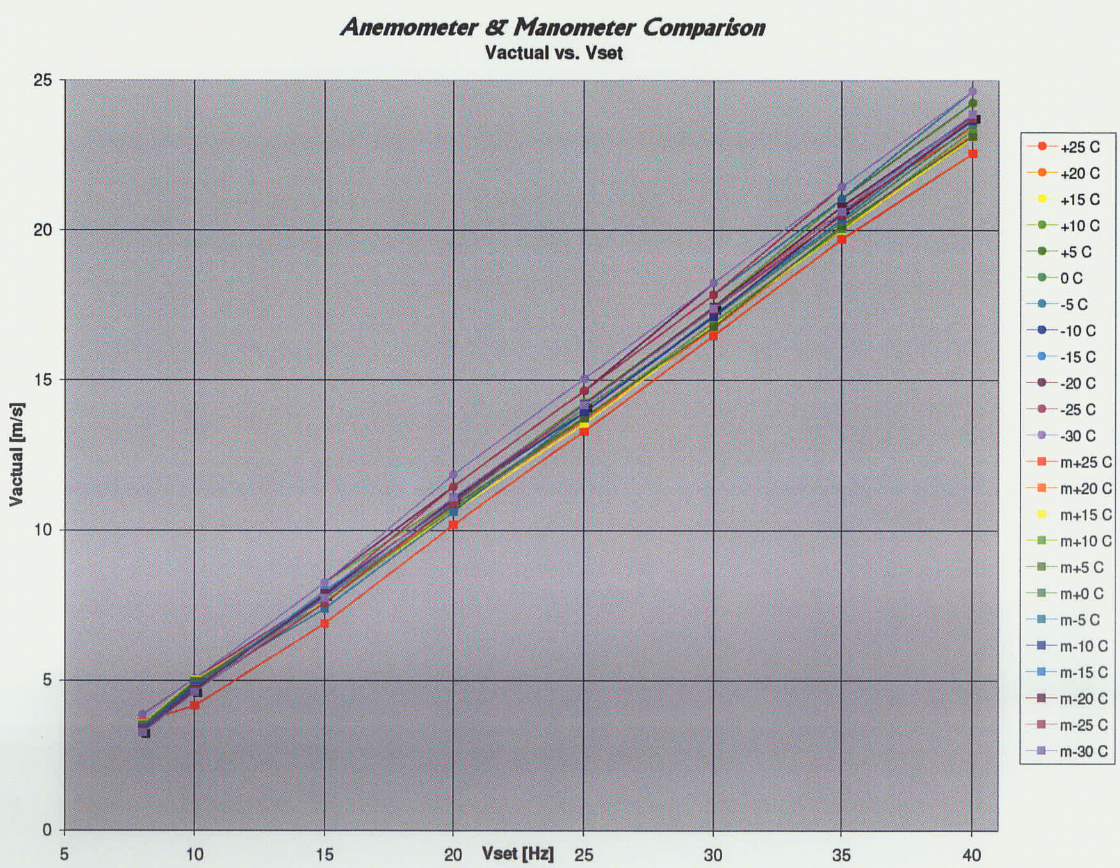
Anemometer & Manometer Comparison
Vactual vs. Vset
Vactual [m/s]
Vset [Hz]
+25 C
+20 C
+15 C
+10 C
+5 C
0 C
-5 C
-10 C
-15 C
-20 C
-25 C
-30 C
m+25 C
m+20 C
m+15 C
m+10 C
m+5 C
m+0 C
m-5 C
m-10 C
m-15 C
m-20 C
m-25 C
m-30 C

Pitot Tube Manometer
Gage Reading with Pitot Tube (Velocity Pressure) [in H2O] vs. Pitot Tube Air Velocity [m/s]

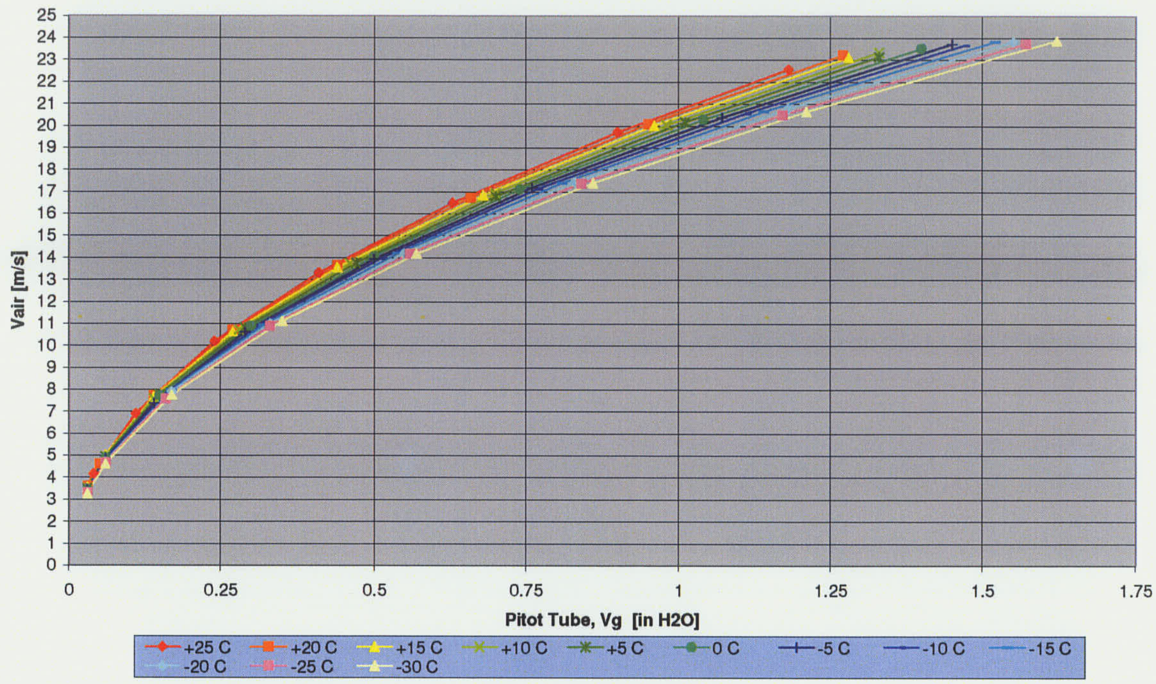

Pitot Tube Manometer
Vactual vs. Vset

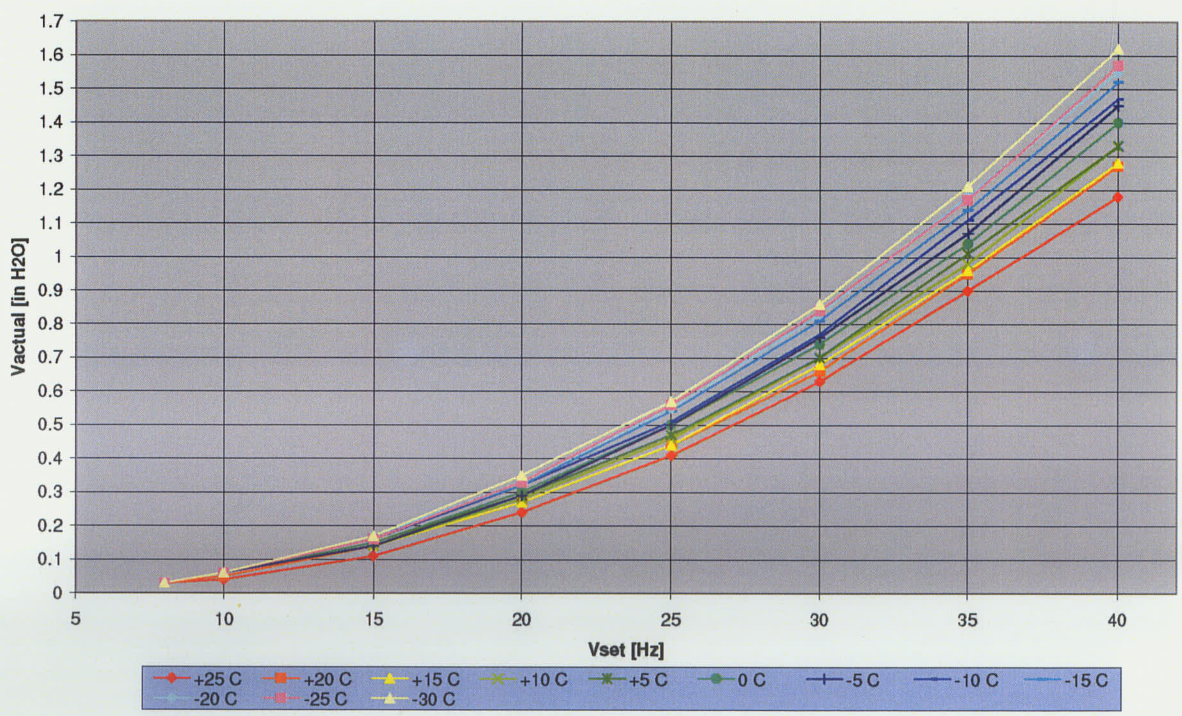

APPENDIX B

SHAPE CATALOGUE

Experiment List					LE Shape Profile Intervals		
Test Description		specimen	thermal regime		1 min	10 mins.	20 mins.
Surface	glaze	plain	-	-			
		icephobic	-	-			
		hydrophobic	-	-			
	rime	plain	-	-			
		icephobic	-	-			
		hydrophobic	-	-			
Thermal	glaze	plain	anti-icing	-			
		plain	-	de-icing			
	rime	plain	anti-icing	-			
		plain	-	de-icing			
Thermface	glaze	icephobic	anti-icing	-			
		hydrophobic	anti-icing	-			
		icephobic	-	de-icing			
		hydrophobic	-	de-icing			
	rime	icephobic	anti-icing	-			
		hydrophobic	anti-icing	-			
		icephobic	-	de-icing			

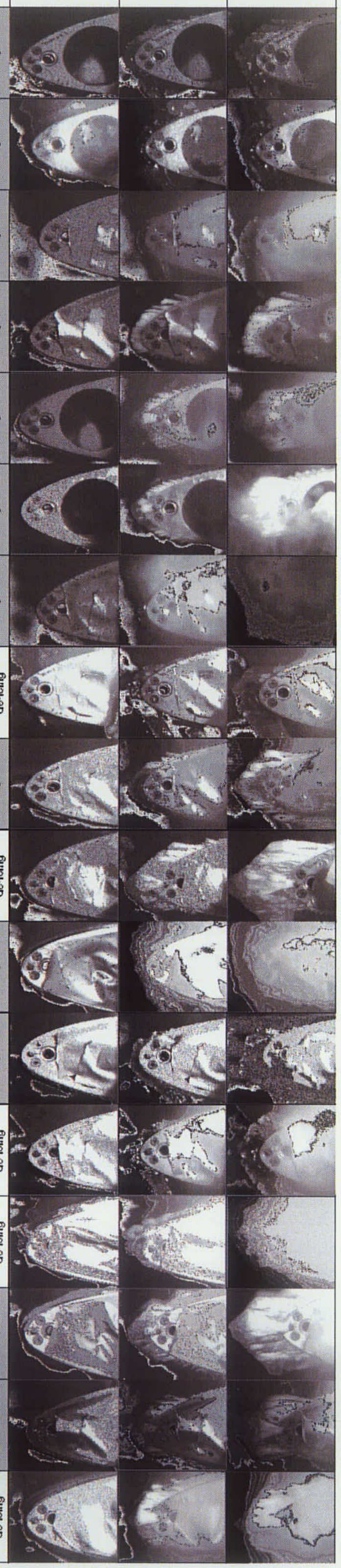

Experiment List					LE Shape Profile Intervals		
Test Description		specimen	thermal regime		1 min	10 mins.	20 mins.
Surface	glaze	plain	-	-		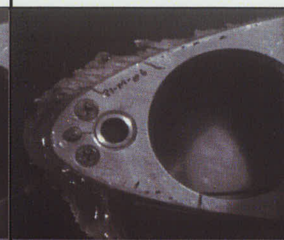	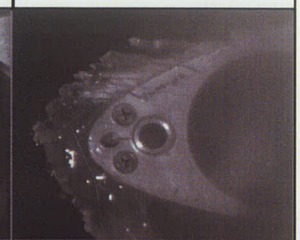
Surface	glaze	icephobic	-	-			
Surface	glaze	hydrophobic	-	-			
Surface	rime	plain	-	-	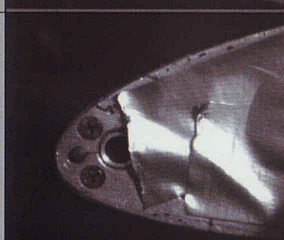		
Surface	rime	icephobic	-	-		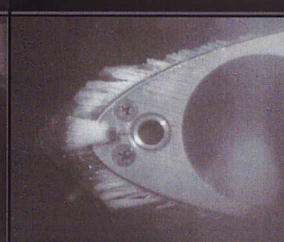	
Surface	rime	hydrophobic	-	-			

Experiment List				LE Shape Profile Intervals		
Test Description		specimen	thermal regime	1 min	10 mins.	20 mins.
Thermal	glaze	plain	anti-icing	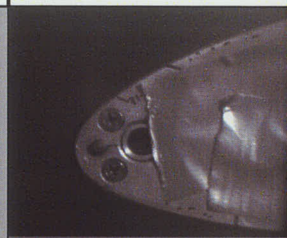		
Thermal	glaze	plain	de-icing	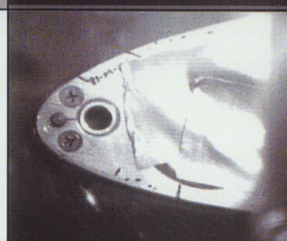		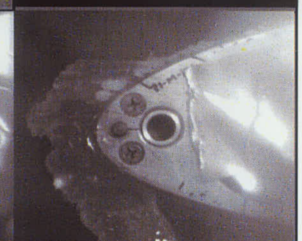
Thermal	rime	plain	anti-icing	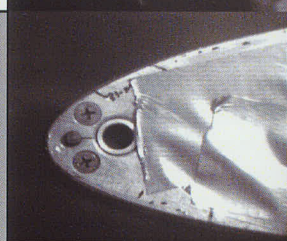	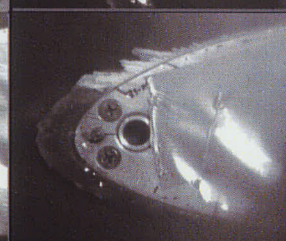	
Thermal	rime	plain	de-icing	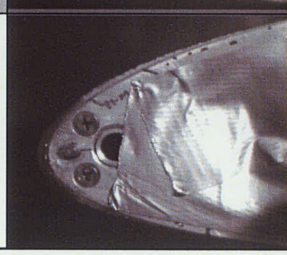		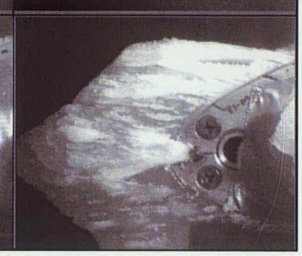

Experiment List					LE Shape Profile Intervals		
Test Description		speci men	thermal regime		1 min	10 mins.	20 mins.
Thermface	glaze	icephobic	anti-icing	-			
		hydrophobic	anti-icing	-			
		icephobic	-	de-icing			
		hydrophobic	-	de-icing			
	rime	icephobic	anti-icing	-			
		hydrophobic	anti-icing	-			
		icephobic	-	de-icing			
		hydrophobic	-	de-icing			

*Incomplete duration of test, limited to 15 mins max, midpoint is at 7 mins.

APPENDIX C

MITIGATION FORECASTING TOOL

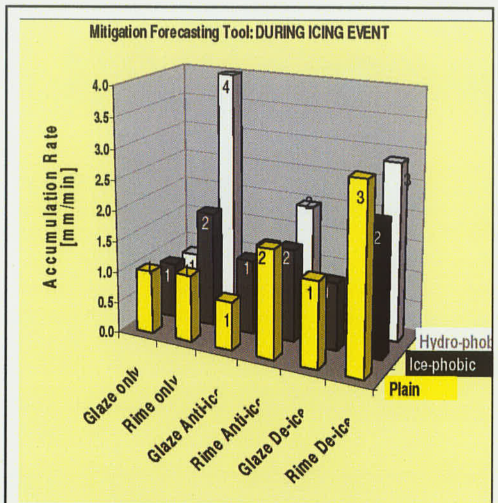
Mitigation Forecasting Tool: DURING ICING EVENT
Accumulation Rate [mm/min]
Glaze only
Rime only
Glaze Anti-ice
Rime Anti-ice
Glaze De-ice
Rime De-ice
Hydro-phobic
Ice-phobic
Plain

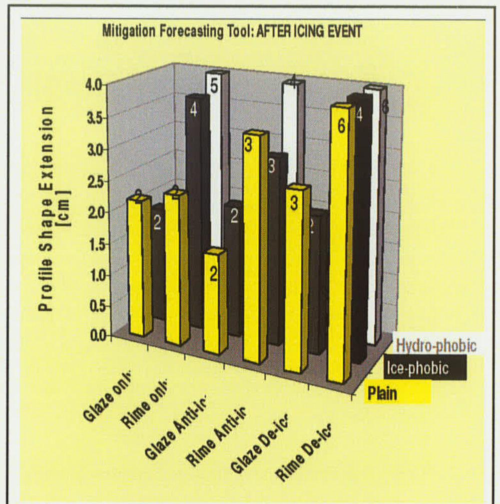
Mitigation Forecasting Tool: AFTER ICING EVENT
Profile Shape Extension [cm]
Glaze only
Rime only
Glaze Anti-ice
Rime Anti-ice
Glaze De-ice
Rime De-ice
Hydro-phobic
Ice-phobic
Plain

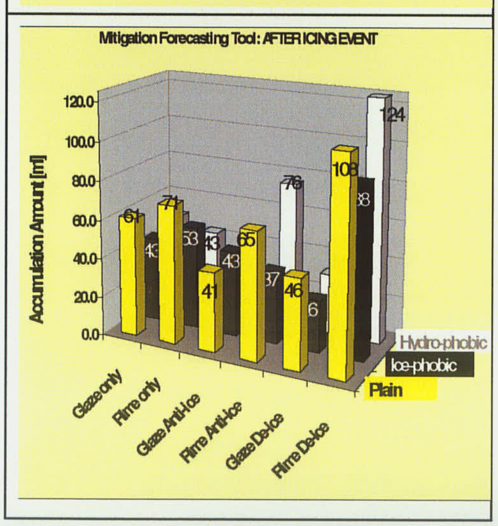
Mitigation Forecasting Tool: AFTER ICING EVENT
Accumulation Amount [ml]
Glaze only
Rime only
Glaze Anti-ice
Rime Anti-ice
Glaze De-ice
Rime De-ice
Hydro-phobic
Ice-phobic
Plain

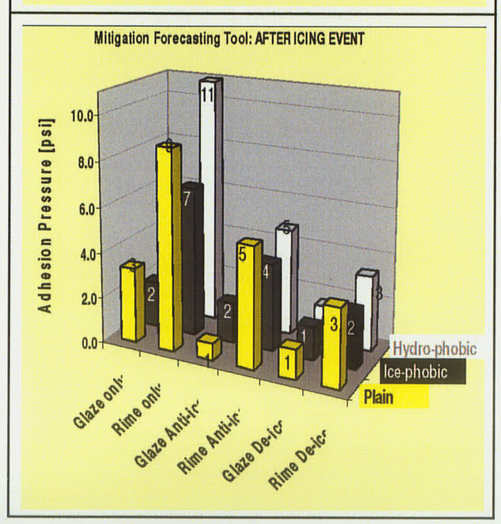
Mitigation Forecasting Tool: AFTER ICING EVENT
Adhesion Pressure [psi]
Glaze only
Rime only
Glaze Anti-ice
Rime Anti-ice
Glaze De-ice
Rime De-ice
Hydro-phobic
Ice-phobic
Plain

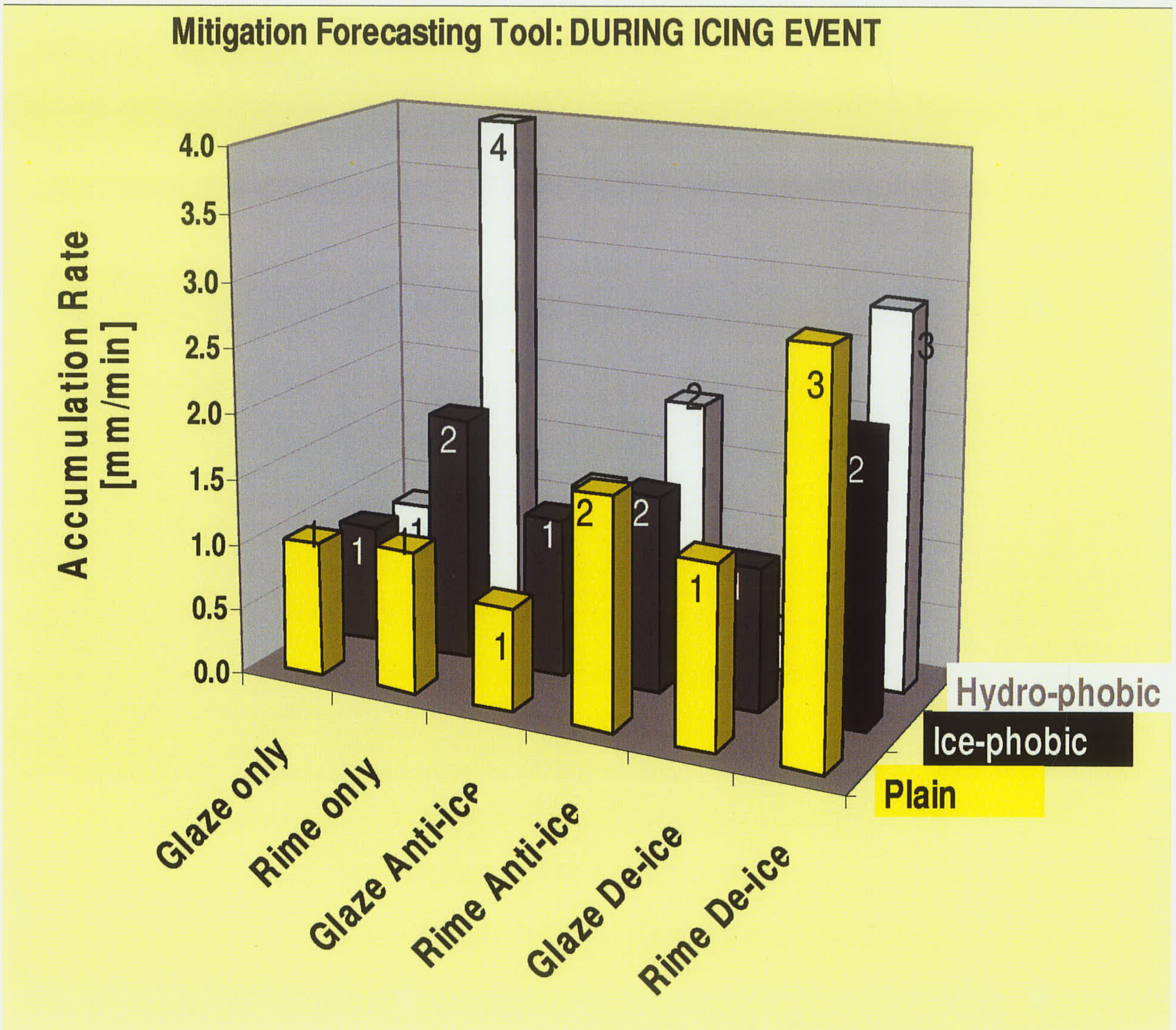
Mitigation Forecasting Tool: DURING ICING EVENT
Accumulation Rate [mm/min]
4.0
3.5
3.0
2.5
2.0
1.5
1.0
0.5
0.0
Glaze only
Rime only
Glaze Anti-ice
Rime Anti-ice
Glaze De-ice
Rime De-ice
Hydro-phobic
Ice-phobic
Plain

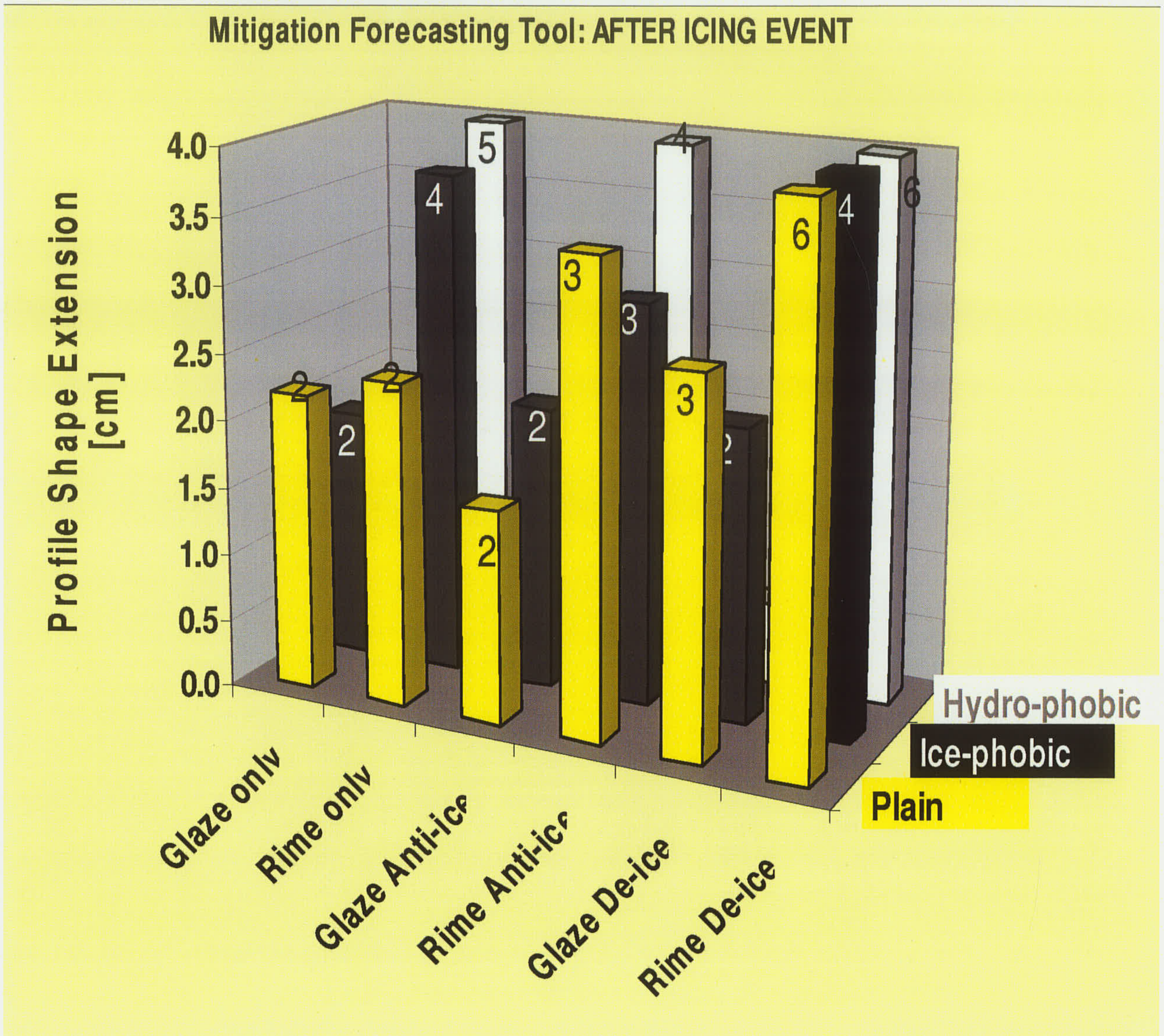

Mitigation Forecasting Tool: AFTER ICING EVENT
Profile Shape Extension
[cm]
4.0
3.5
3.0
2.5
2.0
1.5
1.0
0.5
0.0
Glaze only
Rime only
Glaze Anti-ice
Rime Anti-ice
Glaze De-ice
Rime De-ice
Hydro-phobic
Ice-phobic
Plain

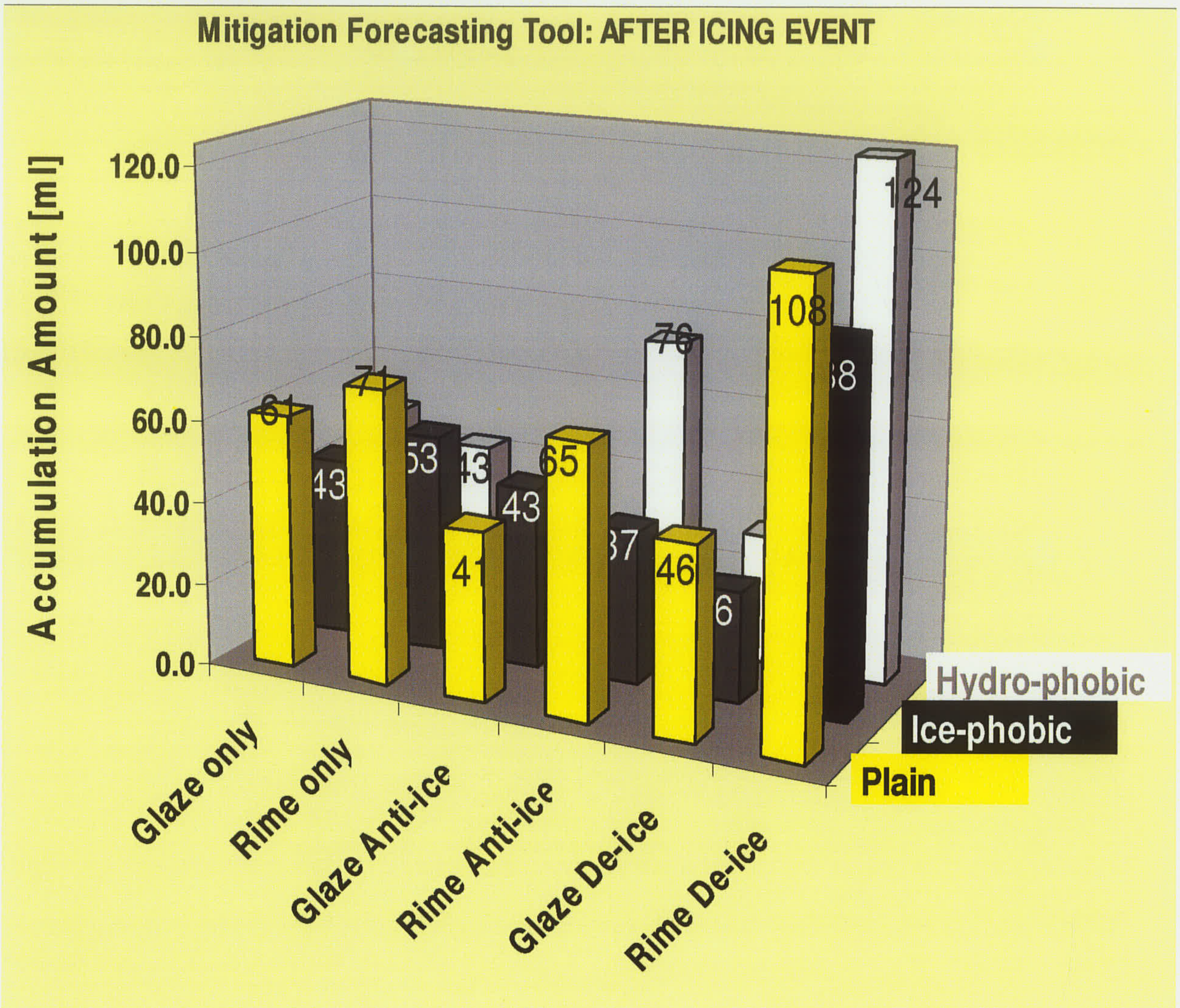
Mitigation Forecasting Tool: AFTER ICING EVENT
Accumulation Amount [ml]
120.0
100.0
80.0
60.0
40.0
20.0
0.0
Glaze only
Rime only
Glaze Anti-ice
Rime Anti-ice
Glaze De-ice
Rime De-ice
Hydro-phobic
Ice-phobic
Plain
124
108
76
71
65
61
53
46
43
43
43
41

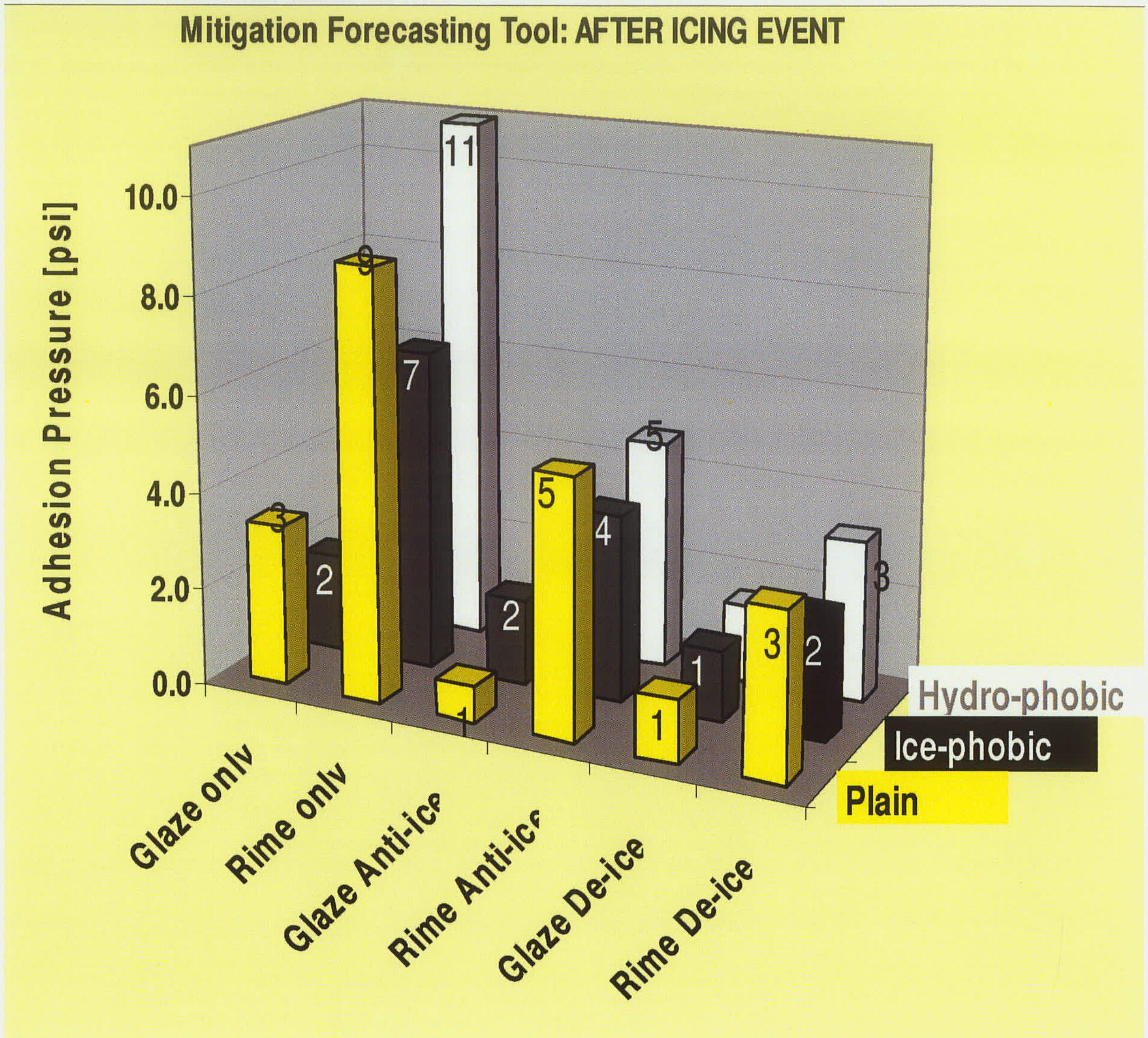
Mitigation Forecasting Tool: AFTER ICING EVENT
Adhesion Pressure [psi]
10.0
8.0
6.0
4.0
2.0
0.0
3
2
9
7
11
1
2
5
4
5
1
1
3
2
3
Glaze only
Rime only
Glaze Anti-ice
Rime Anti-ice
Glaze De-ice
Rime De-ice
Hydro-phobic
Ice-phobic
Plain

APPENDIX D

COST OF THERMAL MITIGATION CALCULATION

The Cost of Heater Mitigation

The selected and tested Thermion heaters have the following parameters

Thermion	Size	Operating Voltage	Output Power	Heated Area	Heated Area Watt Density
imperial	2"x5"	12V	5W	10 in^2	0.5 W/in^2
metric	.0508m x 0.127m	12V	5W	.00645m^2	775W/m^2

12

	Expt Sample		WT blade, Full-Scale	
	metric	imperial	metric	
Length [m]:	0.0635	2.5	40	
Root Chord [m]:	0.5	19.5	3.048	
Tip Chord [m]:	0.5	19.5	0.3048	
Planform Area [m^2]:	0.03175	48.75	67.056	
Surface Area [m^2]:	0.0635	97.5	134.112	
% Heater Area of S.A.	10.1575	10.26	10.00	extrapolated

Req'd Heater Area [m^2]:	13.4112	
Req'd Power [W]:	10393.68	
1 Blade, Req'd Power [KW]:	10.39	per blade
3 Blades, Req'd Power [KW]:	31.18	per turbine
63 Turbines, Wind Farm, Req'd Power	1.96	for St. Leon Wind Farm
For 100MW Wind Farm, [%]:	2	
Protection only 6 months of the year (Nov-May); realistic operational effect [%]:	1	

Note:

*This analysis has been approximated based ona wind farm of 63 turbines, producing a 100MW.
*This results in 1.5 MW per turbine

*The heating required per turbine (of 3 blades) is 31.2 KW
*This translates into ~2% of a turbine's electrical production for heating the blades

Conclusion:

~31 KW/turbine or 2% of 100 MW wind farm or 1% of the annual production of a 100 MW wind farm, goes into heating the blades of the wind turbine, using these electrical heaters

COST OFFSETS:

1. Since Energy production is increased in winter months due to colder more dense air mass, this offsets the cost of the ice-protection heating system.

2. Since the system would have a protection system it can optimize energy production by more readily operating at critical times rather then being shut down. This further offsets the cost of the system, such that the system practically pays for itself while enhancing energy production opportunities.

APPENDIX E

COLLECTED DATA & RESULTS CALCULATIONS

Experimental Test Matrix **RAW DATA**

	Experiment List		specimen	anti-icing	de-icing	rate accumulation [m/s]	adhesion force [lbs]				Avg. adh force [lbs]	LE Area [in^2]				Avg. Adhesion Pressure (Shear) [psi]	accumulation amounts from LE [ml]						Avg. Accm amt [ml]	Shape Profile Length [cm] 20mins
Test Description							readings					readings					readings							
1	Surface	glaze	yellow	only	n/a	1.7E-05	61	10	112	16.75	21.8	7.5	5.63	-	-	3.3	72	52	105	44	55	39	61.2	2.2
		glaze	black	only	n/a	1.5E-05	21	35	42	-	10.2	5.31	4.83	-	-	2.0	65	17	48	-	-	-	43.3	1.8
		glaze	white	only	n/a	1.4E-05	2	41	20	-	6.6	5	7.88	-	-	1.0	92	23	33	-	-	-	49.3	1.6
		rime	yellow	only	n/a	1.8E-05	100	141	46	48	52.7	8.03	7.34	2.53	-	8.8	42	118	126	56	12	-	70.8	2.4
		rime	black	only	n/a	3.1E-05	100	148		-	38.8	2.25	9.5	-	-	6.6	66	13	79	-		-	52.7	3.7
		rime	white	only	n/a	6.9E-05	114	148		-	40.9	2.97	4.5	-	-	11.0	92	15	23	-		-	43.3	4.8
2	Thermal	glaze	yellow	yes	-	1.3E-05	15	1	52	32	7.8	7.19	10.6	8.13	-	0.9	40	46	24	40	53	-	40.6	1.6
		glaze	yellow	-	yes	2.3E-05	33	1	44	58	10.6	8.77	8.75	7.59	-	1.3	60	30	59	24	55	-	45.6	2.7
		rime	yellow	yes	-	2.9E-05	63	115	-		27.8	6.88	3.38	5	5.84	5.3	90	18	53	99	-	-	65.0	3.5
		rime	yellow	-	yes	5.0E-05	76.6	92	103		28.3	8.13	8.75	8.13		3.4	64	158	102	-			108.0	5.8
3	Thermface	glaze	black	yes	-	2.0E-05	20	88	32		14.6	7.54	9.06	-	-	1.8	38	49	43		-	-	43.3	2.1
		glaze	white	yes	-	2.0E-05	15	53	50		12.3	8.75	7.5	-	-	1.5	30	19	53		-	-	34.0	2.4
		glaze	black	-	yes	1.8E-05	20	47	-		10.5	6.88	7.5	-	-	1.5	15	25	39		-	-	26.3	2.2
		glaze	white	-	yes	0.5E-05	22.5	26	44		9.6	7.5	4.78	-	-	1.6	20	35	39		-	-	31.3	0.6
		rime	black	yes	-	2.5E-05	77		-		24.1	6.25	6.25	-	-	3.9	20	54	-		-	-	37.0	3.0
		rime	white	yes	-	3.3E-05	59	125	-		28.8	5.73	6.25	6.25	-	4.7	110	45	72		-	-	75.7	4.0
		rime	black	-	yes	3.6E-05	52.6	60	76	-	19.6	6.27	9.38	8.13		2.5	64	100	100	-			88.0	4.3
		rime	white	-	yes	4.8E-05	81.6	66	84	-	24.1	6.41	7.42	8.13		3.3	46	94	232	-			124.0	6.0

Collected Experimental Data

Adhesion Force

[lbs]	plain	iceph	hydph
Glaze only	21.85	10.21	6.56
Rime only	52.72	38.75	40.94
Glaze Anti-ice	6.25	14.58	12.29
Rime Anti-ice	27.81	24.06	28.75
Glaze De-ice	10.63	10.47	9.64
Rime De-ice	28.29	19.65	24.13

LE H20 Accmulation

[ml]	plain	iceph	hydph
Glaze only	61.17	43.33	49.33
Rime only	70.80	52.67	43.33
Glaze Anti-ice	40.60	43.33	34.00
Rime Anti-ice	65.00	37.00	75.67
Glaze De-ice	45.60	26.33	31.33
Rime De-ice	108.00	88.00	124.00

Accumulation Rate

[m/s]	plain	iceph	hydph
Glaze only	1.02	0.90	0.84
Rime only	1.08	1.86	4.14
Glaze Anti-ice	0.78	1.20	1.20
Rime Anti-ice	1.74	1.50	1.98
Glaze De-ice	1.38	1.08	0.30
Rime De-ice	3.00	2.16	2.88

Shape Profile Extension

[cm]	plain	iceph	hydph
Glaze only	2.19	1.85	1.63
Rime only	2.38	3.73	4.75
Glaze Anti-ice	1.56	2.09	2.44
Rime Anti-ice	3.46	2.95	3.96
Glaze De-ice	2.75	2.16	0.61
Rime De-ice	5.84	4.30	5.99

Adhesion Pressure

[psi]	plain	iceph	hydph
Glaze only	3.33	2.01	1.02
Rime only	8.84	6.60	10.96
Glaze Anti-ice	0.72	1.76	1.51
Rime Anti-ice	5.27	3.85	4.73
Glaze De-ice	1.27	1.46	1.57
Rime De-ice	3.40	2.48	3.30

Calculated Results for Percentage Reduction of Icing Characteristics

Adhesion Force			
[lbs]	plain	iceph	hydph
Glaze only	0.0	53.3	70.0
Rime only	0.0	26.5	22.3
Glaze Anti-ice	71.4	33.2	43.7
Rime Anti-ice	47.2	54.4	45.5
Glaze De-ice	51.4	80.1	81.7
Rime De-ice	46.3	62.7	54.2

LE H20 Accmulation			
[ml]	plain	iceph	hydph
Glaze only	0.0	29.2	19.3
Rime only	0.0	25.6	38.8
Glaze Anti-ice	33.6	29.2	44.4
Rime Anti-ice	8.2	47.7	-6.9
Glaze De-ice	25.4	62.8	55.7
Rime De-ice	-52.5	-24.3	-75.1

Accumulation Rate			
[m/s]	plain	iceph	hydph
Glaze only	0.0	11.8	17.6
Rime only	0.0	-72.2	-283.3
Glaze Anti-ice	23.5	-17.6	-17.6
Rime Anti-ice	-61.1	-38.9	-83.3
Glaze De-ice	-35.3	0.0	72.2
Rime De-ice	-177.8	-100.0	-166.7

Shape Profile Extension			
[cm]	plain	iceph	hydph
Glaze only	0.0	15.7	25.4
Rime only	0.0	-56.5	-99.2
Glaze Anti-ice	28.5	4.4	-11.4
Rime Anti-ice	-45.1	-23.8	-65.9
Glaze De-ice	-25.5	9.4	74.5
Rime De-ice	-145.0	-80.2	-151.3

Adhesion Pressure			
[psi]	plain	iceph	hydph
Glaze only	0.0	39.6	69.4
Rime only	0.0	25.3	-24.1
Glaze Anti-ice	78.3	47.2	54.6
Rime Anti-ice	40.3	56.4	46.4
Glaze De-ice	61.9	83.5	82.2
Rime De-ice	61.6	71.9	62.7

	Experiment List		specimen	anti-icing	de-icing	Rate Accumulation [icebuildup/time]																					metric	imperial
	Test Description					readings																			min.	avg.	avg.	avg.
						1	2	3	4	5	6	7	8	9	10	11	12	13	14	15	16	17	18	19	20	[cm/min]	[m/s]	[in/s]
1	Surface	glaze	yellow	only	n/a	0.227	0.357	0.482	0.568	0.673	0.766	0.854	0.932	1.012	1.128	1.228	1.338	1.432	1.539	1.647	1.77	1.873	1.988	2.096	2.189	0.10326	0.000017	0.00068
			difference				0.13	0.125	0.086	0.105	0.093	0.088	0.078	0.079	0.116	0.101	0.109	0.094	0.108	0.107	0.123	0.104	0.115	0.107	0.094			
			black	only	n/a	0.105	0.184	0.23	0.289	0.367	0.425	0.531	0.668	0.956	1.097	1.129	1.177	1.268	1.378	1.428	1.506	1.653	1.688	1.786	1.846	0.09164	0.000015	0.00060
			difference				0.08	0.046	0.059	0.078	0.058	0.107	0.137	0.287	0.141	0.033	0.048	0.091	0.109	0.051	0.078	0.147	0.035	0.098	0.06			
			white	only	n/a	0.149	0.206	0.279	0.316	0.453	0.514	0.607	0.705	0.769	0.872	0.946	1.041	1.121	1.207	1.294	1.365	1.437	1.557	1.633	1.633	0.08241	0.000014	0.00054
			difference				0.057	0.073	0.038	0.137	0.061	0.093	0.098	0.064	0.103	0.074	0.095	0.08	0.086	0.086	0.072	0.072	0.12	0.075				
		rime	yellow	only	n/a	0.052	0.213	0.382	0.528	0.592	0.715	0.861	0.984	1.108	1.153	1.244	1.346	1.459	1.557	1.617	1.712	1.823	1.896	1.957	2.384	0.12277	0.000020	0.00081
			difference				0.161	0.169	0.147	0.064	0.122	0.146	0.124	0.124	0.045	0.091	0.103	0.113	0.098	0.06	0.095	0.111	0.073	0.06	0.428			
			black	only	n/a	0.174	0.309	0.502	0.629	0.743	0.955	1.402	1.541	1.743	2.035	2.208	2.354	2.476	2.681	2.877	3.064	3.199	3.431	3.575	3.733	0.18732	0.000031	0.00123
			difference				0.136	0.192	0.128	0.114	0.211	0.447	0.139	0.202	0.292	0.173	0.146	0.122	0.205	0.195	0.187	0.135	0.232	0.144	0.157			
			white	only	n/a	0.214	0.737	0.953	1.201	1.613	1.715	1.94	2.095	2.307	2.568	2.83	3.092	3.353	3.615	3.877	4.138	4.4	4.662	4.923	5.185	0.26165	0.000044	0.00172
			difference				0.523	0.216	0.248	0.412	0.102	0.225	0.155	0.212	0.262	0.262	0.262	0.262	0.262	0.262	0.262	0.262	0.262	0.262	0.262	Had to approx. due to experimental outliers+AS85		
2	Thermal	glaze	yellow	yes	-	0.064	0.147	0.315	0.349	0.434	0.563	0.599	0.633	0.778	0.936	0.979	1.063	1.136	1.187	1.259	1.273	1.363	1.439	1.462	1.565	0.07897	0.000013	0.00052
							0.083	0.168	0.033	0.085	0.129	0.036	0.034	0.145	0.158	0.044	0.083	0.074	0.05	0.073	0.014	0.091	0.076	0.023	0.102			
				-	yes	0.236	0.413	0.506	0.644	0.854	0.964	1.157	1.32	1.437	1.562	1.757	1.873	1.974	2.155	2.306	2.373	2.514	2.626	2.748	2.748	0.13954	0.000023	0.00092
							0.177	0.093	0.138	0.211	0.11	0.193	0.163	0.117	0.125	0.195	0.117	0.101	0.181	0.152	0.067	0.141	0.111	0.123				
		rime		yes	-	0.164	0.377	0.573	0.732	0.88	1.009	1.156	1.288	1.444	1.59	1.814	1.986	2.158	2.359	2.549	2.752	2.916	3.09	3.302	3.459	0.17340	0.000029	0.00114
							0.213	0.195	0.16	0.148	0.129	0.147	0.132	0.156	0.145	0.225	0.171	0.172	0.202	0.19	0.203	0.165	0.174	0.212	0.158			
				-	yes	0.719	1.003	1.29	1.597	1.909	2.219	2.517	2.826	3.165	3.42	3.714	4.026	4.529	4.659	4.882	5.213	5.485	5.841	5.841	5.841	0.30125	0.000050	0.00198
							0.283	0.287	0.307	0.312	0.311	0.297	0.309	0.339	0.255	0.294	0.312	0.504	0.13	0.222	0.332	0.271	0.356	0	0			
3	Thermface	glaze	black	yes	-	0.193	0.43	0.591	0.766	0.997	1.148	1.19	1.319	1.415	1.524	1.618	1.741	1.779	1.875	1.929	2.014	2.092	2.092	2.092	2.092	0.11872	0.000020	0.00078
			difference				0.238	0.161	0.175	0.23	0.151	0.042	0.129	0.097	0.109	0.094	0.123	0.037	0.097	0.054	0.085	0.078	0	0	0			
			white	yes	-	0.156	0.286	0.313	0.384	0.461	0.598	0.654	0.744	0.834	0.939	1.168	1.275	1.374	1.482	1.594	1.919	2.051	2.199	2.311	2.439	0.12016	0.000020	0.00079
			difference				0.13	0.027	0.071	0.077	0.137	0.056	0.09	0.09	0.106	0.228	0.107	0.099	0.109	0.111	0.326	0.131	0.149	0.112	0.128			
			black	-	yes	0.137	0.351	0.458	0.537	0.618	0.717	0.872	0.998	1.057	1.125	1.239	1.343	1.459	1.537	1.611	1.793	1.892	1.975	2.048	2.16	0.10650	0.000018	0.00070
			difference				0.215	0.106	0.08	0.081	0.099	0.154	0.126	0.059	0.067	0.114	0.103	0.116	0.078	0.073	0.183	0.099	0.083	0.073	0.112			
			white	-	yes	0.053	0.105	0.135	0.161	0.2	0.229	0.257	0.282	0.315	0.34	0.358	0.382	0.401	0.495	0.515	0.523	0.562	0.579	0.589	0.607	0.02916	0.000005	0.00019
			difference				0.051	0.03	0.026	0.038	0.03	0.028	0.025	0.033	0.025	0.018	0.024	0.019	0.094	0.02	0.008	0.039	0.017	0.011	0.018			
		rime	black	yes	-	0.111	0.191	0.28	0.381	0.582	0.758	0.91	1.058	1.18	1.36	1.494	1.633	1.795	2.067	2.337	2.389	2.501	2.612	2.854	2.953	0.14959	0.000025	0.00098
			difference				0.08	0.089	0.101	0.201	0.176	0.151	0.148	0.122	0.18	0.134	0.139	0.163	0.272	0.27	0.051	0.113	0.111	0.242	0.099			
			white	yes	-	0.171	0.193	0.403	0.646	0.881	1.058	1.268	1.496	1.689	1.939	2.137	2.371	2.581	2.806	3.006	3.221	3.392	3.546	3.793	3.955	0.19916	0.000033	0.00131
			difference				0.022	0.21	0.243	0.236	0.177	0.21	0.228	0.193	0.25	0.197	0.234	0.21	0.225	0.2	0.215	0.172	0.154	0.247	0.162			
			black	-	yes	0.213	0.254	0.344	1.022	1.26	1.474	1.773	1.987	2.198	2.396	2.577	2.802	3.025	3.19	3.386	3.598	3.768	3.961	4.146	4.296	0.21488	0.000036	0.00141
			difference				0.041	0.09	0.678	0.238	0.213	0.299	0.214	0.211	0.198	0.181	0.225	0.223	0.165	0.195	0.212	0.17	0.194	0.184	0.15			
			white	-	yes	0.532	0.861	1.105	1.399	1.68	1.976	2.322	2.642	2.94	3.192	3.542	3.838	4.055	4.375	4.627	4.899	5.263	5.545	5.786	5.991	0.28733	0.000048	0.00189
			difference				0.329	0.244	0.295	0.281	0.297	0.346	0.32	0.298	0.252	0.349	0.297	0.217	0.32	0.252	0.272	0.364	0.282	0.241	0.206			

APPENDIX F

ADHESION FORCE CALCULATIONS

Free body diagram of iced aerofoil specimen in adhesion force test rig:

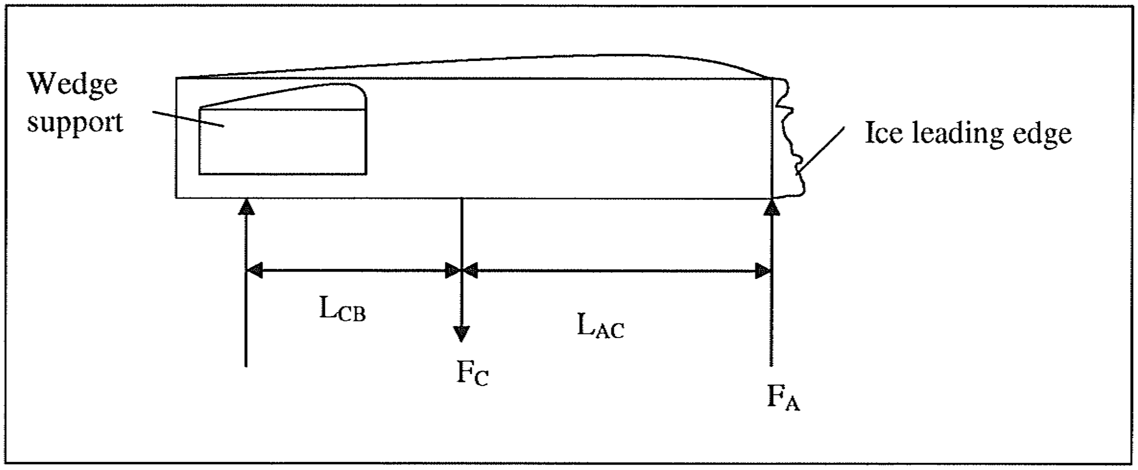

F_A: Force required to shear ice from substrate; a.k.a.: Adhesion Force
F_B: Force due to wedge support for mounting
F_C: Force due to applied load (weights)
L_{AC}: length from leading edge to load application
L_{CB}: length from the load application to the center of the supporting wedge

Taking the sum of moments about the leading edge, point A:

$$(F_C)*(L_{AC}) - F_B*(L_{AC} + L_{CB}) = 0$$

Solving for F_B:

$$F_B = (F_C)*(L_{AC}) /(L_{AC} + L_{CB})$$

Taking the sum of the forces in the vertical direction, positive upwards:

$$F_B + F_A = F_C$$

Solving for the adhesion force, F_A:

$$F_A = F_C - F_B$$

Note: 2 types of specimen geometries were used, due to manufacturing of the components.

	Specimen X	Specimen Y
L_{AC}	7 in.	5 in.
L_{CB}	9 in.	11 in.

APPENDIX G

CHARTS FOR PERCENTAGE REDUCTION OF ICING CHARACTERISTICS

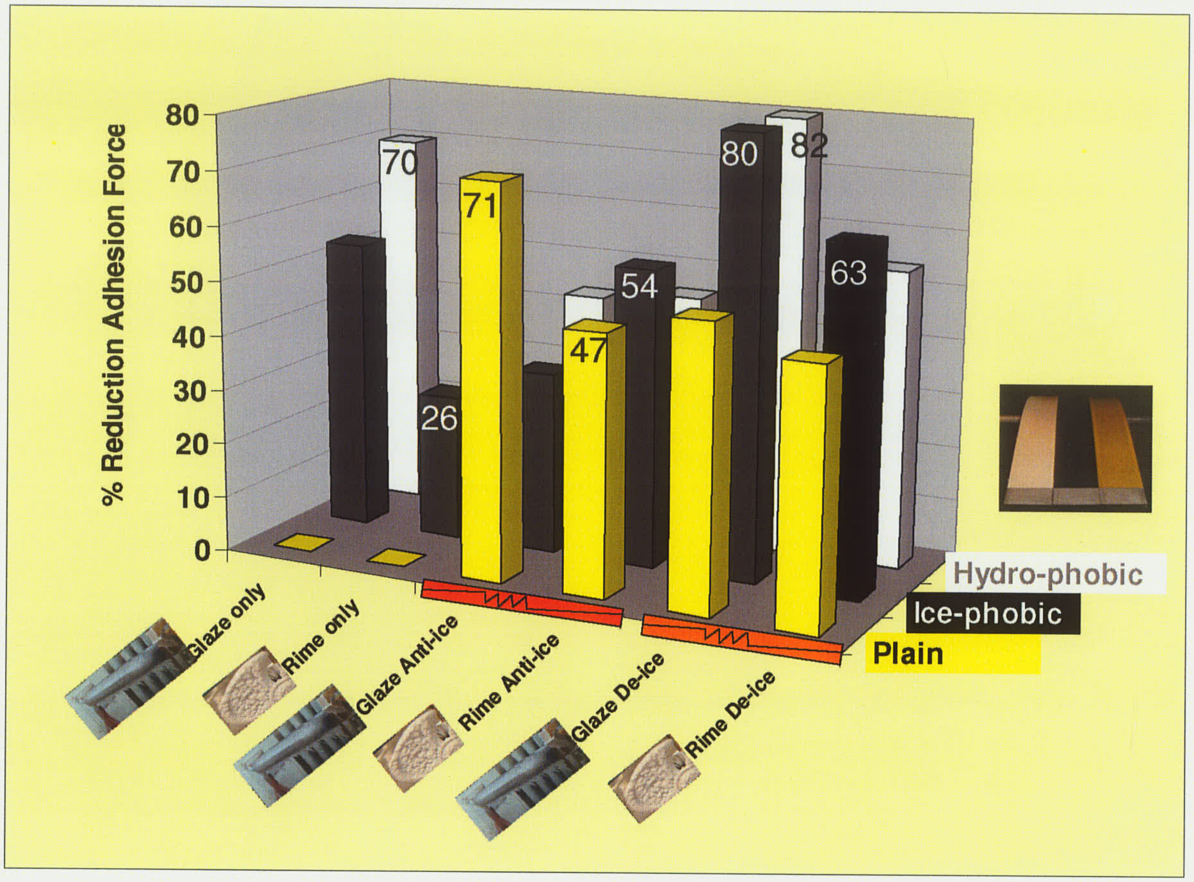
% Reduction Adhesion Force
80
70
60
50
40
30
20
10
0
70
71
26
47
54
80
82
63
Hydro-phobic
Ice-phobic
Plain
Glaze only
Rime only
Glaze Anti-ice
Rime Anti-ice
Glaze De-ice
Rime De-ice

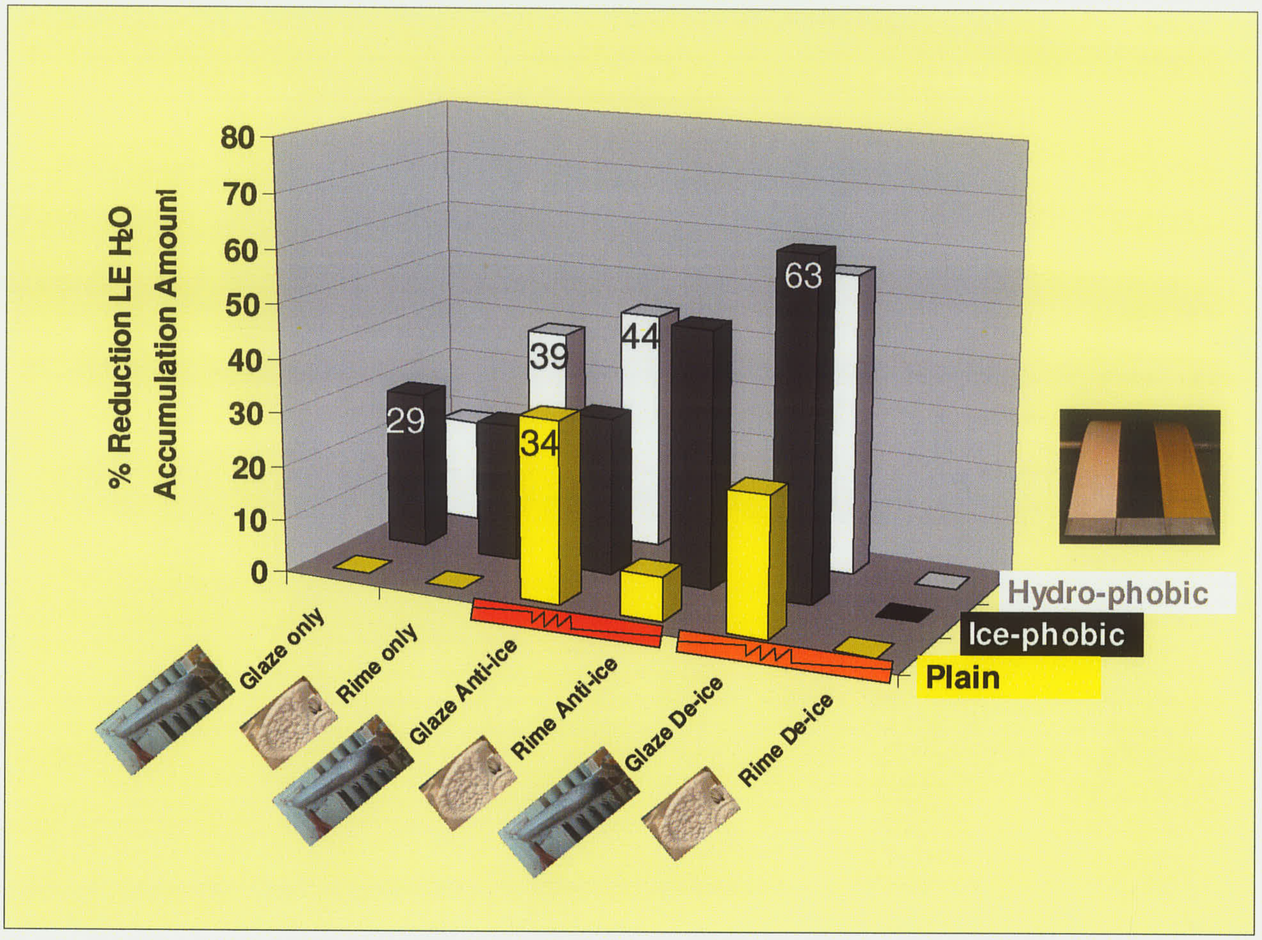
% Reduction LE H_2O Accumulation Amount
80
70
60
50
40
30
20
10
0
29
39
34
44
63
Glaze only
Rime only
Glaze Anti-ice
Rime Anti-ice
Glaze De-ice
Rime De-ice
Hydro-phobic
Ice-phobic
Plain

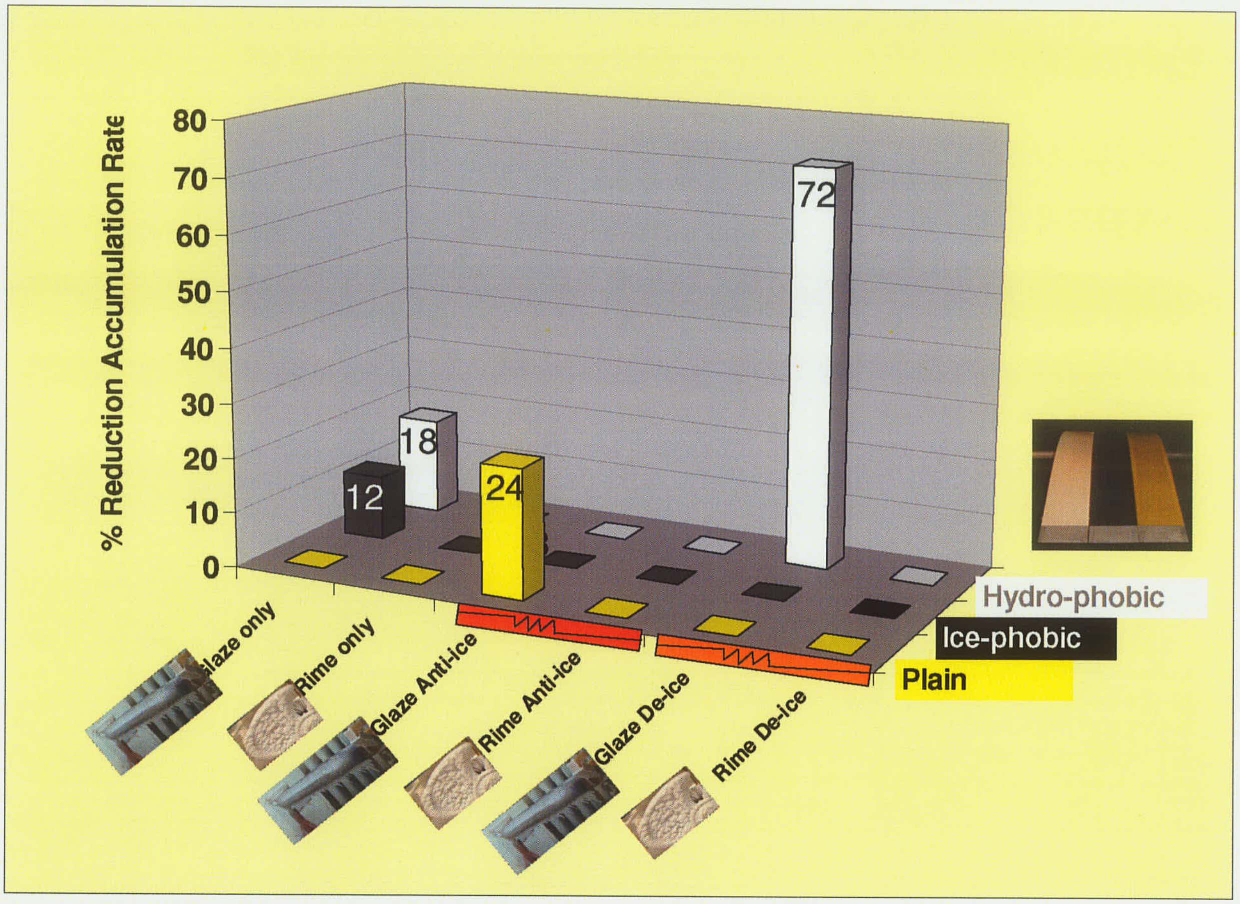

% Reduction Accumulation Rate
80
70
60
50
40
30
20
10
0
72
18
12
24
Hydro-phobic
Ice-phobic
Plain
Glaze only
Rime only
Glaze Anti-ice
Rime Anti-ice
Glaze De-ice
Rime De-ice

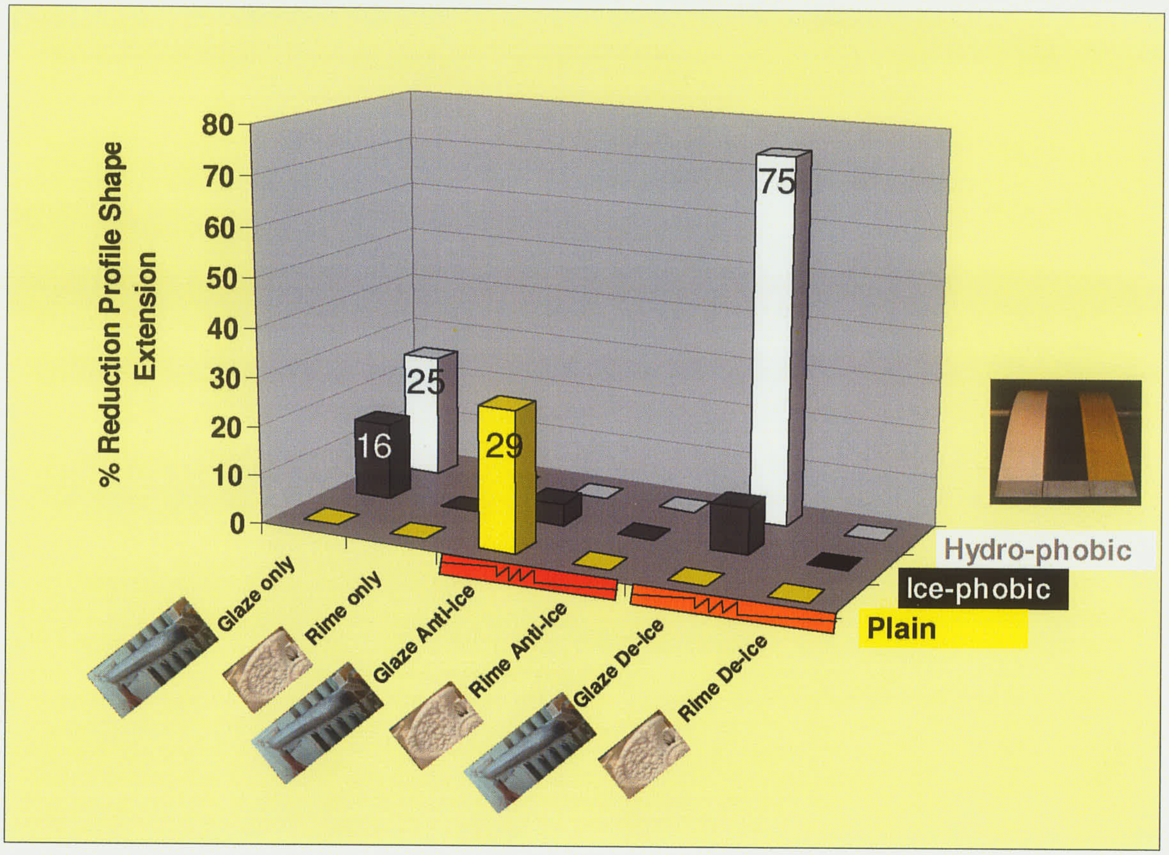
% Reduction Profile Shape Extension
80
70
60
50
40
30
20
10
0
16
25
29
75
Glaze only
Rime only
Glaze Anti-ice
Rime Anti-ice
Glaze De-ice
Rime De-ice
Hydro-phobic
Ice-phobic
Plain

Table 2: Comprehensive Mitigation Results Summary

Comprehensive Results Summary						Adhesion Force				LE H2O Accumulation			
Mitigation						surface	surface	thermal	surface	surface	surface	thermal	surface
		Ice Type	Sample	Anti-icing	De-icing	mit vs. no-mit	thermal vs. no-thermal	surface vs. no-surface	glaze vs. rime	mit vs. no-mit	thermal vs. no-thermal	surface vs. no-surface	glaze vs. rime
1	Surface	glaze	yellow	-	-	0			↓↓	0			↓
			black	-	-	↓↓↓			↓↓↓↓	↓			↓
			white	-	-	↓↓↓↓			↓↓↓↓	↑↑			0
		rime	yellow	-	-	0				0			
			black	-	-	↓				↓			
			white	-	-	↓				↑			
2	Thermal	glaze	yellow	☑	-	↓↓↓↓				↓↓			
			yellow	-	☑	↓↓↓↓				↓↓			
		rime	yellow	☑	-	↓↓				↑			
			yellow	-	☑	↓				↑↑			
3	Thermface	glaze	black	☑	-	↓↓↓	↓	↑↑↑↑+		↓↓	↓↓	↓	
			white	☑	-	↓↓↓↓	S.I.	↑↑↑↑		↓↓↓	↓↓↓	↓↓	
			black	-	☑	↓↓↓↓	↓	↑		↓↓↓↓	↓↓↓↓	↓↓↓	
			white	-	☑	↓↓↓↓	S.I.	↑↑		↓↓↓↓	↓↓↓↓	↓↓↓	
		rime	black	☑	-	↓↓	↓	↑		↓↓↓↓	↓↓↓	↓↓↓↓	
			white	☑	-	↓↓	↓↓	↓		↑↑	↑	↑	
			black	-	☑	↓↓	↓↓	↓↓		↑	↑↑	↓	
			white	-	☑	↓↓	↓↓	↓		↑↑	↑↑	↑	

Legend		
% chng	"-"	"+"
100+	↓↓↓↓+	↑↑↑↑+
75-99	↓↓↓↓	↑↑↑↑
50-75	↓↓↓	↑↑↑
25-50	↓↓	↑↑
1-25	↓	↑
0	No Change	
S.I.: Statistically Insignificant		

APPENDIX H

Icing characteristics and mitigation strategies for wind turbines in cold climates: part 1

World Renewable Energy Conference 2006, Florence, Italy

Icing characteristics and mitigation strategies for wind turbines in cold climates

Andrea G. Kraj[1] and Eric L. Bibeau
Department of Mechanical and Manufacturing Engineering, University of Manitoba
Winnipeg, Manitoba, Canada R3T 5V6
[1]umkrajag@cc.umanitoba.ca

Abstract

Optimized power generation from available wind resources has gained substantial interest by many leaders in the wind power industry worldwide. One issue facing wind power generation in cold climates is ice accumulation on turbine blades, which is not only an energy production and efficiency concern, but also a safety issue. This paper explores various mitigation techniques for delaying and preventing ice accumulation on wind turbines blades. Firstly, a surface mitigation strategy has been applied to blade models involving hydrophobic and ice-phobic coatings. Secondly, a thermal mitigation strategy involving a new composite material has been developed. Subsequently these mitigation techniques are combined to form a third strategy, termed *thermface* mitigation. Stationary blade configurations have been experimentally tested in the University of Manitoba Icing Tunnel Facility. The results of the mitigation techniques depict icing profiles and aerodynamic changes along the blade leading edges during the icing event and quantify the ice adhesion force and accumulation amount over a set period under simulated climatological Glaze and Rime icing conditions. Results are extended to wind turbine performance for estimation of energy production.

Introduction

Wind, as an energy resource, contains the potential to become an important contributor to utility and non-utility power generation in many regions in Canada and in cold climates throughout the world. However, due to extreme climatological factors, many Canadian wind turbine sites are affected by icing problems that impact power generation. Thus, the potential to harness an abundant source of wind for power generation is greatly disadvantaged. Icing is an issue of interest to many groups—from private energy companies, to public utilities and farmers whose land is employed. This paper discusses the experiments performed in the University of Manitoba's Icing Tunnel Facility, (UMITF), for the investigation of icing mitigation strategies for wind turbines, specific to icing conditions in cold climates. Experiments are performed on aerofoils representative of blades currently used in the wind turbine industry, under conditions that simulate actual climatological conditions of severe icing events found in cold climates where wind turbines are employed, similar to those near St. Leon, in Southern Manitoba, where a large 99 MW wind farm is being developed, in a region very well-known for icing events.

Wind turbines are subjected to rime, glaze or mixed ice accretion conditions [1]. In the UMITF, glaze ice forms at temperatures just below freezing in air with high liquid water content, characteristically between 0°C and -6°C. Rime ice forms in colder environmental conditions, traditionally below -10°C, in air of low liquid water content, but also forms when surface temperatures are below -6°C. In rime icing, supercooled water droplets freeze immediately upon impact and form a low-density ice, white and feathery in appearance. In glaze icing, part of the water droplets freeze upon impact and the remaining water runs along the surface before freezing, forming a smooth lumpy profile shape of high-density clear ice. Glaze ice is known to be more difficult to remove than rime ice due to its inherent physical properties.

Icing Mitigation Strategy

Current techniques for ice shedding from aerofoil blades are commonly found in literature related to aerospace and aircraft applications. As Fitt and Pope [2] indicate these methods include anti-icing and de-icing techniques ranging from freezing point depressants and surface deformation, to thermal melting. Reducing the force of ice adhesion from a surface is a key point to improving the ability to shed ice with ease. As explained by Loughborough [3] of the B.F. Goodrich Company, the force of adhesion is approximated to be linear with temperature, increasing 8.5 lbs per sq. in (5976.09 kg/m^2) for each degree centigrade decrease in temperature. The significance of this value indicates that a reduction in the adhesion force of the ice would greatly improve ice shedding and the resulting performance of the turbine. Therefore, a method that reduces the adhesion force of ice on the surface would ideally aid in preventing and delaying the onset of ice accretion. Since environmental conscientiousness is a key factor in the wind turbines systems, hot oil, chemicals and their derivative are not viable mitigation strategies. Furthermore, the use of electrical energy may contradict the purpose of generating electricity, and must be cautiously implemented.

Therefore, the initial preference for an icing mitigation strategy is to implement a passive mitigation technique, such as a surface mitigation to improve the resistance of ice accretion and adhesion to the aerofoil surface. The correlation between a high contact angle for droplets on a surface and their enhanced ability to shed from the surface is highly influenced by the ability of a coating to be hydrophobic or ice-phobic [4]. Thus, the following have been selected for experimentation, for their favourable characteristics in icing conditions: Wearlon *Super-Icephobic* and *Super-Hydrophobic*. The icephobic coating is designed to perform best in icing conditions, whereas the hydrophobic coating is catered more towards repelling water droplets [5, 6]. Subsequently, a less-passive mitigation strategy is be explored. For this experiment it is in the form of a thermal technique. A highly controllable, lightweight system, compatible with modern composite materials has been adapted as an electro-thermal ice protection system where heat is generated at the point of use. Thermion® heaters are made from finely dispersed metal coated carbon fibre elements that may be integrated into composite or polymer material structures and are ideally suited for leading edge blade ice protection applications due to their lightweight and uniform heat distribution capability, contrary to traditional wire heaters [7]. The heat generated by this method is conducted into the ice-substrate interface, where a thin film of water is formed. This breaks the adhesive bond between the ice and the outer surface so that the ice can be swept away by aerodynamic forces. Furthermore, cycling of the heater power helps to control and reduce energy requirements [8], suggesting the use of de-icing regimes to further enhance the effectiveness of the mitigation strategy. By controlling the duration and timing of heat application both anti-icing and various de-icing regimes are be explored.

Finally, the combination of the surface mitigation with the thermal mitigation, termed *thermface*, is explored as means of more controlled-passive deicing, providing insight to the combined effectiveness of these mitigation strategies. The cycling of power for the electro-thermal heaters allows integration with other techniques to optimize mitigation efforts.

Experiment Description

Icing experimentation is performed using the Icing Tunnel Facility located in the Engineering Complex at the University of Manitoba. The UNITF consists of a spray system to emit droplets into the flow and a refrigeration system for cooling of the air as shown in Figure 1 [9].

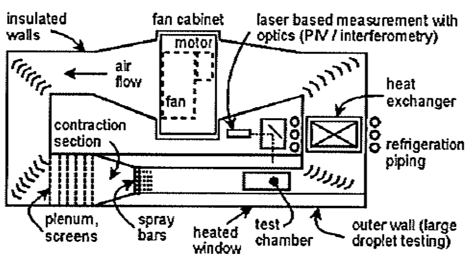

Figure 1: Top view of spray flow and icing tunnel

Experiments are conducted using stationary aerofoils placed within an inner duct ($1 m^2$) of the wind tunnel. Scaled test specimens are subjected to cooled airflows containing water droplets that are released into the flow stream from a customized spray bar located upstream of the aerofoil test piece. Air atomizing nozzles can produce a reliable spray pattern with water mean droplet diameters ranging from 10^{-3} to 10^{-5} meters. The droplets travel in a trajectory towards the test specimen, are cooled along the way and freeze upon impact with the test specimen forming different icing characteristics and shapes, according to the climatological conditions setup for the experiment being conducted.

The test specimen was formed from a NACA 634421 profile aerofoil with aluminum frame and fiberglass sheeting. For this experimental series, six test pieces with various mitigation strategies were required to investigate the surface, `thermal and thermface mitigation strategies. The specimen without a heater or coating was used as a datum. The selected coatings were applied to the aerofoil test specimens using specialized paint application equipment and procedures. The icephobic coated specimen is black, whereas the hydrophobic coated specimen is white, and the plain, uncoated specimen is the original fiberglass composite colour, yellow. All thermally mitigated specimens had two 0.508 x 0.127 m, 12 V / 5 W heaters, each mounted on one of the leading edge upper and lower inner surfaces. All thermface specimens were coated and had heaters. The specimens are shown in Figure 2 as mounted for testing.

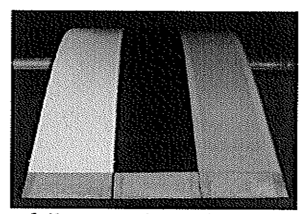

Figure 2: Aerofoil test sections: (L-R) Hydrophobic; Icephobic; Plain

The aerofoil test specimens were mounted at zero angle of attack downstream of the spray bar. Firstly, the surface mitigation technique was performed for the plain, hydro-phobic and icephobic samples under both glaze and rime icing conditions.

Subsequently, the thermal mitigation strategy was applied. For the thermal and thermface mitigation both anti-icing and de-icing regimes were employed in both rime and glaze icing conditions.

The anti-icing regime consisted of applying heat for the complete duration of the 20 minute test, whereas for the de-icing regime, heat was applied for only the second half of the test. The thermface strategy consisted of implementing the thermal strategy with the coated specimens.

Table 1: Experimental Parameters

Parameter	Value
Experimental equipment conditions	
Spray bar water flow (kg/s)	0.00946
Spray bar water temperature (°C)	1.89
Spray bar air pressure (Pa)	206,842
Wind tunnel set velocity, v_t (Hz)	15.5
Test specimen parameters	
Chord length (m)	0.3048
Aerofoil specimen width (m)	0.6350
Angle of attack (degrees)	0.00
Weather conditions for glaze icing	
Liquid water content, LWC (kg/m^3)	0.28e-3
Diameter of droplet, d (m)	0.001
Freestream temperature, T_i (K)	272.0 – 268.0
Freestream pressure, P_o (MPa)	0.1013
Measured local wind velocity, V_w (m/s)	7.7
Weather conditions for rime icing	
Liquid water content, LWC (kg/m^3)	0.28e-3
Diameter of droplet, d (m)	0.001
Free stream temperature, T_i (K)	263.0 – 273.0
Free stream pressure, P_o (MPa)	0.1013
Measured local wind velocity, V_w (m/s)	8.3

Experimental Parameters

A cooled air-water system was used in these experiments. Table 1 indicates the experimental conditions for the wind tunnel and spray bar equipment; the dimensions of the test specimens; and summarizes the implemented climatological conditions. The diameter of the water droplets and the Liquid Water Content (LWC) are approximated.

Experimental Analysis

Leading edge (LE) profiles were compared among all resulting test samples from which ice shape, symmetry and consistency were observed. A high resolution black-white digital camera and data acquisition system was used to collect images of the side-view aerofoil profile and the ice accretion for test duration of 20 minutes. Collected image data was processed using graphics software to determine changes in ice profile shape. Following this test, the shear-adhesion force test was performed on the LE curved surface of the aerofoil to determine the required force to remove the ice from the surface. The iced LE specimens were collected and their geometry was measured. The specimens were melted for a liquid volume measurement to gauge the amount of water that had accumulated along the leading edge.

Results & Discussion

Ice Profile Changes

A visual profile of ice formation on the LE surface, illustrates the varying amounts of ice accumulation and profile shapes between surfaces in glaze icing conditions. The resulting icing profiles are displayed in Figure 3.

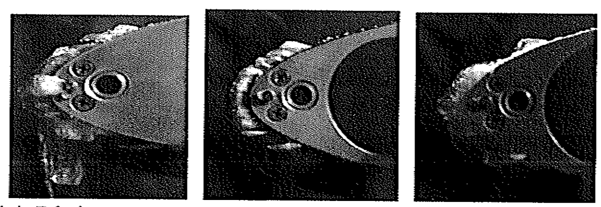

(a) Plain (b) Icephobic (c) Hydrophobic

Figure 3: Experimental icing pictures of leading edge of aerofoil for different coatings

Adhesion Force & Accumulation

The experimental results collected for ice adhesion force and the amount of water accumulation along the leading edge of the aerofoil for the various mitigation techniques is contained in Table 2: Comprehensive Mitigation Results Summary.

Adhesion Force

Comparing glaze and rime icing results indicate that on an uncoated plain surface, the adhesion force of glaze ice is 40% less adhesive than rime ice. The most effective surface mitigation in glaze conditions is the hydrophobic coating which reduces adhesion force by 97%. In rime condition, the icephobic coating is more effective, reducing adhesion by 15%. Evidently, in surface mitigation, the hydrophobic coating is most effective in glaze conditions while the icephobic coating is most effective in rime conditions. This can be attributed to the physical properties of the coatings: the hydrophobic coating is designed to be effective by repelling water as in glaze ice forms, while the icephobic coating is designed to repel solid-ice, as in rime conditions. Thus, the results identify the differences in the surface strategies and indicate that this distinction is related to the applied climatological conditions. This validates the significance and effectiveness of applying the proper coating in their designed-for conditions.

For thermal mitigation, anti-icing is more effective than the deicing regime, in both glaze and rime icing conditions, reducing adhesion 89% and 46% respectively. Furthermore, the results indicate that the glaze responds more effectively than rime to this thermal mitigation strategy.

For the thermface mitigation, in both icing conditions, the anti-icing regime with the hydrophobic coating reducing adhesion by 78% in glaze and 50% in rime is more effective than the icephobic coating. In contrast, for the deicing regime, the icephobic coating is more effective, reducing adhesion by 83% in glaze and 46% in rime. Overall, the deicing regime is more effective and consumes less energy, which is ideal for energy production systems. However, in rime conditions, it appears that both anti-icing and de-icing regimes have similar effectiveness in reducing adhesion force, suggesting that either thermal regime may be selected to optimize the system as needed. Isolating the thermal variable indicates that for glaze icing, both anti-icing and de-icing are 5% more effective when combined with the icephobic coating and are not as effective when combined with the hydrophobic coating. This may be attributed to the designed-for performance characteristics of the coatings. Since the experiments are conducted in icing conditions, the hydrophobic coating is not operating in its design-for conditions, and thus appears to be less effective than the icephobic coating at reducing adhesion force. For rime icing, on a hydrophobic surface, anti-icing is more effective than deicing, while on an icephobic surface, deicing is more effective. Furthermore, isolating the surface variable indicates that for glaze icing, in both anti-icing and deicing regimes there is no apparent adhesion reduction for either coating,

Table 2: Comprehensive Mitigation Results Summary

Comprehensive Results Summary						Adhesion Force				LE H2O Accumulation			
Mitigation						surface	surface	thermal	surface	surface	surface	thermal	surface
		Ice Type	Sample	Anti-icing	De-icing	mit vs. no-mit	thermal vs. no-thermal	surface vs. no-surface	glaze vs. rime	mit vs. no-mit	thermal vs. no-thermal	surface vs. no-surface	glaze vs. rime
1	Surface	glaze	yellow	-	-	0			↓↓	0			↓
			black	-	-	↓↓↓			↓↓↓↓	↓			↓
			white	-	-	↓↓↓↓			↓↓↓↓	↑↑			0
		rime	yellow	-	-	0				0			
			black	-	-	↓				↓			
			white	-	-	↓				↑			
2	Thermal	glaze	yellow	☑	-	↓↓↓↓				↓↓			
			yellow	-	☑	↓↓↓↓				↓↓			
		rime	yellow	☑	-	↓↓				↑			
			yellow	-	☑	↓				↑↑			
3	Thermface	glaze	black	☑	-	↓↓↓	↓	↑↑↑↑+		↓↓	↓↓	↓	
			white	☑	-	↓↓↓↓	S.I.	↑↑↑↑		↓↓↓	↓↓↓	↓↓	
			black	-	☑	↓↓↓↓	↓	↑		↓↓↓↓	↓↓↓↓	↓↓↓	
			white	-	☑	↓↓↓↓	S.I.	↑↑		↓↓↓↓	↓↓↓↓	↓↓↓	
		rime	black	☑	-	↓↓	↓	↑		↓↓↓↓	↓↓↓	↓↓↓↓	
			white	☑	-	↓↓	↓↓	↓		↑↑	↑	↑	
			black	-	☑	↓↓	↓↓	↓↓		↑	↑↑	↓	
			white	-	☑	↓↓	↓↓	↓		↑↑	↑↑	↑	

Legend		
% chng	"-"	"+"
100+	↓↓↓↓+	↑↑↑↑+
75-99	↓↓↓↓	↑↑↑↑
50-75	↓↓↓	↑↑↑
25-50	↓↓	↑↑
1-25	↓	↑
0	No Change	
S.I.: Statistically Insignificant		

suggesting that coatings may impede ice removal by preventing heat transfer by conduction to the surface, as a result of their inherent thickness.

Thus, in both glaze and rime conditions the most effective thermface mitigation strategy is the icephobic coating in the deicing regime.

Accumulation Amount

In comparison of the amount of ice, in liquid state that accumulates along the LE of an aerofoil for both icing conditions, less accumulation exists in glaze than in rime. The most effective surface mitigation in both icing conditions is the icephobic coating which reduces accumulation by 5% in glaze and 23% in rime. Evidently, these results are also dependent on the correlation of the coatings designed-for performance characteristics with climatological conditions; thus, for the given icing conditions, the icephobic coating is expected to, and does, out-perform the hydrophobic coating.

The most effective thermal mitigation strategy on a plain uncoated surface, in glaze conditions, is the anti-icing regime, reducing accumulation by 37%. In rime conditions, accumulation is not significantly reduced; in fact, the amount of accumulation appears to supersede the effectiveness of the mitigation technique, suggesting that it does not have the capacity to be effective in the given conditions.

The most effective thermface regime for glaze conditions involves combining the de-icing regime with the icephobic coating, which reduces accumulation 83%. In rime conditions, the icephobic coating is effective with either anti-icing or deicing regime, reducing accumulation 78% and 19% respectively. The lesser effectiveness of the mitigation strategy with the deicing regime in rime conditions indicates that the thermal technique has nearly reached its max capacity of effectiveness, yet the combination with the surface mitigation remains more effective than the thermal technique alone. In light of energy consumption, the deicing regime is utilizes less energy and is effective in either icing condition, suggesting that is it preferred regime.

Evidently, both the thermal and surface mitigation strategies, independently, have significant effects in reducing accumulation along the leading edge of an aerofoil. However, the combined mitigation of the thermface strategy provides the most substantial reduction in accumulation. Thus, the recommended mitigation strategy for reducing accumulation either glaze or rime conditions would be the implementation of an icephobic coating in combination with a deicing regime. Furthermore, this strategy is effective at reducing adhesion force as well.

Wind Turbine Performance Measures

Optimized wind turbine performance is dependent on the lift to drag ratio created by the blades. Ice accumulation changes the aerodynamic profile shape of the blade and directly affects the lift, as well as creates trigger points for non-laminar flow over the blade surface resulting in less-efficient energy capture; furthermore, ice adds weight to the aerofoil. With a less-effective lift-to-drag ratio the turbine is not capable of efficient wind energy production. Additionally, an effective mitigation strategy, must not consume more energy than the system produces. Therefore, an optimal mitigation strategy would best balance these performance measures.

Conclusion

Wind Energy production in adverse cold climates is enhanced by implementing the presented mitigation strategies, which significantly reduce the adhesion force and accumulation amount of ice on a blade surface and influence the formation of a more symmetric LE ice profile. It is shown that in glaze or rime conditions, the thermface strategy employing the de-icing thermal regime with the icephobic surface coating is the most effective, mitigation. Furthermore, the combination of mitigation strategies must be carefully designed so that they are employed in the climatological conditions best suited for their use and within their scope of capability so that they do not adversely affect the capabilities of one another—specifically, in the case of coating thickness impeding heat transfer by conduction to the surface.

Acknowledgments

Funding from the Manitoba Hydro, NRCAN, and NSERC Alternative Energy Chair is gratefully acknowledged. Discussions with Manitoba Hydro, and the crew at the St. Leon Wind Turbine Farm in Southern Manitoba were helpful in defining icing conditions used in this study to applicable cases.

References

[1] Bose, N., Icing on a small horizontal-axis wind turbine- part 1: Glaze ice profiles, Journal of wind engineering and industrial aerodynamics, v45, n1 (1992), 75-85.

[2] Fitt, A.D. and Pope, M.P., De-icing by slot injection, Acta Mechanica. v147, n1-4 (2001) 73-86.

[3] Loughborough, D.L., Physics of mechanical removal of ice from aircraft, Aeronautical Engineering Review, v11, n2 (Feb 1952) 29-34.

[4] Mohammadi, R., Wassink, J., Amirfazli, A., Effect of Surfactants on Wetting of Super-Hydrophobic Surfaces, American Chemical Society, (Aug 6, 2004), 1-6.

[5] Garti, N. et al, New Non-Stick Epoxy-Silicone Water-Based Coatings Part 1: Physical and Surface Properties, Proceeding of the 5th International Zebra Mussel and Other Aquatic Nuisance Organisms Conference, Toronto, Canada, (Feb, 1995), 151-169.

[6] http://www.wearlon.com/Eproducts.htm

[7] http://www.thermion.com/heaters/advantages.html

[8] Thomas, Scott K. et al., Aircraft anti-icing and de-icing techniques and modeling, Journal of Aircraft, v33, No. 5, September-October 1996, 841-854.

[9] Naterer, G. F. et al, Experimental Facility for New Hybrid Ice/Spray Flow Tunnel with Laser Based Droplet Measurement, AIAA 2002-2867, 1-10.

APPENDIX I

Icing characteristics and mitigation strategies for wind turbines in cold climates, part 2: profile shape extension

Global Wind Energy Conference 2006, Adelaide, Australia

Icing characteristics and mitigation strategies for wind turbines in cold climates, part 2: profile shape extension

Andrea G. Kraj[1] and Eric L. Bibeau
Department of Mechanical and Manufacturing Engineering, University of Manitoba
Winnipeg, Manitoba, Canada R3T 5V6
[1]umkrajag@cc.umanitoba.ca

Abstract

Optimized power generation from available wind resources has gained substantial interest by many leaders in the wind power industry worldwide. One issue facing wind power generation in cold climates is ice accumulation on turbine blades, which is not only an energy production and efficiency concern, but also a safety issue. This paper explores various mitigation techniques for delaying and preventing ice accumulation on wind turbines blades. Firstly, a surface mitigation strategy has been applied to blade models involving hydrophobic and ice-phobic coatings. Secondly, a thermal mitigation strategy involving a new composite material has been developed. Subsequently these mitigation techniques are combined to form a third strategy, termed *thermface* mitigation. Stationary blade configurations have been experimentally tested in the University of Manitoba Icing Tunnel Facility. The results of the mitigation techniques depict icing profiles and aerodynamic changes along the blade leading edges during the icing event and quantify the profile shape extension, ice adhesion force and accumulation amount over a set period under simulated climatological Glaze and Rime icing conditions. Results are extended to wind turbine performance for estimation of energy production.

Introduction

Wind, as an energy resource, contains the potential to become an important contributor to utility and non-utility power generation in many regions in Canada and in cold climates throughout the world. However, due to extreme climatological factors, many Canadian wind turbine sites are affected by icing problems that impact power generation. Thus, the potential to harness an abundant source of wind for power generation is greatly disadvantaged. Icing is an issue of interest to many groups—from private energy companies, to public utilities and landowners. This paper discusses the experiments performed in the University of Manitoba's Icing Tunnel Facility, (UMITF), for the investigation of icing mitigation strategies for wind turbines, specific to icing conditions in cold climates. Experiments are performed on aerofoils representative of blades currently used in the wind turbine industry, under conditions that simulate actual climatological conditions of severe icing events found in cold climates where wind turbines are employed, similar to those near St. Leon, in Southern Manitoba, where a large 99 MW wind farm is being developed, in a region very well-known for icing events.

Wind turbines are subjected to rime, glaze or mixed ice accretion conditions [1]. In the UMITF, glaze ice forms at temperatures just below freezing in air with high liquid water content, characteristically between 0°C and -6°C. Rime ice forms in colder environmental conditions, traditionally below -10°C, in air of low liquid water content, but also forms when surface temperatures are below -6°C. In rime icing, supercooled water droplets freeze immediately upon impact and form a low-density ice, white and feathery in appearance. In glaze icing, part of the water droplets freeze upon impact and the remaining water runs along the surface before freezing, forming a smooth lumpy profile shape of high-density clear ice. Glaze ice is known to be more difficult to remove than rime ice due to its inherent physical properties.

Icing Mitigation Strategy

Current techniques for ice shedding from aerofoil blades are commonly found in literature related to aerospace and aircraft applications. As Fitt and Pope [2] indicate these methods include anti-icing and de-icing techniques ranging from freezing point depressants and surface deformation, to thermal melting. Reducing the force of ice adhesion from a surface is a key point to improving the ability to shed ice with ease. As explained by Loughborough [3] of the B.F. Goodrich Company, the force of adhesion is approximated to be linear with temperature, increasing 8.5 lbs per sq. in (5976.09 kg/m^2) for each degree centigrade decrease in temperature. The significance of this value indicates that a reduction in the adhesion force of the ice would greatly improve ice shedding and the resulting performance of the turbine. Therefore, a method that reduces the adhesion force of ice on the surface would ideally aid in preventing and delaying the onset of ice accretion. Since environmental conscientiousness is a key factor in the wind turbines systems, hot oil, chemicals and their derivative are not viable mitigation strategies. Furthermore, the use of electrical energy may contradict the purpose of generating electricity, and must be cautiously implemented. Therefore, the initial preference for an icing mitigation strategy is to implement a passive mitigation technique, such as a surface mitigation to improve the resistance of ice accretion and adhesion to the aerofoil surface. The correlation between a high contact angle for droplets on a surface and their enhanced ability to shed from the surface is highly influenced by the ability of a coating to be hydrophobic or ice-phobic [4]. Thus, the following have been selected for experimentation, for their favourable characteristics in icing conditions: Wearlon *Super-Icephobic* and *Super-Hydrophobic*. The icephobic coating is designed to perform best in icing conditions, whereas the hydrophobic coating is catered more towards repelling water droplets [5, 6]. Subsequently, a less-passive mitigation strategy is be explored. For this experiment it is in the form of a thermal technique. A highly controllable, lightweight system, compatible with modern composite materials has been adapted as an electro-thermal ice protection system where heat is generated at the point of use. Thermion® heaters are made from finely dispersed metal coated carbon fibre elements that may be integrated into composite or polymer material structures and are ideally suited for leading edge blade ice protection applications due to their lightweight and uniform heat distribution capability, contrary to traditional wire heaters [7]. The heat generated by this method is conducted into the ice-substrate interface, where a thin film of water is formed. This breaks the adhesive bond between the ice and the outer surface so that the ice can be swept away by aerodynamic forces. Furthermore, cycling of the heater power helps to control and reduce energy requirements [8], suggesting the use of de-icing regimes to further enhance the effectiveness of the mitigation strategy. By controlling the duration and timing of heat application both anti-icing and various de-icing regimes are be explored.

Finally, the combination of the surface mitigation with the thermal mitigation, termed *thermface*, is explored as means of more controlled-passive deicing, providing insight to the combined effectiveness of these mitigation strategies. The cycling of power for the electro-thermal heaters allows integration with other techniques to optimize mitigation efforts.

Experiment Description

Icing experimentation is performed using the Icing Tunnel Facility located in the Engineering Complex at the University of Manitoba. The UMITF consists of a spray system to emit droplets into the flow and a refrigeration system for cooling of the air as shown in Figure 1 [9].

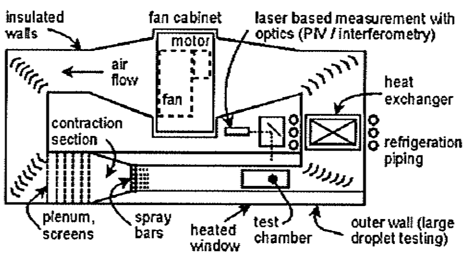

Figure 1: Top view of spray flow and icing tunnel

Experiments are conducted using stationary aerofoils placed within an inner duct ($1m^2$) of the wind tunnel. Scaled test specimens are subjected to cooled airflows containing water droplets that are released into the flow stream from a customized spray bar located upstream of the aerofoil test piece. Air atomizing nozzles can produce a reliable spray pattern with water mean droplet diameters ranging from 10^{-3} to 10^{-5} meters. The droplets travel in a trajectory towards the test specimen, are cooled along the way and freeze upon impact with the test specimen forming different icing characteristics and shapes, according to the climatological conditions set for the conducted experiment.

The test specimen was formed from a NACA 634421 profile aerofoil with aluminum frame and fiberglass sheeting. For this experimental series, six test pieces with various mitigation strategies were required to investigate the surface, thermal and thermface mitigation strategies. The specimen without a heater or coating was used as a datum. The selected coatings were applied to the aerofoil test specimens using specialized paint application equipment and procedures. The icephobic coated specimen is black, whereas the hydrophobic coated specimen is white, and the plain, uncoated specimen is the original fiberglass composite colour, yellow. All thermally mitigated specimens had two 0.508 x 0.127 m, 12 V / 5 W heaters, each mounted on one of the leading edge upper and lower inner surfaces. All thermface specimens were coated and had heaters. The specimens are shown in Figure 2 as mounted for testing.

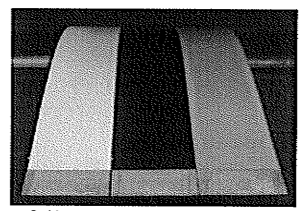

Figure 2: Aerofoil test sections: (L-R) Hydrophobic; Icephobic; Plain

The aerofoil test specimens were mounted at zero angle of attack downstream of the spray bar. Firstly, the surface mitigation technique was performed for the plain, hydro-phobic and icephobic samples under both glaze and rime icing conditions.

Subsequently, the thermal mitigation strategy was applied. For the thermal and thermface mitigation both anti-icing and de-icing regimes were employed in both rime and glaze icing conditions.

The anti-icing regime consisted of applying heat for the complete duration of the 20 minute test, whereas for the de-icing regime, heat was applied for only the second half of the test. The thermface strategy consisted of implementing the thermal strategy with the coated specimens.

Parameter	Value
Experimental equipment conditions	
Spray bar water flow (kg/s)	0.00946
Spray bar water temperature (°C)	1.89
Spray bar air pressure (Pa)	206,842
Wind tunnel set velocity, v_t (Hz)	15.5
Test specimen parameters	
Chord length (m)	0.3048
Aerofoil specimen width (m)	0.6350
Angle of attack (degrees)	0.00
Weather conditions for glaze icing	
Liquid water content, LWC (kg/m^3)	0.28e-3
Diameter of droplet, d (m)	0.001
Freestream temperature, T_i (K)	268.0
Freestream pressure, P_o (MPa)	0.1013
Measured local wind velocity, V_w (m/s)	7.37
Weather conditions for rime icing	
Liquid water content, LWC (kg/m^3)	0.28e-3
Diameter of droplet, d (m)	0.001
Free stream temperature, T_i (K)	258.0
Free stream pressure, P_o (MPa)	0.1013
Measured local wind velocity, V_w (m/s)	7.97

Experimental Parameters

A cooled air-water system was used in these experiments. Table 1 indicates the experimental conditions for the wind tunnel and spray bar equipment; the dimensions of the test specimens; and summarizes the implemented climatological conditions. The diameter of the water droplets and the Liquid Water Content (LWC) are approximated.

Table 1: Experimental Parameters

Experimental Analysis

Leading edge (LE) profiles were compared among all resulting test samples from which ice shape, symmetry and consistency were observed. A high resolution black-white digital camera and data acquisition system was used to collect images of the side-view aerofoil profile and the ice

Table 1: Experimental Parameters

accretion for test duration of 20 minutes. Collected image data was processed using graphics software to determine changes in ice profile shape. Following this test, the shear-adhesion force test was performed on the LE curved surface of the aerofoil to determine the required force to remove the ice from the surface. The iced LE specimens were collected and their geometry was measured. The specimens were melted for a liquid volume measurement to gauge the amount of water that had accumulated along the leading edge.

Results & Discussion

Ice Profile Changes

A visual profile of ice formation on the LE surface, illustrates the varying amounts of ice accumulation and profile shapes between surfaces in glaze icing conditions. The resulting icing profiles are displayed in Figure 3.

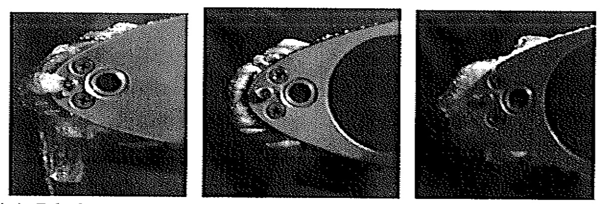

(a) Plain (b) Icephobic (c) Hydrophobic

Figure 3: Experimental icing pictures of leading edge of aerofoil for different coatings

LE Profile Shape Extension

In comparison of the amount of ice, in solid state that accumulates at the LE of an aerofoil, causing an extension in shape profile, for both icing conditions, less shape extension occurs in glaze than in rime ice by 8%. Results indicate that surface mitigation efforts are only effective in glaze conditions, in which the hydrophobic coating reduces shape extension by 25% and the icephobic coating by 16%. Evidently the hydrophobic coating is slightly more effective. Surface mitigation in rime conditions is not effective, suggesting that the rime icing conditions subdue surface mitigation efforts for reducing shape extension.

The most effective thermal mitigation strategy on a plain uncoated surface, in glaze conditions, is the anti-icing regime, reducing shape extension by 29%, whereas the deicing regime does not effectively reduce shape extension. In rime conditions, shape extension is not significantly reduced by either de-icing or anti-icing regimes, suggesting that the mitigation effort does not have the capacity to be effective in the given conditions.

The most effective thermface regime for glaze conditions involves combining the de-icing regime with the hydrophobic coating, which reduces shape extension by 70%. The next best option is the icephobic coating with the de-icing regime. In rime conditions, the best mitigation strategy is to employ the icephobic coating with the anti-icing thermal regime, which has an overall effectiveness of reducing shape extension by 12%.

Evidently, it is more difficult to control profile shape extension in rime than in glaze conditions, however it is not impossible. Both surface and thermal techniques are independently effective, and when combined are substantially more effective, as is evident in glaze conditions, and even slightly in rime conditions. The best performing mitigation strategies for controlling profile shape extension are depicted in Table 2, at the beginning, mid and end stages of ice accumulation for the three mitigation strategies in both glaze and rime icing conditions.

Table 2: Shape Catalogue Profile Extension

Best Performers at Reducing Profile Shape Extension						
Expt List	ice	[illegible]	anti-icing	de-icing	LE Shape Profile Intervals	
Test Description					1 min / 10 mins. / 20 mins.	
Surface	glaze	white	n/a	n/a		
	rime	yellow	n/a	n/a	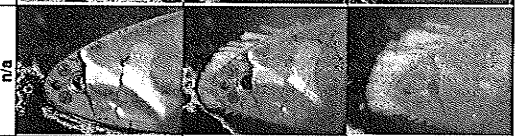	
Thermal	glaze	yellow	yes	-	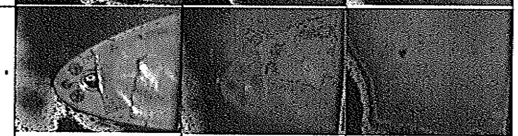	
	rime	yellow	yes	-		
Thermface	glaze	white	-	yes		
	rime	black	yes	-	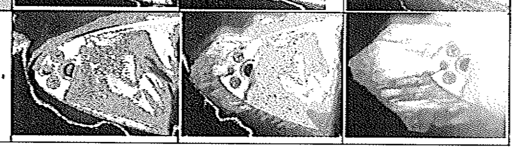	

Adhesion Force & Accumulation

The experimental results collected for ice adhesion force and the amount of water accumulation along the leading edge of the aerofoil for the various mitigation techniques is contained in Table 3: Comprehensive Mitigation Results Summary.

<u>Adhesion Force</u>

Comparing glaze and rime icing results indicate that on an uncoated plain surface, the adhesion force of glaze ice is 40% less adhesive than rime ice. The most effective surface mitigation in glaze conditions is the hydrophobic coating which reduces adhesion force by 97%. In rime condition, the icephobic coating is more effective, reducing adhesion by 15%. Evidently, in surface mitigation, the hydrophobic coating is most effective in glaze conditions while the icephobic coating is most effective in rime conditions. This can be attributed to the physical properties of the coatings: the hydrophobic coating is designed to be effective by repelling water as in glaze ice forms, while the icephobic coating is designed to repel solid-ice, as in rime conditions. Thus, the results identify the differences in the surface strategies and indicate that this distinction is related to the applied climatological conditions. This validates the significance and effectiveness of applying the proper coating in their designed-for conditions.

For thermal mitigation, anti-icing is more effective than the deicing regime, in both glaze and rime icing conditions, reducing adhesion 89% and 46% respectively. Furthermore, the results indicate that the glaze responds more effectively than rime to this thermal mitigation strategy.

For the thermface mitigation, in both icing conditions, the anti-icing regime with the hydrophobic coating reducing adhesion by 78% in glaze and 50% in rime is more effective than the icephobic coating. In contrast, for the deicing regime, the icephobic coating is more effective, reducing adhesion by 83% in glaze and 46% in rime. Overall, the deicing regime is more effective and consumes less energy, which is ideal for energy production systems. However, in rime conditions, it appears that both anti-icing and de-icing regimes have similar effectiveness in reducing adhesion force, suggesting that either thermal regime may be selected to optimize the system as needed.

Table 3: Comprehensive Mitigation Results Summary

Comprehensive Results Summary						Adhesion Force				LE H2O Accumulation			
Mitigation						surface	surface	thermal	surface	surface	surface	thermal	surface
		Ice Type	Sample	Anti-icing	De-icing	mit vs. no-mit	thermal vs. no-thermal	surface vs. no-surface	glaze vs. rime	mit vs. no-mit	thermal vs. no-thermal	surface vs. no-surface	glaze vs. rime
1	Surface	glaze	yellow	-	-	0			↓↓	0			↓
			black	-	-	↓↓↓			↓↓↓↓	↓			↓
			white	-	-	↓↓↓↓			↓↓↓↓	↑↑			0
		rime	yellow	-	-	0				0			
			black	-	-	↓				↓			
			white	-	-	↓				↑			
2	Thermal	glaze	yellow	☑	-	↓↓↓↓				↓↓			
			yellow	-	☑	↓↓↓↓				↓↓			
		rime	yellow	☑	-	↓↓				↑			
			yellow	-	☑	↓				↑↑			
3	Thermface	glaze	black	☑	-	↓↓↓	↓	↑↑↑↑+		↓↓	↓↓	↓	
			white	☑	-	↓↓↓↓	S.I.	↑↑↑↑		↓↓↓	↓↓↓	↓↓	
			black	-	☑	↓↓↓↓	↓	↑		↓↓↓↓	↓↓↓↓	↓↓↓	
			white	-	☑	↓↓↓↓	S.I.	↑↑		↓↓↓↓	↓↓↓↓	↓↓↓	
		rime	black	☑	-	↓↓	↓	↑		↓↓↓↓	↓↓↓	↓↓↓↓	
			white	☑	-	↓↓	↓↓	↓		↑↑	↑	↑	
			black	-	☑	↓↓	↓↓	↓↓		↑	↑↑	↓	
			white	-	☑	↓↓	↓↓	↓		↑↑	↑↑	↑	

Legend		
% chng	"-"	"+"
100+	↓↓↓↓+	↑↑↑↑+
75-99	↓↓↓↓	↑↑↑↑
50-75	↓↓↓	↑↑↑
25-50	↓↓	↑↑
1-25	↓	↑
0	No Change	
S.I.: Statistically Insignificant		

Isolating the thermal variable indicates that for glaze icing, both anti-icing and de-icing are 5% more effective when combined with the icephobic coating and are not as effective when combined with the hydrophobic coating. This may be attributed to the designed-for performance characteristics of the coatings. Since the experiments are conducted in icing conditions, the hydrophobic coating is not operating in its design-for conditions, and thus appears to be less effective than the icephobic coating at reducing adhesion force. For rime icing, on a hydrophobic surface, anti-icing is more effective than deicing, while on an icephobic surface, deicing is more effective. Furthermore, isolating the surface variable indicates that for glaze icing, in both anti-icing and deicing regimes there is no apparent adhesion reduction for either coating, suggesting that coatings may impede ice removal by preventing heat transfer by conduction to the surface, as a result of their inherent thickness.

Thus, in both glaze and rime conditions the most effective thermface mitigation strategy is the icephobic coating in the deicing regime.

Accumulation Amount

In comparison of the amount of ice, in liquid state that accumulates along the LE of an aerofoil for both icing conditions, less accumulation exists in glaze than in rime. The most effective surface mitigation in both icing conditions is the icephobic coating which reduces accumulation by 5% in glaze and 23% in rime. Evidently, these results are also dependent on the correlation of the coatings designed-for performance characteristics with climatological conditions; thus, for the given icing conditions, the icephobic coating is expected to, and does, out-perform the hydrophobic coating.

The most effective thermal mitigation strategy on a plain uncoated surface, in glaze conditions, is the anti-icing regime, reducing accumulation by 37%. In rime conditions, accumulation is not significantly reduced; in fact, the amount of accumulation appears to supersede the effectiveness of the mitigation technique, suggesting that it does not have the capacity to be effective in the given conditions.

The most effective thermface regime for glaze conditions involves combining the de-icing regime with the icephobic coating, which reduces accumulation 83%. In rime conditions, the icephobic coating is effective with either anti-icing or deicing regime, reducing accumulation 78% and 19% respectively. The lesser effectiveness of the mitigation strategy with the deicing regime in rime conditions indicates that the thermal technique has nearly reached its max capacity of effectiveness, yet the combination with the surface mitigation remains more effective than the thermal technique alone. In light of energy consumption, the deicing regime utilizes less energy and is effective in either icing condition, suggesting that it is the preferred regime.

Evidently, both the thermal and surface mitigation strategies, independently, are significantly effective at reducing accumulation along the leading edge of an aerofoil. However, the combined mitigation of the thermface strategy provides the most substantial reduction in accumulation. Thus, the recommended mitigation strategy for reducing accumulation in either glaze or rime conditions would be to implement the icephobic coating in combination with a deicing regime. Furthermore, this strategy is effective at reducing adhesion force as well.

Wind Turbine Performance Measures

Optimized wind turbine performance is dependent on the lift to drag ratio created by the blades. Ice accumulation changes the aerodynamic profile shape of the blade and directly affects the lift, as well as creates trigger points for non-laminar flow over the blade surface resulting in less-efficient energy capture; furthermore, ice adds weight to the aerofoil. With a less-effective lift-to-drag ratio the turbine is not capable of efficient wind energy production. As shown in the shape catalogue summary, the transient change in chord length of the aerofoil can result in a significant change in chord length after only a period of 10 minutes, for which aerodynamic blades are not designed. Additionally, an effective mitigation strategy, must not consume more energy than the system produces. Therefore, an optimal mitigation strategy would best balance these performance measures.

Conclusion

Wind Energy production in adverse cold climates can be enhanced by implementing the presented mitigation strategies, which significantly reduce the profile shape extension, adhesion force and accumulation amount of ice on a blade surface and influence the formation of a more symmetric LE ice profile. It is shown that in glaze or rime conditions, the thermface strategy employing the de-icing thermal regime with the icephobic surface coating is the most effective mitigation for reducing adhesion force and accumulation amount; while for reducing shape extension in glaze conditions the de-icing regime with the hydrophobic coating is the most effective and in rime conditions the icephobic coating with the anti-icing regime.

Furthermore, the combination of mitigation strategies must be carefully designed so that they are employed in the climatological conditions best suited for their use and within their scope of capability so that they do not adversely affect the capabilities of one another—specifically, in the case of coating thickness impeding heat transfer by conduction to the surface.

Acknowledgments

Funding from the Manitoba Hydro NSERC Alternative Energy Chair, NRCAN, and support from the St. Leon Wind Farm Personnel, is gratefully acknowledged.

References

[1] Bose, N., Icing on a small horizontal-axis wind turbine- part 1: Glaze ice profiles, Journal of wind engineering and industrial aerodynamics, v45, n1 (1992), 75-85.
[2] Fitt, A.D. and Pope, M.P., De-icing by slot injection, Acta Mechanica. v147, n1-4 (2001) 73-86.
[3] Loughborough, D.L., Physics of mechanical removal of ice from aircraft, Aeronautical Engineering Review, v11, n2 (Feb 1952) 29-34.
[4] Mohammadi, R., Wassink, J., Amirfazli, A., Effect of Surfactants on Wetting of Super-Hydrophobic Surfaces, American Chemical Society, (Aug 6, 2004), 1-6.
[5] Garti, N. et al, New Non-Stick Epoxy-Silicone Water-Based Coatings Part 1: Physical and Surface Properties, Proceeding of the 5th International Zebra Mussel and Other Aquatic Nuisance Organisms Conference, Toronto, Canada, (Feb, 1995), 151-169.
[6] http://www.wearlon.com/Eproducts.htm
[7] http://www.thermion.com/heaters/advantages.html
[8] Thomas, Scott K. et al., Aircraft anti-icing and de-icing techniques and modeling, Journal of Aircraft, v33, No. 5, September-October 1996, 841-854.
[9] Naterer, G. F. et al, Experimental Facility for New Hybrid Ice/Spray Flow Tunnel with Laser Based Droplet Measurement, AIAA 2002-2867, 1-10.

APPENDIX J

Icing characteristics and mitigation strategies for wind turbines in cold climates, part 3: accumulation rate

Renewable Energy 2006 Conference, Makuhari, Japan

Icing characteristics and mitigation strategies for wind turbines in cold climates, part 3: accumulation rate

Andrea G. Kraj[1] and Eric L. Bibeau
Department of Mechanical and Manufacturing Engineering, University of Manitoba
Winnipeg, Manitoba, Canada R3T 5V6
[1]umkrajag@cc.umanitoba.ca

Abstract

Optimized power generation from available wind resources has gained substantial interest by many leaders in the wind power industry worldwide. One issue facing wind power generation in cold climates is ice accumulation on turbine blades, which is not only an energy production and efficiency concern, but also a safety issue. This paper explores various mitigation techniques for delaying and preventing ice accumulation on wind turbines blades. Firstly, a surface mitigation strategy has been applied to blade models involving hydrophobic and ice-phobic coatings. Secondly, a thermal mitigation strategy involving a new composite material has been developed. Subsequently these mitigation techniques are combined to form a third strategy, termed *thermface* mitigation. Stationary blade configurations have been experimentally tested in the University of Manitoba Icing Tunnel Facility. The results of the mitigation techniques depict icing profiles and aerodynamic changes along the blade leading edges during the icing event and quantify ice adhesion force, accumulation amount and rate of accumulation over a set period under simulated climatological Glaze and Rime icing conditions. Results are extended to wind turbine performance for estimation of energy production.

Introduction

Wind, as an energy resource, contains the potential to become an important contributor to utility and non-utility power generation in many regions in Canada and in cold climates throughout the world. However, due to extreme climatological factors, many Canadian wind turbine sites are affected by icing problems that impact power generation. Thus, the potential to harness an abundant source of wind for power generation is greatly disadvantaged. Icing is an issue of interest to many groups—from private energy companies, to public utilities and landowners. This paper discusses the experiments performed in the University of Manitoba's Icing Tunnel Facility, (UMITF), for the investigation of icing mitigation strategies for wind turbines in cold climates. Experiments are performed on aerofoils representative of blades currently used in the wind turbine industry, under simulated climatological conditions for severe icing events found in cold climates where wind turbines are commonly employed. Of particular interest is the 99.9 MW wind farm in St. Leon, Manitoba, which has been developed in a region very well-known for icing events.

Wind turbines are subjected to rime, glaze or mixed ice accretion conditions [1]. In the UMITF, glaze ice forms at temperatures just below freezing in air with high liquid water content, characteristically between 0°C and -6°C. Rime ice forms in colder environmental conditions, traditionally below -10°C, in air of low liquid water content, but also forms when surface temperatures are below -6°C. In rime icing, supercooled water droplets freeze immediately upon impact and form a low-density ice, white and feathery in appearance. In glaze icing, part of the water droplets freeze upon impact and the remaining water runs along the surface before freezing, forming a smooth lumpy profile shape of high-density clear ice.

Icing Mitigation Strategy

Current techniques for ice shedding from aerofoil blades are commonly found in literature related to aerospace and aircraft applications. As Fitt and Pope [2] indicate these methods include anti-icing and de-icing techniques ranging from freezing point depressants and surface deformation, to thermal melting. Reducing the force of ice adhesion from a surface is a key point to improving the ability to shed ice with ease. As explained by Loughborough [3] of the B.F. Goodrich Company, the force of adhesion is approximated to be linear with temperature, increasing 8.5 lbs per sq. in (5976.09 kg/m^2) for each degree centigrade decrease in temperature. The significance of this value indicates that a reduction in the adhesion force of the ice would greatly improve ice shedding and the resulting performance of the turbine. Therefore, a method that reduces the adhesion force of ice on the surface would ideally aid in preventing and delaying the onset of ice accretion. Since environmental conscientiousness is a key factor in the wind turbines systems, hot oil, chemicals and their derivative are not viable mitigation strategies. Furthermore, the use of electrical energy may contradict the purpose of generating electricity, and must be cautiously implemented. Therefore, the initial preference for an icing mitigation strategy is to implement a passive mitigation technique, such as a surface mitigation to improve the resistance of ice accretion and adhesion to the aerofoil surface. The correlation between a high contact angle for droplets on a surface and their enhanced ability to shed from the surface is highly influenced by the ability of a coating to be hydrophobic or ice-phobic [4]. Thus, the following have been selected for experimentation, for their favourable characteristics in icing conditions: Wearlon *Super-Icephobic* and *Super-Hydrophobic*. The icephobic coating is designed to perform best in icing conditions, whereas the hydrophobic coating is catered more towards repelling water droplets [5, 6]. Subsequently, a less-passive mitigation strategy can be explored. For this experiment, a thermal technique is selected. A highly controllable, lightweight system, compatible with modern composite materials has been adapted as an electro-thermal ice protection system where heat is generated at the point of use. Thermion® heaters are made from finely dispersed metal coated carbon fibre elements that may be integrated into composite or polymer material structures and are ideally suited for leading edge blade ice protection applications due to their lightweight and uniform heat distribution capability, contrary to traditional wire heaters [7]. The heat generated by this method is conducted into the ice-substrate interface, where a thin film of water is formed. This breaks the adhesive bond between the ice and the outer surface so that the ice can be swept away by aerodynamic forces. Furthermore, cycling of the heater power helps to control and reduce energy requirements [8], suggesting the use of various thermal regimes to further enhance the effectiveness of the mitigation strategy. By controlling the duration and timing of heat application both anti-icing and various de-icing regimes can be explored.

Finally, the combination of the surface mitigation with the thermal mitigation, termed *thermface*, is explored as means of more controlled-passive deicing technique, providing insight to the combined effectiveness of these mitigation strategies. The cycling of power for the electro-thermal heaters allows integration with other techniques to optimize mitigation efforts.

Experiment Description

Icing experimentation is performed in the Icing Tunnel Facility located in the Engineering Complex at the University of Manitoba. The UMITF consists of a spray system to emit droplets into the flow and a refrigeration system for cooling of the air as shown in Figure 1 [9].

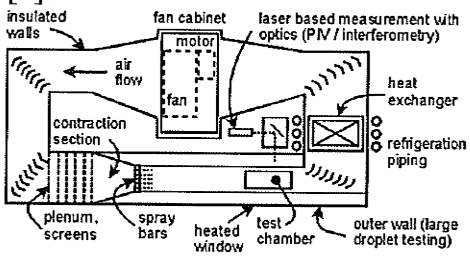

Figure 1: Top view of spray flow and icing tunnel

Experiments are conducted using stationary aerofoils placed within an inner duct ($1m^2$) of the wind tunnel. Scaled test specimens are subjected to cooled airflows containing water droplets that are released into the flow stream from a customized spray bar located upstream of the aerofoil test piece. Air atomizing nozzles can produce a reliable spray pattern with water mean droplet diameters ranging from 10^{-3} to 10^{-5} meters. The droplets travel in a trajectory towards the test specimen, are cooled along the way and freeze upon impact with the test specimen forming different icing characteristics and shapes, according to the climatological conditions set for the conducted experiment.

The test specimen is in the forms of a NACA 634421 profile aerofoil with aluminum frame and fiberglass sheeting. For this experimental series, six test pieces with various mitigation strategies were required to investigate the surface, thermal and thermface mitigation strategies. The specimen without a heater or coating was used as a datum.

The selected coatings were applied to the aerofoil test specimens using specialized paint application equipment and procedures. The icephobic coated specimen is black, whereas the hydrophobic coated specimen is white, and the plain, uncoated specimen is the original fiberglass composite colour, yellow. All thermally mitigated specimens had two 0.508 x 0.127 m, 12 V / 5 W heaters, mounted on each of the upper and lower leading edge surfaces. All thermface specimens contained both coatings and heaters. The specimens are shown in Figure 2 as mounted for testing.

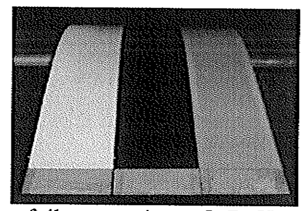

Figure 2: Aerofoil test sections: (L-R) Hydrophobic; Icephobic; Plain

The aerofoil test specimens were mounted at zero angle of attack downstream of the spray bar. Firstly, the surface mitigation technique was performed for the plain, hydrophobic and icephobic samples under both glaze and rime icing conditions.

Subsequently, the thermal mitigation strategy was applied. For the thermal and thermface mitigation both anti-icing and de-icing regimes were employed in both rime and glaze icing conditions. The anti-icing regime consisted of applying heat for the complete duration of the 20 minute test, whereas for the de-icing regime, heat was applied for only the second half of the test. The thermface strategy consisted of implementing the thermal strategy with the coated specimens.

Experimental Parameters

A cooled air-water system was used in these experiments. Table 1 indicates the experimental conditions for the wind tunnel and spray bar equipment; the dimensions of the test specimens; and summarizes the implemented

Parameter	Value
Experimental equipment conditions	
Spray bar water flow (kg/s)	0.00946
Spray bar water temperature (°C)	1.89
Spray bar air pressure (Pa)	206,842
Wind tunnel set velocity, v_t (Hz)	15.5
Test specimen parameters	
Chord length (m)	0.3048
Aerofoil specimen width (m)	0.6350
Angle of attack (degrees)	0.00
Weather conditions for glaze icing	
Liquid water content, LWC (kg/m^3)	0.28e-3
Diameter of droplet, d (m)	0.001
Freestream temperature, T_i (K)	268.0
Freestream pressure, P_o (MPa)	0.1013
Measured local wind velocity, V_w (m/s)	7.37
Weather conditions for rime icing	
Liquid water content, LWC (kg/m^3)	0.28e-3
Diameter of droplet, d (m)	0.001
Free stream temperature, T_i (K)	258.0
Free stream pressure, P_o (MPa)	0.1013
Measured local wind velocity, V_w (m/s)	7.97

Table 1: Experimental Parameters

climatological conditions. The diameter of the water droplets and the Liquid Water Content (LWC) are approximated.

Experimental Analysis

Leading edge (LE) profiles were compared among all resulting test samples from which ice shape, symmetry and consistency were observed. A high resolution black-white digital camera and data acquisition system was used to collect images of the side-view aerofoil profile and the ice accretion for test duration of 20 minutes. Collected image data was processed using graphics software to determine changes in ice profile shape and accumulation rate. Following this test, the shear-adhesion force test was performed on the LE curved surface of the aerofoil to determine the required force to remove the ice from the surface. The iced LE specimens were collected and their geometry was measured. The specimens were melted for a liquid volume measurement to gauge the amount of water that had accumulated along the leading edge.

Results & Discussion

Ice Profile Changes

A visual profile of ice formation on the LE surface, illustrates the varying amounts of ice accumulation and profile shapes between surfaces in glaze icing conditions. The resulting icing profiles are displayed in Figure 3.

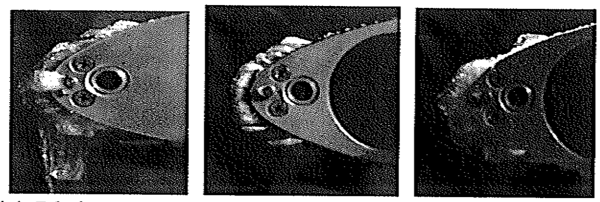

(a) Plain (b) Icephobic (c) Hydrophobic

Figure 3: Experimental icing pictures of leading edge of aerofoil for different coatings

Adhesion Force & Accumulation

The experimental results collected for ice adhesion force and the amount of water accumulation along the leading edge of the aerofoil for the various mitigation techniques are contained in Figures 4 and 5.

Adhesion Force

Comparing glaze and rime icing results indicate that on an uncoated plain surface, the adhesion force of glaze ice is 60% less adhesive than rime ice. The most effective surface mitigation in glaze conditions is the hydrophobic coating which reduces adhesion force by 70%. In rime condition, the icephobic coating is more effective, reducing adhesion by 26%. Evidently, in surface mitigation, the hydrophobic coating is most effective in glaze conditions while the icephobic coating is most effective in rime conditions. This can be attributed to the physical properties of the coatings: the hydrophobic coating is designed to be effective by repelling water as in glaze ice forms, while the icephobic coating is designed to repel solid-ice, as in rime conditions. Thus, the results identify the differences in the surface strategies and indicate that this distinction is related to the applied climatological conditions. This validates the significance and effectiveness of applying the proper coating in their designed-for conditions.

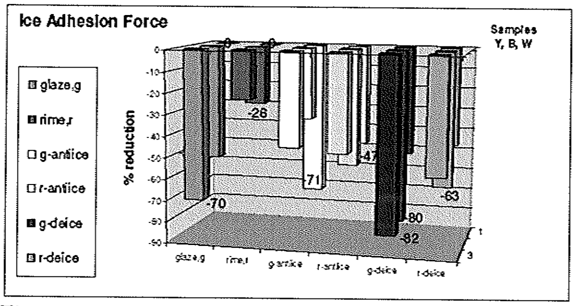

Figure 4: Percentage Reduction in Adhesion Force

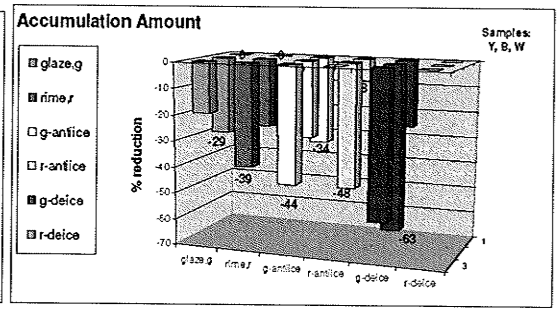

Figure 5: Percentage Reduction in Accumulation

For thermal mitigation, anti-icing is more effective than the deicing regime, in both glaze and rime icing conditions, reducing adhesion 71% and 47% respectively. Furthermore, the results indicate that the glaze responds more effectively than rime to this thermal mitigation strategy.

For the thermface mitigation, in both icing conditions, the de-icing regime is more effective than the anti-icing regime. In glaze conditions it performs equally well among the icephobic and hydrophobic coatings, reducing adhesion by 80%; whereas in rime conditions, it is best paired with the icephobic coating, reducing adhesion by 63%. Furthermore, the deicing regime also consumes less energy, which is ideal for energy production systems. Isolating the thermal variable indicates that for glaze icing, the thermal regimes are not solitarily effective at reducing adhesion force, and are thus most effective when paired with a secondary mitigation strategy. Furthermore, isolating the surface variable indicates that for glaze icing, there is no apparent adhesion reduction for either coating with the anti-icing regime, suggesting a supplementary result that the coatings may impede ice removal by preventing conductive heat transfer to the surface, as a result of their inherent thickness.

Thus, in both glaze and rime conditions the recommended strategy would be to employ the thermface mitigation technique with the icephobic coating in the deicing regime.

Accumulation Amount

In comparison of the amount of ice, in liquid state that accumulates along the LE of an aerofoil for both icing conditions, there is 14% less accumulation in glaze than in rime. The most effective surface mitigation in glaze icing is the icephobic coating, reducing accumulation by 29%, and in rime is the hydrophobic coating reducing accumulation 39%.

The most effective thermal mitigation strategy on a plain uncoated surface, in glaze conditions, is the anti-icing regime, reducing accumulation by 34%. In rime conditions, accumulation is not significantly reduced; in fact, only the anti-icing regime reduces accumulation by 8%, whereas for deicing, the amount of accumulation appears to supersede the effectiveness of the mitigation technique, suggesting that it does not have the capacity to be effective in the given conditions.

The most effective thermface regime for glaze conditions involves combining the de-icing regime with the icephobic coating, which reduces accumulation 63%. In rime conditions, the only effective solution is the icephobic coating with the anti-icing regime, reducing accumulation 48%.

The inability of the mitigation strategy to be effective with the de-icing regime in rime conditions indicates that the thermal technique has nearly reached its max capacity of effectiveness, yet the combination with the surface mitigation remains more effective than the thermal technique alone. In light of energy consumption, the deicing regime utilizes less energy, however it is limited in effectiveness of reducing accumulation in rime conditions, despite being the preferred regime.

Evidently, both the thermal and surface mitigation strategies, independently, are significantly effective at reducing accumulation along the leading edge of an aerofoil. However, the combined mitigation of the thermface strategy provides the most substantial reduction in accumulation. Thus, the recommended mitigation strategy for reducing accumulation in either glaze or rime conditions would be to implement the icephobic coating in combination with a deicing regime, but with attention to enhanced thermal duration as needed in rime conditions due to the limitation of de-icing to effectively reduce accumulation. Furthermore, this strategy is effective at reducing adhesion force as well.

Rate of Ice Accumulation

The experimental results collected for ice accumulation rate for various mitigation techniques are contained in Figures 6.

Comparing the rate of accumulation between glaze and rime icing conditions, it has been found that on an uncoated plain surface, glaze ice accumulates at a rate of 5% less than rime. When surface mitigation is used, the rate of ice accumulations on a wind turbine blade is more effectively reduced. By employing the icephobic coating, icing accumulation rate (IAR) is 52% less in glaze than in rime, while using the hydrophobic coating IAR is 80% in glaze than in rime.

Comparing the surface mitigation techniques, in glaze conditions, the IAR is reduced by 12% with the icephobic coating and 18% by the hydrophobic coating. In rime conditions, surface mitigation does not effectively reduce IAR, suggesting that the mitigation strategy has reached its maximum capacity for the given climatological conditions.

In comparison of the thermal mitigation techniques, for glaze conditions, the anti-icing regime effectively reduces IAR by 24%, whereas the deicing regime is ineffective for reducing IAR. In rime conditions, neither thermal mitigation regime effectively reduces IAR suggesting that the technique has reached its maximum capacity to be effective in the given conditions.

The thermface strategy employing the hydrophobic coating with the deicing regime reduces IAR by 72% in glaze conditions and is the only thermface strategy to perform effectively. In rime conditions, not one mitigation strategy overall indicates a reduction in IAR. Isolating individual variables for further insight to these results indicates that the icephobic coating with anti-icing provides a reduction in IAR when compared to both surface and thermal mitigations individually. This thermface technique effectively reduces IAR by 20% over surface mitigation alone and 14% over anti-icing thermal mitigation alone; thereby suggesting that it would be the most effective mitigation strategy in rime conditions for controlling IAR.

Evidently, IAR is more easily mitigated in glaze than in rime conditions. The most effective mitigation strategy is the thermface technique, where in glaze the hydrophobic coating with the de-icing regime is employed, and in rime, the icephobic coating with the anti-icing regime is employed. These results are indicative of the correlation between the sensitivity of the behaviour of the ice to the employed mitigation strategy, i.e. rime icing being more severe and requiring a more intense mitigation technique to effectively control the icing accumulation rate.

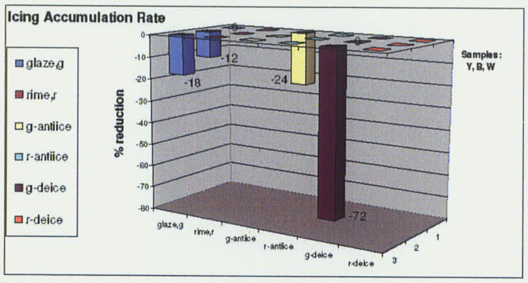

Figure 6: Percentage Reduction in Accumulation Rate

Wind Turbine Performance Measures

Optimized wind turbine performance is dependent on the lift to drag ratio created by the blades. Ice accumulation changes the aerodynamic profile shape of the blade and directly affects the lift, as well as creates trigger points for non-laminar flow over the blade surface resulting in less-efficient energy capture; furthermore, ice adds weight to the aerofoil. With a less-effective lift-to-drag ratio the turbine is not capable of efficient wind energy production. As shown in the change in ice profile shapes and accumulation rate over the capture period, the transient change in chord length of the aerofoil can result in a significant extension in chord length after only a period of 10 minutes, for which the aerodynamic blades are not designed. Additionally, an effective mitigation strategy, must not consume more energy than the system produces. Therefore, an optimal mitigation strategy would best balance these performance measures.

Conclusion

Wind Energy production in adverse cold climates can be enhanced by implementing the presented mitigation strategies, which significantly control the ice profile shapes, reduce the accumulation rate, adhesion force and accumulation amount of ice on a blade surface and influence the formation of a more symmetric LE ice profile. It is shown that in glaze or rime conditions, the thermface strategy employing the de-icing thermal regime with the icephobic surface coating is the most effective mitigation for reducing adhesion force and accumulation amount, with the necessity to extend the duration of the thermal regime to best mitigate accumulation amount; while for controlling icing accumulation rate, glaze icing will be effectively mitigated with the minimalist strategy while rime icing requires the most intense strategy.

Furthermore, the combination of mitigation strategies must be carefully designed so that they are employed in the climatological conditions best suited for their use and within their scope of capability so that they do not adversely affect the capabilities of one another—specifically, in the case of coating thickness impeding heat transfer by conduction to the surface.

Acknowledgments

Funding from the Manitoba Hydro NSERC Alternative Energy Chair, NRCAN, and support from the St. Leon Wind Farm Personnel, is gratefully acknowledged.

References

[1] Bose, N., Icing on a small horizontal-axis wind turbine-part 1: Glaze ice profiles, Journal of wind engineering and industrial aerodynamics, v45, n1 (1992), 75-85.
[2] Fitt, A.D. and Pope, M.P., De-icing by slot injection, Acta Mechanica. v147, n1-4 (2001) 73-86.
[3] Loughborough, D.L., Physics of mechanical removal of ice from aircraft, Aeronautical Engineering Review, v11, n2 (Feb 1952) 29-34.
[4] Mohammadi, R., Wassink, J., Amirfazli, A., Effect of Surfactants on Wetting of Super-Hydrophobic Surfaces, American Chemical Society, (Aug 6, 2004), 1-6.
[5] Garti, N. et al, New Non-Stick Epoxy-Silicone Water-Based Coatings Part 1: Physical and Surface Properties, Proceeding of the 5th International Zebra Mussel and Other Aquatic Nuisance Organisms Conference, Toronto, Canada, (Feb, 1995), 151-169. [6] http://www.wearlon.com/Eproducts.htm
[7] http://www.thermion.com/heaters/advantages.html
[8] Thomas, Scott K. et al., Aircraft anti-icing and de-icing techniques and modeling, Journal of Aircraft, v33, No. 5, September-October 1996, 841-854.
[9] Naterer, G. F. et al, Experimental Facility for New Hybrid Ice/Spray Flow Tunnel with Laser Based Droplet Measurement, AIAA 2002-2867, 1-10.

APPENDIX K

Impact of mitigation strategies on icing accumulation rate for wind turbines in cold climates

CanWEA 2006 Conference, Winnipeg, Manitoba, Canada

Impact of mitigation strategies on icing accumulation rate for wind turbines in cold climates

Andrea G. Kraj[1] and Eric L. Bibeau
Department of Mechanical and Manufacturing Engineering, University of Manitoba
Winnipeg, Manitoba, Canada R3T 5V6
[1]umkrajag@cc.umanitoba.ca

Abstract
Wind, as a potential resource for alternative energy and power generation has gained substantial interest worldwide. Optimization of wind generation systems is a key factor to establish this resource as an economic means for power generation. With a great amount of untapped wind resources in cold climates there is immense potential that is hindered by the uncertainty of the characteristics of the extreme climatological conditions. One issue facing the optimization of wind power generation in cold climates is ice accumulation on turbine blades, which is not only an energy production and efficiency concern, but also a safety issue. This paper explores mitigation techniques employed to prevent or delay ice accumulation on wind turbines blades in an effort to enhance the understanding of the icing characteristics and the means to optimize wind turbine systems in extreme conditions. Mitigation strategies involve surface, thermal and, the newly developed, *thermface* techniques in both anti-icing and de-icing regimes for both glaze and rime icing conditions. Experiments are conducted on stationary blade configurations in the state-of-the-art University of Manitoba Icing Tunnel Facility. The results of the mitigation techniques depict icing profiles and aerodynamic changes along the blade leading edge during the icing event and quantify the ice accumulation rate over a set period under simulated climatological icing conditions. Results are extended to an interpretive *Mitigation Forecasting Tool*, prior, during and after an icing event.

Introduction
Wind, as an energy resource, contains the potential to become an important contributor to utility and non-utility power generation in many regions in Canada and in cold climates throughout the world. However, due to extreme climatological factors, many Canadian wind turbine sites are affected by icing problems that impact power generation. Thus, the potential to harness an abundant source of wind for power generation is greatly disadvantaged. Icing is an issue of interest to many groups—from private energy companies, to public utilities and landowners. This paper discusses the experiments performed in the University of Manitoba's Icing Tunnel Facility, (UMITF), for the investigation of icing mitigation strategies for wind turbines in cold climates. Experiments are performed on aerofoils representative of blades currently used in the wind turbine industry, under simulated climatological conditions for severe icing events found in cold climates where wind turbines are commonly employed. Of particular interest is the 99.9 MW wind farm in St. Leon, Manitoba, which has been developed in a region very well-known for icing events.

Wind turbines are subjected to rime, glaze or mixed ice accretion conditions [1]. In the UMITF, glaze ice forms at temperatures just below freezing in air with high liquid water content, characteristically between 0°C and -6°C. Rime ice forms in colder environmental conditions, traditionally below -10°C, in air of low liquid water content, but also forms when surface temperatures are below -6°C. In rime icing, supercooled water droplets freeze immediately upon impact and form a low-density ice, white and feathery in appearance. In glaze icing, part of the water droplets freeze upon impact and the remaining water runs along the surface before freezing, forming a smooth lumpy profile shape of high-density clear ice.

Wind Turbine Performance Measures

Optimized aerodynamic performance is dependent on the blade lift to drag ratio [2]. Ice accumulation changes the wind turbine blade aerodynamic profile shape and directly affects the lift, as well as creates trigger points for non-laminar flow over the blade surface resulting in less-efficient energy capture; furthermore, ice adds weight to the aerofoil [3]. With a less-effective lift-to-drag ratio the turbine is not capable of efficient wind energy production. As shown in changes of ice profile shapes [4], the transient change in chord length of the aerofoil due to ice accumulation can result in a significant extension in chord after only a period of 10 minutes, for which the aerodynamic blades are not designed. Additionally, an effective mitigation strategy, must not consume more energy than the system produces. Therefore, an optimal mitigation strategy would best balance these performance measures.

Icing Mitigation Strategy

Current techniques for ice shedding from aerofoil blades are commonly found in literature related to aerospace and aircraft applications. As Fitt and Pope [5] indicate these methods include anti-icing and de-icing techniques ranging from freezing point depressants and surface deformation, to thermal melting. Reducing the force of ice adhesion from a surface is a key point to improving the ability to shed ice with ease. As explained by Loughborough [6] of the B.F. Goodrich Company, the force of adhesion is approximated to be linear with temperature, increasing 8.5 lbs per sq. in (5976.09 kg/m^2) for each degree centigrade decrease in temperature. The significance of this value indicates that a reduction in the adhesion force of the ice would greatly improve ice shedding and the resulting performance of the turbine. Therefore, a method that reduces the adhesion force of ice on the surface would ideally aid in preventing and delaying the onset of ice accretion. Since environmental conscientiousness is a key factor in the wind turbines systems, hot oil, chemicals and their derivative are not viable mitigation strategies. Furthermore, the use of electrical energy may contradict the purpose of generating electricity, and must be cautiously implemented. Therefore, the initial preference for an icing mitigation strategy is to implement a passive mitigation technique, such as a surface mitigation to improve the resistance of ice accretion and adhesion to the aerofoil surface. The correlation between a high contact angle for droplets on a surface and their enhanced ability to shed from the surface is highly influenced by the ability of a coating to be hydrophobic or ice-phobic [7]. Thus, the following have been selected for experimentation, for their favourable characteristics in icing conditions: Wearlon *Super-Icephobic* and *Super-Hydrophobic*. The icephobic coating is designed to perform best in icing conditions, whereas the hydrophobic coating is catered towards repelling water droplets [7, 8].

Subsequently, a less-passive mitigation strategy is explored. For this experiment, a thermal technique is selected. A highly controllable, lightweight system, compatible with modern composite materials has been adapted as an electro-thermal ice protection system where heat is generated at the point of use. Thermion® heaters are made from finely dispersed metal coated carbon fibre elements that may be integrated into composite or polymer material structures and are ideally suited for leading edge blade ice protection applications due to their lightweight and uniform heat distribution capability, contrary to traditional wire heaters [9]. The heat generated by this method is conducted into the ice-substrate interface, where a thin film of water is formed. This breaks the adhesive bond between the ice and the outer surface so that the ice can be swept away by aerodynamic forces. Furthermore, cycling of the heater power helps to control and reduce energy requirements [10], suggesting the use of various thermal regimes to further enhance the effectiveness of the mitigation strategy. By controlling the duration and timing of heat application both anti-icing and various de-icing regimes can be explored.

Finally, the combination of the surface mitigation with the thermal mitigation, termed *thermface*, is explored as means of more controlled-passive deicing technique, providing insight to the combined effectiveness of these mitigation strategies. The cycling of power for the electro-thermal heaters allows integration with other techniques to optimize mitigation efforts.

Experiment Description

Icing experimentation is performed in the Icing Tunnel Facility located in the Engineering Complex at the University of Manitoba. The UMITF consists of a spray system to emit droplets into the flow and a refrigeration system for cooling of the air as shown in Figure 1 [12].

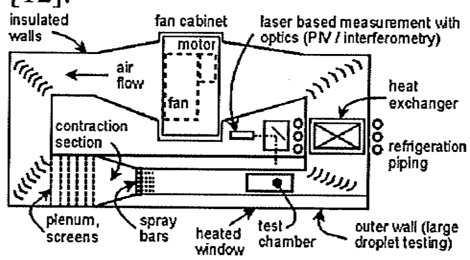

Figure 1: Top view of spray flow and icing tunnel

Experiments are conducted using stationary aerofoils placed within an inner duct ($1m^2$) of the wind tunnel. Scaled test specimens are subjected to cooled airflows containing water droplets that are released into the flow stream from a customized spray bar located upstream of the aerofoil test piece. Air atomizing nozzles can produce a reliable spray pattern with water mean droplet diameters ranging from 10^{-3} to 10^{-5} meters. The droplets travel in a trajectory towards the test specimen, are cooled along the way and freeze upon impact with the test specimen forming different icing characteristics and shapes, according to

the climatological conditions set for the conducted experiment.
The test specimen is in the form of a NACA 634421 profile aerofoil with aluminum frame and fiberglass sheeting. For this experimental series, six test pieces with various mitigation strategies were required to investigate the surface, thermal and thermface mitigation strategies. The specimen without a heater or coating was used as a datum. The selected coatings were applied to the aerofoil test specimens using specialized paint application equipment and procedures. The icephobic coated specimen is black, whereas the hydrophobic coated specimen is white, and the plain, uncoated specimen is the original fiberglass composite colour, yellow. All thermally mitigated specimens had two 0.508 x 0.127 m, 12 V / 5 W heaters, mounted on each of the upper and lower leading edge surfaces. All thermface specimens contained both coatings and heaters. The specimens are shown in Figure 2 as mounted for testing.

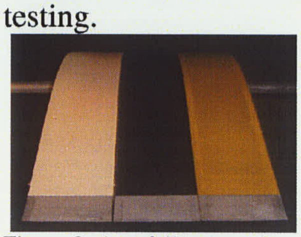

Figure 2: Aerofoil test sections: (L-R) Hydrophobic; Icephobic; Plain

The aerofoil test specimens were mounted at zero angle of attack downstream of the spray bar. Firstly, the surface mitigation technique was performed for the plain, hydrophobic and icephobic samples under both glaze and rime icing conditions. Subsequently, the thermal mitigation strategy was applied. For the thermal and thermface mitigation both anti-icing and de-icing regimes were employed in both rime and glaze icing conditions. The anti-icing regime consisted of applying heat for the complete duration of the 20 minute test, whereas for the de-icing regime, heat was applied for only the second half of the test. The thermface strategy consisted of implementing the thermal strategy with the coated specimens.

Table 1: Experimental Parameters

Parameter	Value
Experimental equipment conditions	
Spray bar water flow (kg/s)	0.00946
Spray bar water temperature (°C)	1.89
Spray bar air pressure (Pa)	206,842
Wind tunnel set velocity, v_t (Hz)	15.5
Test specimen parameters	
Chord length (m)	0.3048
Aerofoil specimen width (m)	0.6350
Angle of attack (degrees)	0.00
Weather conditions for glaze icing	
Liquid water content, LWC (kg/m^3)	0.28e-3
Diameter of droplet, d (m)	0.001
Freestream temperature, T_i (K)	268.0
Freestream pressure, P_o (MPa)	0.1013
Measured local wind velocity, V_w (m/s)	7.37
Weather conditions for rime icing	
Liquid water content, LWC (kg/m^3)	0.28e-3
Diameter of droplet, d (m)	0.001
Free stream temperature, T_i (K)	258.0
Free stream pressure, P_o (MPa)	0.1013
Measured local wind velocity, V_w (m/s)	7.97

Experimental Parameters

A cooled air-water system was used in these experiments. Table 1 indicates the experimental conditions for the wind tunnel and spray bar equipment; the dimensions of the test specimens; and summarizes the implemented climatological conditions. The diameter of the water droplets and the Liquid Water Content (LWC) are approximated.

Experimental Analysis

Leading edge (LE) profiles were compared among all resulting test samples from which ice shape, symmetry and consistency were observed. A high resolution black-white digital camera and data acquisition system was used to collect images of the side-view aerofoil profile and the ice accretion for test duration of 20 minutes. Collected image data was processed using graphics software to determine changes in ice profile shape and accumulation rate. Following this test, the shear-adhesion force test was performed on the LE curved surface of the aerofoil to determine the required force to remove the ice from the surface. The iced LE specimens were collected and their geometry was measured. The specimens were melted for a liquid volume measurement to gauge the amount of water that had accumulated along the leading edge.

Results & Discussion

Ice Profile Changes

A visual profile of ice formation on the LE surface, illustrates the varying amounts of ice accumulation and profile shapes between surfaces in glaze icing conditions. The resulting icing profiles are displayed in Figure 3.

(a) Plain (b) Icephobic (c) Hydrophobic

Figure 3: Experimental icing pictures of leading edge of aerofoil for different coatings

Rate of Ice Accumulation

The experimental results collected for ice accumulation rate for various mitigation techniques are contained in Figures 4.

Comparing the rate of accumulation between glaze and rime icing conditions, it has been found that on an uncoated plain surface, glaze ice accumulates at a rate of 5% less than rime. When surface mitigation is used, the rate of ice accumulations on a wind turbine blade is more effectively reduced. By employing the icephobic coating, icing accumulation rate (IAR) is 52% less in glaze than in rime, while using the hydrophobic coating IAR is 80% less in glaze than in rime.

Comparing the surface mitigation techniques, in glaze conditions, the IAR is reduced by 12% with the icephobic coating and 18% by the hydrophobic coating. In rime conditions, surface mitigation does not effectively reduce IAR, suggesting that the mitigation strategy has reached its maximum capacity for the given climatological conditions.

In comparison of the thermal mitigation techniques, for glaze conditions, the anti-icing regime effectively reduces IAR by 24%, whereas the deicing regime is ineffective for reducing IAR. In rime conditions, neither thermal mitigation regime effectively reduces IAR suggesting that the technique has reached its maximum capacity to be effective in the given conditions.

The thermface strategy employing the hydrophobic coating with the deicing regime reduces IAR by 72% in glaze conditions and is the only thermface strategy to perform effectively. In rime conditions, not one mitigation strategy overall indicates a reduction in IAR. Isolating individual variables for further insight to these results indicates that the icephobic coating with anti-icing provides a reduction in IAR when compared to both surface and thermal mitigations individually. This thermface technique effectively reduces IAR by 20% over surface mitigation alone and 14% over anti-icing thermal mitigation alone; thereby suggesting that it would be the most effective mitigation strategy in rime conditions for controlling IAR.

Evidently, IAR is more easily mitigated in glaze than in rime conditions. The most effective mitigation strategy is the thermface technique, where in glaze the hydrophobic coating with the de-icing regime is employed, and in rime, the icephobic coating with the anti-icing regime is employed. These results are indicative of the correlation between the sensitivity of the behaviour of the ice to the employed mitigation strategy, i.e. rime icing being more severe and requiring a more intense mitigation technique to effectively control the icing accumulation rate.

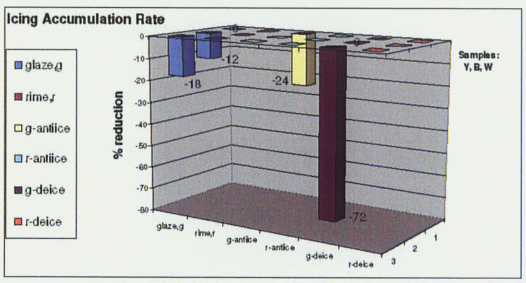

Figure 4: Percentage Reduction in Accumulation Rate

Mitigation Forecasting Tool (MFT)

Results have been consolidated, within the scope of this experiment, into a Mitigation Forecasting Tool (MFT). The MFT is composed of relevant icing characteristic data during and after an icing event for the proposed mitigation strategies in the given simulated climatological conditions. It has been designed to provide an idea of what to expect during and after an icing event in terms of accumulation rate, profile shape extension, weight amount of ice accumulation and adhesion pressure. Adhesion pressure provides an idea of "how sticky" the ice is to the surface, or in other words, how difficult the ice is to remove from the substrate per square inch. Profile shape extension is used to determine the changes in blade aerodynamics in terms of extended chord length which is a direct influential parameter for blade optimization, while ice weight accumulation provides the information to assess how much "heavier" and unstable the blade can become, which has a direct influence on turbine vibration and blade aerodynamics. Icing accumulation rate indicates the amount of ice to accumulate (length scale) at the leading edge, in a given time frame and provides an indication to the required intensity of a mitigation strategy to effectively mitigate an icing event. Figure 5 relates the collected data in a timeline format during and after an icing event. The figure is used to forecast icing characteristics and performance measures of mitigation strategies, as well as provide a comparison of values amongst strategies for a given icing characteristic.

Conclusion

Wind Energy production in adverse cold climates can be enhanced by implementing the presented mitigation strategies, which significantly control the ice profile shapes, reduce the accumulation rate, adhesion force and accumulation amount of ice on a blade surface and influence the formation of a more symmetric LE ice profile. For controlling icing accumulation rate, glaze icing will be effectively mitigated with the minimalist strategy while rime icing requires the most intense strategy, indicating the sensitivity of the behaviour of the ice to the employed mitigation strategy. The specific solution for each icing condition is the hydrophobic coating with the de-icing regime in glaze, and the icephobic coating with the anti-icing regime in rime.

The Mitigation Forecasting Tool indicates the performance measures for various mitigation strategies as a means to predict results and resolve an optimal solution, when a critical icing characteristic is selected.

Furthermore, the combination of mitigation strategies must be carefully designed so that they are employed in the climatological conditions best suited for their use and within their scope of capability so that they do not adversely affect the capabilities of one another.

References

[1] Bose, N., Icing on a small horizontal-axis wind turbine- part 1: Glaze ice profiles, Journal of wind engineering and industrial aerodynamics, v45, n1 (1992), 75-85.

[2] Kraj, A. G., Aerodynamic Optimization of a Biplane Configuration Through Differential Evolution, Department of Mechanical and Industrial Engineering, University of Manitoba, 2003.

[3] Kraj, A. G. and Bibeau, E. L., Icing characteristics and mitigation strategies for wind turbines in cold climates-part 1, WREC 2006.

[4] Kraj, A. G. and Bibeau, E. L., Icing characteristics and mitigation strategies for wind turbines in cold climates-part 2, Global Wind Power, 2006.

[5] Fitt, A.D. and Pope, M.P., De-icing by slot injection, Acta Mechanica. v147, n1-4 (2001) 73-86.

[6] Loughborough, D.L., Physics of mechanical removal of ice from aircraft, Aeronautical Engineering Review, v11, n2 (Feb 1952) 29-34.

[7] Mohammadi, R., Wassink, J., Amirfazli, A., Effect of Surfactants on Wetting of Super-Hydrophobic Surfaces, American Chemical Society, (Aug 6, 2004), 1-6.

[8] Garti, N. et al, New Non-Stick Epoxy-Silicone Water-Based Coatings Part 1: Physical and Surface Properties, Proceeding of the 5th International Zebra Mussel and Other Aquatic Nuisance Organisms Conference, Toronto, Canada, (Feb, 1995), 151-169.

[9] www.wearlon.com/Eproducts.htm

[10] www.thermion.com/heaters/advantages.html

[11] Thomas, Scott K. et al., Aircraft anti-icing and de-icing techniques and modeling, Journal of Aircraft, v33, No. 5, September-October 1996, 841-854.

[12] Naterer, G. F. et al, Experimental Facility for New Hybrid Ice/Spray Flow Tunnel with Laser Based Droplet Measurement, AIAA 2002-2867, 1-10.

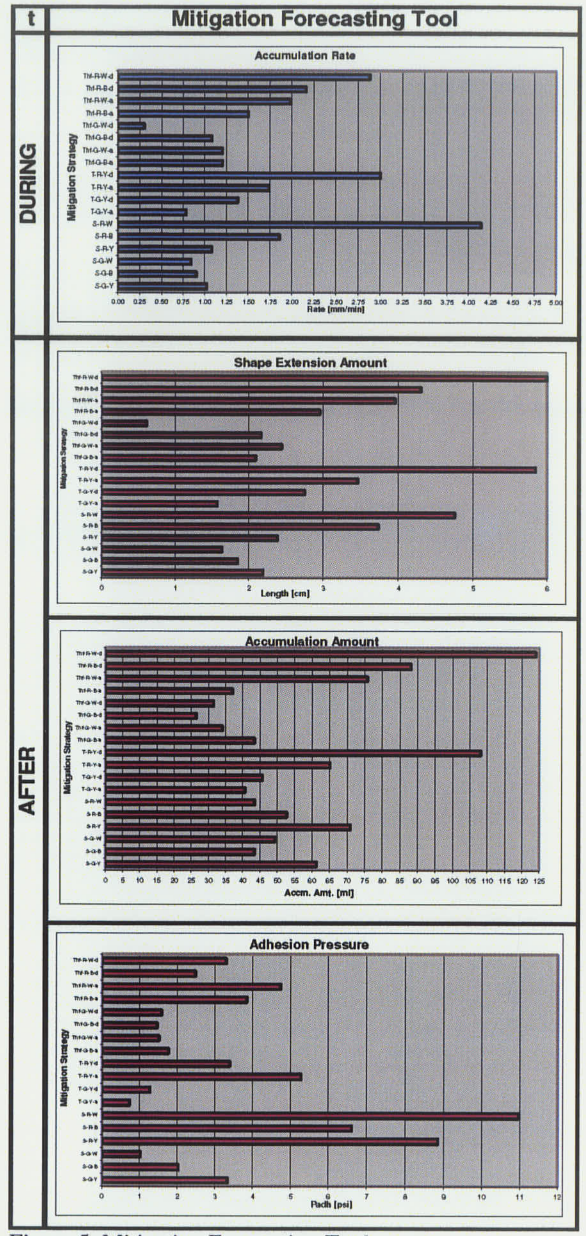

Figure 5: Mitigation Forecasting Tool

Acknowledgments

Funding from the Manitoba Hydro NSERC Alternative Energy Chair, NRCAN, and support from the St. Leon Wind Farm Personnel, is gratefully acknowledged.

APPENDIX L

Application of coatings for icing mitigation of wind turbines in cold climates

Renewable Energy 2006 Conference, Makuhari, Japan

Application of Coatings for Icing Mitigation of Wind Turbines in Cold Climates

Andrea G. Kraj[1] and Eric L. Bibeau
Department of Mechanical and Manufacturing Engineering, University of Manitoba
Winnipeg, Manitoba, Canada R3T 5V6
[1]umkrajag@cc.umanitoba.ca

Need For Icing Mitigation

•Ice removal from blades is critical to safe & efficient power generation

•Private sector, public utilities, land owners

•St. Leon, Manitoba, Canada: 99MW wind farm

Objectives

•Reduce the adhesion force of ice on the surface

•Prevent and delay ice accretion

Limitations

•Environmental: hot oil, chemicals and their derivatives are not viable strategies.

•Electrical: contradict the purpose of generating electricity, and must be cautiously implemented.

Stage 1: Surface Mitigation
•passive • improve resistance of ice accretion and adhesion to the aerofoil surface
• COATINGS Wearlon Super-Icephobic (black) Wearlon Super-Hydrophobic (white) Uncoated (yellow)
• Desired Properties: non-stick ability, good wear properties, excellent adhesion and water resistance, weatherability, low surface energy

Icing Tunnel Facility

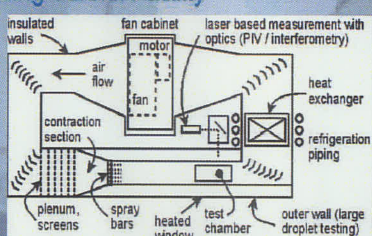

Experiment Description

•Experiments performed in the University of Manitoba Icing Tunnel Facility, (UMITF)

•Simulated climatological conditions of severe icing events

•Specimens: Stationary Aerofoils at Zero A.O.A. downstream

•Icing: Cooled airflows + Spray Bar + H20 droplets

•Variables: Glaze & Rime ice conditions
Plain, Icephobic, & Hydrophobic surfaces

UMITF Experimental Parameters	Glaze	Rime
Water Flow [GPH]	9.0	9.0
Tunnel Temp. [C]	-5	-15
Wind Speed [m/s]	7.37	7.97
Air-line pressure [psi]	50	50
Ice Density	HIGH	LOW
LWC	HIGH	LOW
Appearance	Clear & Uneven	White & Feathery

Experimental Analysis

•Collected image data processed using graphics software to determine changes in ice profiles: ice shape, symmetry and consistency observed

•Shear-adhesion force test:
 •New test apparatus designed to measure ice adhesion on curved surface
 •Performed on the LE to determine the required force to remove the ice from the surface

•Accumulation Amount:
 •Specimens melted for a liquid volume measurement due to variance in solid shapes between tests

Test Specimen

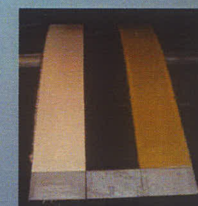

•NACA 634421 aerofoil

•Al frame + fiberglass substrate

•Planform Dimensions: 0.30m x 0.64m

Results

Ice Profile Changes

• LE aerofoil has greatest ice accretion

• Overall ice accretion: Plain > Hydrophobic > Icephobic

• Icephobic most controlled & symmetric ice profile

(a) Plain (b) Icephobic (c) Hydrophobic

One example: varying amounts of ice accumulation and profile shapes between surfaces in glaze icing conditions

Adhesion Force

•Glaze vs. Rime: uncoated plain surface, glaze ice 40% less adhesive than rime

•Glaze conditions
 Hydrophobic coating which reduces adhesion force by 97%.

•Rime conditions
 Ice phobic coating is more effective, reducing adhesion by 15%.

➢*Apply the proper coating in its designed-for conditions.*

Accumulation Amount

•Glaze vs. Rime: Less ice accumulates in glaze then in rime.

•Most effective coating: *Icephobic*
 •reduces accumulation by 5% in glaze and 23% in rime.

•Results are dependent on the climatological designed-for coating performance characteristics for the given icing conditions
 • icephobic coating outperforms the hydrophobic coating in icing conditions

Conclusion

Surface mitigation:
 •significantly reduces the adhesion force and accumulation amount of ice on a blade surface
 •influences the formation of a more symmetric LE ice profile
 •Enhances wind energy production in adverse cold climates

Mitigation strategies must be carefully designed:
 •employed in the climatological conditions best suited for their use and within their scope of capability
 •do not adversely affect the capabilities of other possible combinations

coating material characteristic, k, influences the thermal gradient; ice removal is more difficult.